

AD-A269 053

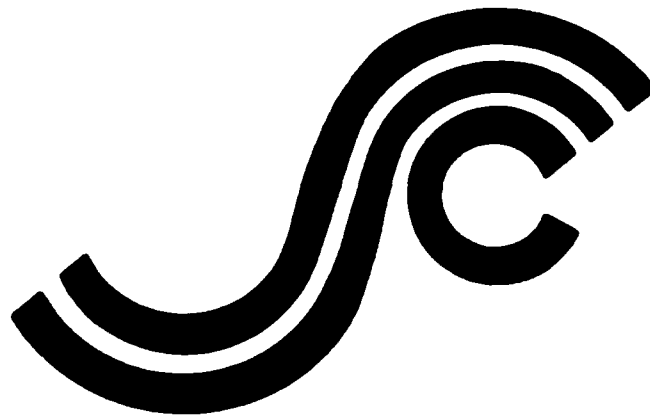


①
HJH

SSC-367

FATIGUE TECHNOLOGY ASSESSMENT AND STRATEGIES FOR FATIGUE AVOIDANCE IN MARINE STRUCTURES

APPENDICES



DTIC
ELECTE
AUG 25 1993
S B D

This document has been approved
for public release and sale; its
distribution is unlimited

93-19855

SHIP STRUCTURE COMMITTEE

1993

93 8 24 184

SHIP STRUCTURE COMMITTEE

The SHIP STRUCTURE COMMITTEE is constituted to prosecute a research program to improve the hull structures of ships and other marine structures by an extension of knowledge pertaining to design, materials, and methods of construction.

RADM A. E. Henn, USCG (Chairman)
Chief, Office of Marine Safety, Security
and Environmental Protection
U. S. Coast Guard

Mr. Thomas H. Peirce
Marine Research and Development
Coordinator
Transportation Development Center
Transport Canada

Mr. H. T. Haller
Associate Administrator for Ship-
building and Ship Operations
Maritime Administration

Dr. Donald Liu
Senior Vice President
American Bureau of Shipping

Mr. Alexander Malakhoff
Director, Structural Integrity
Subgroup (SEA OSP)
Naval Sea Systems Command

Mr. Thomas W. Allen
Engineering Officer (N7)
Military Sealift Command

CDR Stephen E. Sharpe, USCG
Executive Director
Ship Structure Committee
U. S. Coast Guard

CONTRACTING OFFICER TECHNICAL REPRESENTATIVE

Mr. William J. Siekierka
SEA 05P4
Naval Sea Systems Command

SHIP STRUCTURE SUBCOMMITTEE

The SHIP STRUCTURE SUBCOMMITTEE acts for the Ship Structure Committee on technical matters by providing technical coordination for determining the goals and objectives of the program and by evaluating and interpreting the results in terms of structural design, construction, and operation.

AMERICAN BUREAU OF SHIPPING

Mr. Stephen G. Arntson (Chairman)
Mr. John F. Conlon
Dr. John S. Spencer
Mr. Glenn M. Ashe

NAVAL SEA SYSTEMS COMMAND

Dr. Robert A. Sielski
Mr. Charles L. Null
Mr. W. Thomas Packard
Mr. Allen H. Engle

TRANSPORT CANADA

Mr. John Grinstead
Mr. Ian Bayly
Mr. David L. Stocks
Mr. Peter Timonin

MILITARY SEALIFT COMMAND

Mr. Robert E. Van Jones
Mr. Rickard A. Anderson
Mr. Michael W. Touma
Mr. Jeffrey E. Beach

MARITIME ADMINISTRATION

Mr. Frederick Seibold
Mr. Norman O. Hammer
Mr. Chao H. Lin
Dr. Walter M. Maclean

U. S. COAST GUARD

CAPT T. E. Thompson
CAPT W. E. Colburn, Jr.
Mr. Rubin Scheinberg
Mr. H. Paul Cojeen

SHIP STRUCTURE SUBCOMMITTEE LIAISON MEMBERS

U. S. COAST GUARD ACADEMY

LCDR Bruce R. Mustain

U. S. MERCHANT MARINE ACADEMY

Dr. C. B. Kim

U. S. NAVAL ACADEMY

Dr. Ramswar Bhattacharyya

STATE UNIVERSITY OF NEW YORK MARITIME COLLEGE

Dr. W. R. Porter

SOCIETY OF NAVAL ARCHITECTS AND MARINE ENGINEERS

Dr. William Sandberg

OFFICE OF NAVAL RESEARCH

Dr. Yapa D. S. Rajapaske

NATIONAL ACADEMY OF SCIENCES - MARINE BOARD

Mr. Alexander B. Stavovy

NATIONAL ACADEMY OF SCIENCES - COMMITTEE ON MARINE STRUCTURES

Mr. Peter M. Palermo

WELDING RESEARCH COUNCIL

Dr. Martin Prager

AMERICAN IRON AND STEEL INSTITUTE

Mr. Alexander D. Wilson

DEPARTMENT OF NATIONAL DEFENCE - CANADA

Dr. Neil G. Pegg

Member Agencies:

*United States Coast Guard
Naval Sea Systems Command
Maritime Administration
American Bureau of Shipping
Military Sealift Command
Transport Canada*



**Ship
Structure
Committee**

An Interagency Advisory Committee

Address Correspondence to:

Executive Director
Ship Structure Committee
U. S. Coast Guard (G-M/R)
2100 Second Street, S.W.
Washington, D.C. 20593-0001
PH: (202) 267-0003
FAX: (202) 267-4677

May 17, 1993

SSC-367
SR-1324

**FATIGUE TECHNOLOGY ASSESSMENT AND STRATEGIES FOR FATIGUE
AVOIDANCE IN MARINE STRUCTURES**

This report synthesizes the state-of-the-art in fatigue technology as it relates to the marine field. Over the years more sophisticated methods have been developed to anticipate the life cycle loads on structures and more accurately predict the failure modes. As new design methods have been developed and more intricate and less robust structures have been built it has become more critical than ever that the design tools used be the most effective for the task. This report categorizes fatigue failure parameters, identifies strengths and weaknesses of the available design methods, and recommends fatigue avoidance strategies based upon variables that contribute to the uncertainties of fatigue life.

This set of Appendices includes more in-depth presentations of the methods used in modeling the loads from wind and waves, linear system response to random excitation, stress concentration factors, vortex shedding and fatigue damage calculation.

A. E. HENN

Rear Admiral, U.S. Coast Guard
Chairman, Ship Structure Committee

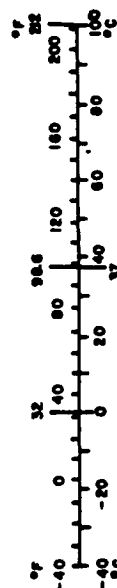
1. Report No.	2. Government Accession No.	3. Recipient's Catalog No.	
4. Title and Subtitle FATIGUE DESIGN PROCEDURES		5. Report Date June 1992	
		6. Performing Organization Code	
7. Author(s) Cuneyt C. Capanoglu		8. Performing Organization Report No. SR-1324	
9. Performing Organization Name and Address EARL AND WRIGHT 180 Howard Street San Francisco, CA 94105		10. Work Unit No. (TRAIS)	
		11. Contract or Grant No. DTCG23-88-C-20029	
12. Sponsoring Agency Name and Address Ship Structure Committee U.S. Coast Guard (G-M) 2100 Second Street, SW Washington, DC 20593		13. Type of Report and Period Covered Final Report	
		14. Sponsoring Agency Code G-M	
15. Supplementary Notes Sponsored by the Ship Structure Committee and its members agencies.			
16. Abstract <p style="text-align: center;"><u>ABSTRACT</u></p> <p>This report provides an up-to-date assessment of fatigue technology, directed specifically toward the marine industry. A comprehensive overview of fatigue analysis and design, a global review of fatigue including rules and regulations and current practices, and a fatigue analysis and design criteria, are provided as a general guideline to fatigue assessment. A detailed discussion of all fatigue parameters is grouped under three analysis blocks:</p> <ul style="list-style-type: none">• Fatigue stress model, covering environmental forces, structure response and loading, stress response amplitude operations (RAOs) and hot-spot stresses• Fatigue stress history model covering long-term distribution of environmental loading• Fatigue resistance of structures and damage assessment methodologies <p>The analyses and design parameters that affect fatigue assessment are discussed together with uncertainties and research gaps, to provide a basis for developing strategies for fatigue avoidance. Additional in-depth discussions of wave environment, stress concentration factors, etc. are presented in the appendixes.</p>			
17. Key Words Assessment of fatigue technology, fatigue stress models, fatigue stress history models, fatigue resistance, fatigue parameters and fatigue avoidance strategies		18. Distribution Statement Available from: National Technical Information Serv. U. S. Department of Commerce Springfield, VA 22151	
19. Security Classif. (of this report) Unclassified	20. Security Classif. (of this page) Unclassified	21. No. of Pages 194 Excl. Appendixes	22. Price

METRIC CONVERSION FACTORS

Approximate Conversions to Metric Measures			
Symbol	When You Know	Multiply by	To Find
LENGTH			
in	inches	2.5	centimeters
ft	feet	30	centimeters
yd	yards	0.9	meters
mi	miles	1.6	kilometers
AREA			
in ²	square inches	6.5	square centimeters
ft ²	square feet	0.09	square meters
yd ²	square yards	0.8	square meters
mi ²	square miles	2.6	square kilometers
	acres	0.4	hectares
MASS (weight)			
oz	ounces	28	grams
lb	pounds	0.45	kilograms
	short tons (2000 lb)	0.9	tonnes
VOLUME			
cup	teaspoons	5	milliliters
fl oz	tablespoons	15	milliliters
	fluid ounces	30	milliliters
c	cups	0.24	liters
pt	pints	0.47	liters
qt	quarts	0.95	liters
gal	gallons	3.8	liters
cu ft	cubic feet	0.03	cubic meters
yd ³	cubic yards	0.76	cubic meters
TEMPERATURE (exact)			
°F	Fahrenheit temperature	5/9 (after subtracting 32)	Celsius temperature
°C	Celsius temperature	9/5 (then add 32)	Fahrenheit temperature

*1 in = 2.54 exactly. For other exact conversions and more detailed tables, see NBS Mon. Publ. 286, Units of Weight and Measures, Price \$2.75, SO Catalog No. C13.10-286.

Approximate Conversions from Metric Measures			
Symbol	When You Know	Multiply by	To Find
LENGTH			
mm	millimeters	0.04	inches
cm	centimeters	0.4	inches
m	meters	3.3	feet
km	kilometers	1.1	miles
		0.6	miles
AREA			
cm ²	square centimeters	0.16	square inches
m ²	square meters	1.2	square yards
km ²	square kilometers	0.4	square miles
ha	hectares (10,000 m ²)	2.5	acres
MASS (weight)			
g	grams	0.035	ounces
kg	kilograms	2.2	pounds
t	tonnes (1000 kg)	1.1	short tons
VOLUME			
ml	milliliters	0.03	fluid ounces
l	liters	2.1	pints
		1.06	quarts
		0.26	gallons
m ³	cubic meters	35	cubic feet
		1.3	cubic yards
TEMPERATURE (exact)			
°C	Celsius temperature	9/5 (then add 32)	Fahrenheit temperature



**FATIGUE TECHNOLOGY
ASSESSMENT AND STRATEGIES
FOR FATIGUE AVOIDANCE IN
MARINE STRUCTURES**

APPENDICES

CONTENTS

APPENDIX A Review of the Ocean Environment

APPENDIX B Review of Linear System Response to Random Excitation

APPENDIX C Stress Concentration Factors

APPENDIX D Vortex Shedding Avoidance and Fatigue Damage Computation

DTIC QUALITY INSPECTED 8

Accession For	
NTIS GRA&I	<input checked="checked" type="checkbox"/>
DTIC TAB	<input type="checkbox"/>
Unannounced	<input type="checkbox"/>
Justification	
By _____	
Distribution/	
Availability Codes	
Dist	Avail and/or Special
A-1	

APPENDIX A

REVIEW OF OCEAN ENVIRONMENT

CONTENTS

- A. REVIEW OF OCEAN ENVIRONMENT
 - A.1 IRREGULAR WAVES
 - A.2 PROBABILITY CHARACTERISTICS OF WAVE SPECTRA
 - A.2.1 Characteristic Frequencies and Periods
 - A.2.2 Characteristic Wave Heights
 - A.3 WAVE SPECTRA FORMULAS
 - A.3.1 Bretschneider and ISSC Spectrum
 - A.3.2 Pierson-Moskowitz Spectrum
 - A.3.3 JONSWAP and Related Spectra
 - A.3.4 Scott and Scott-Wiegel Spectra
 - A.4 SELECTING A WAVE SPECTRUM
 - A.4.1 Wave Hindcasting
 - A.4.2 Direct Wave Measurements
 - A.5 WAVE SCATTER DIAGRAM
 - A.6 WAVE EXCEEDANCE CURVE
 - A.7 WAVE HISTOGRAM AND THE RAYLEIGH DISTRIBUTION
 - A.8 EXTREME VALUES AND THE WEIBULL DISTRIBUTION
 - A.9 WIND ENVIRONMENT
 - A.9.1 Air Turbulence, Surface Roughness and Wind Profile
 - A.9.2 Applied, Mean and Cyclic Velocities
 - A.9.3 Gust Spectra
 - A.10 REFERENCES

A. REVIEW OF OCEAN ENVIRONMENT

The ocean environment is characterized by waves, wind and current. The waves are typically irregular (confused or random seas). Some waves are generated locally by the wind, and some waves are generated great distances away. The wind is unsteady, with gusts. The wind varies with height above water. The current is caused by the wind, by waves, by the tide, and by global temperature differences. The current varies with depth. All of these characteristics vary with time.

A.1 IRREGULAR WAVES

Irregular waves (a random sea) can be described as the sum of an infinite number of individual regular (sinusoidal) waves of different amplitude, frequency, and phase (Figure A-1). Therefore, the randomly varying sea surface elevation can be represented by a Fourier series.

$$\eta(t) = \sum_{i=1}^N a_i \cos(\omega_i t + \phi_i)$$

where $\eta(t)$ is the water surface elevation measured from still water level,

a_i is the amplitude of each component regular wave,

ω_i is the frequency of each component regular wave,

ϕ_i is the phase angle of each component regular wave, and

t is time.

The most distinctive feature of a random sea is that it never repeats its pattern and it is impossible to predict its shape. Therefore, total energy is used to define a particular sea. The energy (E) in an individual regular wave per unit surface area is,

$$E = \frac{1}{2} \rho g a^2$$

and the total energy of the sea is the sum of the energies of the constituent regular waves.

$$E = \frac{1}{2} \rho g \sum_{i=1}^N a_i^2$$

The total energy of the sea is distributed according to the frequencies of the various wave components. The amount of energy per unit surface area within the small frequency band $(\omega_i, \omega_i + d\omega)$ is,

$$E(\omega_i) = \frac{1}{2} \rho g a_i^2 d\omega$$

The total energy of the sea is then the sum of the energies within the individual wave components. If the sea is made up of an infinite number of waves, the energies of the waves form a smooth curve, and the above summation may be replaced by an integral.

$$E = \rho g \int_0^{\infty} \frac{1}{2} a^2 d\omega$$

The smooth distribution of the wave energy is called the energy spectrum or wave spectrum of the random sea, and is often designated as $S(\omega)$. A wave spectrum is normally depicted as a curve with an ordinate of energy and an abscissa of frequency. A typical wave spectrum has a central peak with a tapered energy distribution either side of the peak.

The recommended form of displaying a wave spectrum is with an ordinate of $\frac{1}{2}a^2$ and an abscissa of ω , radial frequency. However, since the engineer will encounter wave spectra equations in a number of forms, using various bases and units, the applicable conversion factors are provided in the following sections.

Spectrum Basis

The recommended spectrum basis is half amplitude squared or energy. Often spectrum equations having a different basis are encountered. Before any statistical calculations are performed with a spectrum equation, the equation should be converted to the recommended basis.

For a "half amplitude" or "energy" spectrum, the basis is one-half times the amplitude squared.

$$S(\omega) = \frac{1}{2}a^2$$

$$S(\omega)d\omega = E / (pg)$$

where,

S is the spectral ordinate,

ω is the radial frequency,

a is the wave amplitude of the constituent wave of frequency,

E is the energy content of the constituent wave of frequency, ω .

For an "amplitude" spectrum, the basis is amplitude squared.

$$S(\omega) = a^2$$

$$S(\omega) = 2 * (\frac{1}{2} * \eta^2)$$

For a "height" spectrum, the basis is height squared.

$$S(\omega) = h^2$$

$$S(\omega) = 8 * (\frac{1}{2} * \eta^2)$$

where,

h is the height of the constituent wave of frequency, ω .

For a "height double" spectrum, the basis is two times the height squared.

$$S(\omega) = s * h^2$$

$$S(\omega) = 16 * (\frac{1}{2} * \eta^2)$$

The basis of the spectrum must be determined before the spectrum is used in an analysis, because the ordinate of one representation of the spectrum may be as much as 16 times as great as the ordinate of another representation.

Units

The spectrum equation may be expressed in terms of radial frequency, circular frequency, or period. Conversion between circular frequency and radial frequency is accomplished by multiplying by the constant, 2π .

$$\omega = 2\pi * f$$

$$S(\omega) = S(f) / (2\pi)$$

where,

f is the circular frequency.

The conversion between period and radial frequency is more complicated.

$$\omega = 2\pi/T$$

$$S(f) = T^2 * S(T)$$

$$S(\omega) = T^2 * S(T) / (2\pi)$$

where,

T is the period.

When converting between period and frequency, the abscissa axis is reversed. Zero period becomes infinite frequency, and infinite period becomes zero frequency.

Wave spectrum equations may be used with any length units by remembering that the spectrum ordinate is proportional to amplitude squared or height squared.

$$S(\omega)_{\text{meter}} = (0.3048)^2 * S(\omega)_{\text{feet}}$$

The mathematical formulation for the wave spectrum equation will often include the significant height squared or the gravitational constant squared, which when entered in the appropriate units will convert the equation to the desired length units.

A.2 PROBABILITY CHARACTERISTICS OF WAVE SPECTRA

The characteristics of ocean waves are determined by assuming that the randomness of the surface of the sea can be described by two

common probability distributions, the Gaussian (or normal) distribution and the Rayleigh distribution. These probability distributions are used to define the distribution of wave elevations, η , and of wave heights, H , respectively.

A.2.1 Characteristic Frequencies and Periods

For design purposes sea spectra equations are selected to represent middle aged seas that would exist some time after a storm, yet which are still young enough to have a good dispersion of wave frequencies. The primary assumption about the design seas is that the wave elevations follow a Gaussian or normal distribution. Samples of wave records tend to support this assumption. In conjunction with the Gaussian distribution assumption, the wave elevations are assumed to have a zero mean. Digitized wave records tend to have a slight drift of the mean away from zero, usually attributed to tide or instrument drift. The Gaussian distribution assumption is equivalent to assuming that the phase angles of the constituent waves within a wave spectrum, are uniformly distributed.

The Gaussian distribution allows one to calculate statistical parameters which are used to describe the random sea. The mean elevation of the water surface is the first moment of the Gaussian probability density function. The mean-square is the second moment taken about zero, and the root-mean-square is the positive square root of the mean-square. The variance is the second moment taken about the mean value. The standard deviation is the positive square root of the variance. Since the wave elevations are assumed to have a zero mean value, the variance is equal to the mean-square, and the standard deviation is equal to the root-mean-square. In present practice, the area under a random wave energy spectrum is equated to the variance.

In a similar way, the characteristic frequencies and periods of a wave spectrum are defined in terms of the shape, the area, and/or the area moments of the $\frac{1}{2} \sigma^2$ wave spectrum. Depending upon the

particular wave spectrum formula, these characteristic periods may or may not reflect any real period. The area and area moments are calculated as follows.

Area:

$$m_0 = \int_0^{\infty} \omega^0 S(\omega) d\omega$$

Nth Area Moment:

$$m_n = \int_0^{\infty} \omega^n S(\omega) d\omega$$

The characteristic frequencies and periods are defined as follows.

ω_m : Peak frequency

The peak frequency is the frequency at which the spectral ordinate, $S(\omega)$ is a maximum.

T_p : Peak period

The peak period is the period corresponding to the frequency at which $S(\omega)$ is a maximum.

$$T_p = 2\pi/\omega_m$$

T_m : Modal period

The modal period is the period at which $S(T)$ is a maximum. Since the spectrum equations in terms of frequency and in terms of period differ by the period squared factor, the modal period is shifted away from the peak period.

T_v : Visually Observed Period, or Mean Period, or Apparent Period

The visually observed period is the centroid of the $S(\omega)$ spectrum. The International Ship Structures Congress (ISSC) and some environmental reporting agencies have adopted T_v as the period visually estimated by observers.

$$T_v = 2\pi \cdot (m_0/m_2)^{1/2}$$

T_z : Average Zero-upcrossing period or Average Period

The average zero-upcrossing period is the average period between successive zero up-crossings. The average period may be obtained from a wave record with reasonable accuracy.

$$T_z = 2\pi \cdot (m_0/m_2)^{1/2}$$

T_c : Crest Period

The crest period is the average period between successive crests. The crest period may be taken from a wave record, but its accuracy is dependent upon the resolution of the wave measurement and recording equipment and the sampling rate.

$$T_c = 2\pi \cdot (m_2/m_4)^{1/2}$$

T_s : Significant Period

The significant period is the average period of the highest one-third of the waves. Some environmental reporting agencies give the sea characteristics using T_s and H_s , the significant wave height. There are two equations relating T_s to T_p .

$$T_s = 0.8568 \cdot T_p, \quad \text{Old}$$

$$T_s = 0.9457 * T_p, \quad \text{New}$$

The first equation applies to original Bretschneider wave spectrum, and the second is the result of recent wave studies (See Reference A.1).

The peak period, T_p , is an unambiguous property of all common wave spectra, and is therefore the preferred period to use in describing a random sea.

A.2.2 Characteristic Wave Heights

From the assumption that the wave elevations tend to follow a Gaussian distribution, it is possible to show that the wave heights follow a Rayleigh distribution. Since wave heights are measured from a trough to succeeding crest, wave heights are always positive which agrees with the non-zero property of the Rayleigh probability density. From the associated property that the wave heights follow a Rayleigh distribution, the expected wave height, the significant wave height, and extreme wave heights may be calculated. The equation for the average height of the one-over-nth of the highest waves is as follows.

$$H_{1/n} / (m_0)^{1/2} = 2 * [2 * \ln(n)]^{1/2} + \frac{1}{n * (2\pi)^{1/2} * [1 - \text{erf}[(\ln(n))^{1/2}]]}$$

where:

m_0 is the variance or the area under the energy spectrum,

\ln is the natural logarithm,

erf is the error function, (the error function is explained and tables of error function values are available in mathematics table books.)

The characteristic wave heights of a spectrum are related to the total energy in the spectrum. The energy is proportional to the area under the $\frac{1}{2}a^2$ spectrum.

H_a : Average Wave Height

The average or mean height of all of the waves is found by setting $n=1$.

$$H_a = 2.51*(m_0)^{\frac{1}{2}}$$

H_s : Significant Height

The significant height is the average height of the highest one-third of all the waves, often denoted as $H_{1/3}$.

$$H_s = 4.00*(m_0)^{\frac{1}{2}}$$

H_{max} : Maximum Height

The maximum height is the largest wave height expected among a large number of waves, (n on the order of 1000), or over a long sampling period, (t on the order of hours).

The maximum wave height is often taken to be the average of the 1/1000th highest waves.

$$H_{1/1000} = 7.94*(m_0)^{\frac{1}{2}} = 1.985*H_s$$

Using the one-over-nth equation and neglecting the second term gives the following equation.

$$H_{1/n} = 2*[\ln(n)]^{\frac{1}{2}}*(m_0)^{\frac{1}{2}}$$

or

$$H_{1/n} = 2*[2*\ln(n)]^{1/2} * H_s$$

For $n = 1000$, this gives,

$$H_{1/1000} = 7.43*(m_0)^{1/2} = 1.86*H_s$$

For a given observation time, t , in hours, the most probable extreme wave height is given by the following equation.

$$H_{max} = 2*[2*m_0*\ln(3600*t/T_z)]^{1/2}$$

The $3600*t/T_z$ is the average number of zero up-crossings in time, t .

A.3 WAVE SPECTRA FORMULAS

The Bretschneider and Pierson-Moskowitz spectra are the best known of the one-dimensional frequency spectra that have been used to describe ocean waves. The JONSWAP spectrum is a recent extension of the Bretschneider spectrum and has an additional term which may be used to give a spectrum with a sharper peak.

A.3.1 Bretschneider and ISSC Spectrum

The Bretschneider (Reference A.2) spectrum and the spectrum proposed as a modified Pierson-Moskowitz spectrum by the Second International Ship Structures Congress (Reference A.4) are identical. The Bretschneider equation in terms of radial frequency is as follows.

$$S(\omega) = (5/16)*(H_s)^2*(\omega_m^4/\omega^5)* \exp [-1.25*(\omega/\omega_m)^{-4}]$$

where:

H_s is the significant wave height, and

ω_m is the frequency of maximum spectral energy.

The Bretschneider equation may be written in terms of the peak period instead of the peak frequency, by substituting $\omega_m = 2\pi/T_p$.

$$S(\omega) = (5/16) * (H_s)^2 * [(2\pi)^4 / (\omega^5 * (T_p)^4)] * \exp[-1.25 * (2\pi^4 / (\omega * T_p)^4)]$$

A.3.2 Pierson-Moskowitz Spectrum

The Pierson-Moskowitz (Reference A.4) spectrum was created to fit North Atlantic weather data. The P-M spectrum is the same as the Bretschneider spectrum, but with the H_s and ω_m dependence merged into a single parameter. The frequency used in the exponential has also been made a function of reported wind speed. The equation for the Pierson-Moskowitz spectrum is as follows.

$$S(\omega) = \alpha * g^2 / \omega^5 * \exp[-\beta * (\omega_0 / \omega)^4]$$

where:

$$\alpha : 0.0081$$

$$\beta = 0.74$$

$$\omega_0 = g/U$$

and, U is the wind speed reported by the weather ships.

The Pierson-Moskowitz spectrum equation may be obtained from the Bretschneider equation by using one of the following relations between H_s and ω_m .

$$H_s = 0.1610 * g / (\omega_m)^2$$

or

$$\omega_m = 0.40125 * g / (H_s)^{1/2}$$

An interesting point that may be noted is that if β were set equal to 0.75 instead of 0.74, the ω_0 would be the frequency corresponding to the modal period, T_m .

A.3.3 JONSWAP and Related Spectra

The JONSWAP wave spectrum equation resulted from the Joint North Sea Wave Project (Reference A.5). The JONSWAP equation is the original Bretschneider wave spectrum equation with an extra term added. The extra term may be used to produce a sharply peaked spectrum with more energy near the peak frequency. The JONSWAP spectrum can be used to represent the Bretschneider wave spectrum, the original Pierson-Moskowitz wave spectrum, and the ISSC modified P-M spectrum. The full JONSWAP equation is as follows.

$$S(\omega) = (\alpha_j * g^2 \omega^5) * \exp[-1.25 * \omega / \omega_m^{-4}] * \gamma^a$$

where:

$$a = \exp \left[-\frac{1}{2} * (\omega - \omega_m)^2 / (\sigma * \omega_m)^2 \right]$$

ω_m is the frequency of maximum spectral energy.

The Joint North Sea Wave Project recommended the following mean values to represent the North Sea wave spectra.

$$\gamma = 3.3$$

$$\sigma = 0.07, \quad \text{for } \omega < \omega_m$$

$$\alpha = 0.09, \quad \text{for } \omega > \omega_m$$

The value of α is found by integrating the spectrum and adjusting ω to give the desired area.

The Bretschneider equation and the ISSC equation can be obtained by setting the following parameter values.

$$\gamma = 1.0$$

$$\alpha = (5/16) * (H_s)^2 * (\omega_m)^4 / g^2$$

The Pierson-Moskowitz equation is obtained from the further restriction that H_s and ω_m are related.

$$H_s = 0.1610 * g / (\omega_m)^2$$

or

$$\omega_m = 0.140125 * (g / H_s)^{1/2}$$

or

$$\alpha = 0.0081$$

When γ is set to one the JONSWAP term is effectively turned off. Without the JONSWAP term, the wave spectrum equation can be mathematically integrated to give the following relationships among the characteristic wave periods.

$$T_p = 1.1362 * T_m$$

$$T_p = 1.2957 * T_v$$

$$T_p = 1.4077 * T_z$$

$$T_p = 1.1671 * T_s$$

For $\gamma = 1$, the fourth area moment is infinite. The crest period, T_c , is therefore zero.

For values of γ other than one, the JONSWAP equation cannot be mathematically integrated. The period relationships as a function of γ can be calculated by numerical integration of the wave spectrum equation over the range from three-tenths of the peak frequency to ten times the peak frequency.

The shape of the JONSWAP spectrum can be further adjusted by changing the values of e . The e values are sometimes varied when the JONSWAP spectrum is used to fit measured wave spectra.

A.3.4 Scott and Scott-Wiegel Spectra

The Scott (Reference A.6) spectrum was also formulated to fit North Atlantic weather data. The Scott spectrum is the Darbyshire (Reference A.7) spectrum with slight modifications to the constants in the equation. The spectrum equation is as follows.

$$S(\omega) = 0.214 * (H_s)^2 * \exp[-(\omega - \omega_m) / \{0.065 * (\omega - \omega_m + 0.26)\}^{1/2}]$$

for $-0.26 < \omega - \omega_m < 1.65$

= 0, elsewhere.

where

H_s is the significant height,

$$\omega_m = 3.15*T^{-1} + 8.98*T^{-2},$$

T is the characteristic period of the waves.

The ω_m is the frequency of the peak spectral energy, but unfortunately, the period, T , used in the equation for ω_m does not correspond to any of the mathematical characteristics of the spectrum. The equation for ω_m was derived as a curve fit to real data.

The Scott-Wiegel spectrum is a Scott spectrum modification that was proposed by Wiegel (Reference A.8). The constants are adjusted to match the equation to a "100-year storm" wave condition. The new equation is as follows.

$$S(\omega) = 0.300*(H_s)^2 * \exp[-(\omega - \omega_m)^2 / \{0.0353*(\omega - \omega_m + 0.26)\}]$$

The ω_m in this equation is 1.125 times that specified for the Scott equation.

A.4 SELECTING A WAVE SPECTRUM

Information about the random sea characteristics in a particular area is derived by either 'wave hindcasting' or by direct wave measurement. For many areas of the world's oceans, the only data available is measured wind speeds and visually estimated wave heights. Sometimes the estimated wave heights are supplemented by estimated wave periods. For a few areas of intense oil development, such as the North Sea, direct wave measurement projects have produced detailed wave spectra information.

A.4.1 Wave Hindcasting

Wave hindcasting is a term used to describe the process of estimating the random sea characteristics of an area based upon meteorological or wind data. Various researchers (References A.2, A.4, A.6, A.7 and A.8) have attempted to derive a relationship between the wind speed over a recent period of time and the spectrum of the random sea generated by the particular wind. The wind speed data is usually qualified by two additional parameters, the duration that the wind has been blowing at that speed and the fetch or distance over open ocean that the wind has been blowing.

A set of equations as derived by Bretschneider (Reference A.2), which relate wind speed, duration and fetch are as follows.

$$g \cdot H_s / U^2 = 0.283 \cdot \tanh[0.125 \cdot (g \cdot F / U^2)^{0.42}]$$

$$g \cdot T_s / (2 \pi \cdot U) = 1.2 \cdot \tanh[0.077 \cdot (g \cdot F / U^2)^{0.42}]$$

$$g \cdot t_{\min} / U = 6.5882 \cdot \exp\{[0.161 \cdot \Lambda^2 - 0.3692 \cdot \Lambda + 2.024]^{1/2} + 0.8798 \cdot \Lambda\}$$

where

U is the wind speed,

F is the fetch,

$\Lambda = \ln[g \cdot F / U^2],$

t_{\min} is the minimum duration for which the fetch will determine the significant height and period, and

\tanh is the hyperbolic tangent.

If the wind duration is less than t_{min} , then the third equation is used to find the fetch which would correspond to $t_{min} = t$.

For a fully arisen sea, the above equations simplify to the following.

$$g*H_s/U^2 = 0.283$$

$$g*T_s/(2\pi*U) = 1.2$$

Other relationships have been developed in the references. Often specialized weather/wave research companies have developed elaborate wave hindcasting models to derive the wave spectra characteristics for particular areas. However, the assumptions incorporated into these models have very profound impact on the outcome.

A.4.2 Direct Wave Measurements

By installing a wave probe or a wave buoy in the ocean area of interest, wave elevation histories may be directly measured. The elevation of the sea at a particular point is either recorded by analog means or is sampled at short time intervals (typically one second) and recorded digitally. The wave elevations are usually recorded intermittently, ie. the recorder is turned on for say 30 min every four hours.

The wave records are then reduced by computer, and the wave characteristics are summarized in various ways. Two common ways of summarizing the data are as a wave scatter diagram and/or as a wave height exceedance diagram.

The wave scatter diagram is a grid with each cell containing the number or occurrences of a particular significant wave height range and wave period range. The wave period range may be defined in terms of either peak period or zero-upcrossing period.

The wave height exceedance diagram is a curve showing the percentage of the wave records for which the significant wave height was greater than the particular height.

A5

WAVE SCATTER DIAGRAM

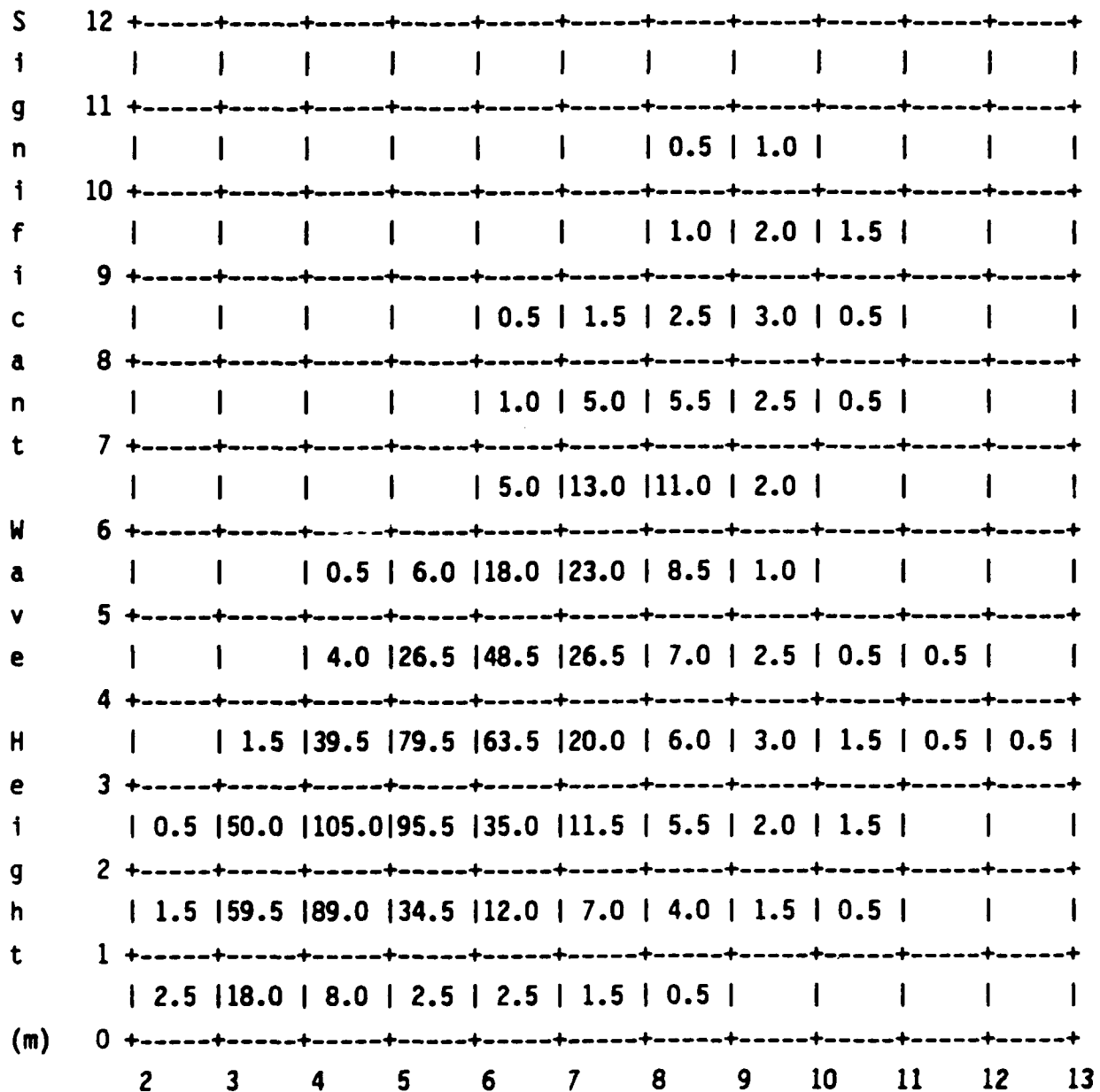
Wave scatter diagrams show the occurrences of combinations of significant wave height and average zero-upcrossing period over an extended time period such as many years.

Wave height distribution over time can be obtained by actual wave measurements. The heights and periods of all waves in a given direction are observed for short periods of time at regular intervals. A short time interval of several hours may be considered constant. For this sea state, defined as "stationary", the mean zero up-crossing period, T_z , and the significant wave height, H_s , are calculated. The H_s and T_z pairs are ordered and their probabilities of occurrence written in a matrix form, called a wave scatter diagram.

Sometimes wave scatter diagrams are available for the sea and for the swell. The sea scatter diagram includes the sea spectra generated locally. The swell scatter diagram contains the swell spectra (or regular waves) generated far from the area, days before. Due to greater energy losses in high frequency waves and the continual phase shifting caused by viscosity, the energy in irregular seas tends to shift toward longer periods, and the spectra becomes more peaked as time passes. The energy in the swell is concentrated about a single long period/low frequency, and often the swell is treated as a single regular wave.

A typical wave scatter diagram, presenting statistical data on the occurrence of significant wave height and zero up-crossing period per wave direction is shown on Figure A-2.

Sample Wave Scatter Diagram



Zero Up-crossing Period, T_z (sec)

Sum of Occurances 999.5

Figure A-2 A Typical Wave Scatter Diagram for the Central North Sea

Using the significant wave height and zero up-crossing period from the wave scatter diagram and selecting a representative sea spectrum formulation, the energy of each sea state can be reconstructed.

A.6 WAVE EXCEEDANCE CURVE

A wave exceedance curve shows the number (percentage) of waves that are greater than a given wave height for consistent wave height intervals. Table A-1 shows the type of data contained on a wave exceedance curve.

Wave Height (ft)	Number of Waves (N)
0	35,351,396
5	3,723,300
10	393,887
15	41,874
20	4,471
25	480
30	51
35	5
40	1

Table A-1 Wave Exceedance Data for Campos Basin
(Number of Waves from Northeast)

This data can be plotted on semi-log paper and closely approximated by a straight line plot. Typically, a wave exceedance H-N curve can be defined with the following equation.

$$H = H_m + m_z * \log N_h$$

where

H_m is the maximum wave height for the design life,

m_z is the slope of the H-log N curve, $-H_m/\log N_h$.

N_m is the total number of waves in the design life, and

N_h is the number of occurrences of waves with height exceeding H .

A.7 WAVE HISTOGRAM AND THE RAYLEIGH DISTRIBUTION

Actual wave height measurements can be plotted to show the number of waves of a given height at equal wave height intervals. The histogram obtained can be defined by a simple curve.

A simple curve that fits most wave histograms is the Rayleigh distribution. Past work have shown that the Rayleigh distribution often allows accurate description of observed wave height distributions over a short term.

The Rayleigh distribution is typically given as,

$$P(H_i) = 2 * H_i * \text{EXP}(-H_i^2/\underline{H}^2) * (1/\underline{H}^2)$$

where

$P(H_i)$ is the wave height percentage of occurrences,

H_i is the wave heights at constant increments,

\underline{H}^2 is the average of all wave heights squared.

A.8 EXTREME VALUES AND THE WEIBULL DISTRIBUTION

For design purposes an estimate of the maximum wave height (extreme value) is required. The Rayleigh distribution provides such an estimate over a short duration. However, in order to estimate the extreme wave that may occur in say 100 years, the Weibull distribution is often used.

The equation for the Weibull distribution is as follows.

$$P(H) = 1 - \text{EXP} [- ((H-\epsilon)/\theta)^\alpha]$$

where

$P(H)$ is the cumulative probability,

H is the extreme height,

ϵ is the location parameter that locates one end of the density function,

θ is the scale parameter, and

α is the shape parameter.

By plotting the wave exceedance data on Weibull graph paper, the distribution can be fit with a straight line and the extreme value for any cumulative probability can be found by extrapolation.

A.9 WIND ENVIRONMENT

The wind environment, source of most ocean waves, is random in nature. The wind speed, its profile and its directionality are therefore best described by probabilistic methods.

A.9.1 Air Turbulence, Surface Roughness and Wind Profile

Air turbulence and wind speed characteristics are primarily influenced by the stability of the air layer and terrain. For extreme wind gusts the influence of stability is small, making

turbulence largely a function of terrain roughness. In an ocean environment, the wave profile makes prediction of wind characteristics more difficult. As the wind speed increases, the wave height also increases, thereby increasing the surface roughness. A surface roughness parameter is used as a measure of the retarding effect of water surface on the wind speed.

A simple relationship developed by Charnock (Reference A.9) is often used to define the surface roughness parameter and the frictional velocity in terms of mean wind speed. Further discussion on surface roughness parameter and drag factor is presented in an ESDU document (Reference A.10).

Full scale experiments carried out by Bell and Shears (Reference A.11) may indicate that although turbulence will decay with the distance above sea surface, it may be reasonably constant to heights that are applicable for offshore structures.

Considering that wind flow characteristics are primarily influenced by energy loss due to surface friction, the mean wind profile for an ocean environment may be assumed to be similar to that on land and to follow this power law:

$$V_{mz} = V_{mz1} (z/z_1)^{\alpha}$$

where:

V_{mz} = mean wind velocity at height z above LAT

V_{mz1} = mean wind velocity of reference height above LAT

z = height at point under consideration above LAT

z_1 = reference height, 30 ft (10 M), above LAT
(typical)

α = height exponent, typically 0.13 to 0.15.

A.9.2 Applied, Mean and Cyclic Velocities

The random wind velocity at height z can be thought of as a combination of time-averaged mean velocity, V_{mz} , and a time varying cyclic component, $v_z(t)$.

$$V_z(t) = V_{mz} + v_z(t)$$

A range of mean and associated cyclic wind speeds can be extracted from an anemogram and divided into one- to four-hour groups over which the cyclic component of the wind speed is approximately equal. By describing cyclic wind speeds associated with an average value of the mean component of the wind speed over a particular period of time, a number of pairs of mean and associated cyclic speeds can be obtained. In addition to the applied, mean and cyclic wind speeds shown on Table A-2, their probability of occurrence is necessary to generate a scatter diagram. If sufficient data are not available, the number of occurrences can be extrapolated based on similar data. Table A-2 is given only to illustrate the wind make-up and the uncertainties associated with wind data.

Applied Wind Speed Vz(t) ft/s (m/s)	Mean Wind Speed Vmz ft/s (m/s)	Cyclic Wind Speed vz(t) ft/s (m/s)	Probability of Occurrence %
-----	-----	-----	-----
4.26 (13)	29.5 (9)	13.1 (4)	16.7
78.7 (24)	62.3 (19)	16.4 (5)	45.8
101.7 (31)	78.7 (24)	23.0 (7)	12.5
134.5 (41)	101.7 (31)	32.8 (10)	16.7
154.0 (50)	124.6 (38)	39.4 (12)	4.2
180.4 (55)	131.2 (40)	49.2 (15)	4.2

Table A-2 Applied, Mean and Cyclic Wind Speed Distribution for an Extreme Gust Environment

A.9.3 Gust Spectra

The power spectral density function provides information on the energy content of fluctuating wind flow at each frequency component. A study of 90 strong winds over terrains of different roughness in the United States, Canada, Great Britain, and Australia at heights ranging from 25 feet (8m) to 500 feet (150m) allowed Davenport (Reference A.12) to propose a power density spectrum of along-wind gust (the longitudinal component of gust velocity).

A modified version of the Davenport spectrum, due to Harris (Reference ??), is given by:

$$\frac{nS(n)}{k V_m^2} = \frac{4f}{(2 + f^2)^{5/6}}$$

where:

n	=	fluctuating frequency 2
$S(n)$	=	power density [(m/sec)/Hz]
k	=	surface roughness drag factor corresponding to the mean velocity at 30 ft (10m) (i.e. 0.0015)
V	=	mean hourly wind speed at 30 ft (10m) m
f	=	non-dimensional frequency (nL/V) m
L	=	length scale of turbulence (1200 to 1800m, typical)

The Harris spectra may be used to develop the wind spectra for each one of the mean wind speeds associated with the scatter diagram.

A.10**REFERENCES**

- A.1 **Mechanics of Wave Forces on Offshore Structures, Sarpkaya, T. and Isaacson, M., Van Nostrand Reinhold Company, 1981.**

- A.2 **Bretschneider, C.L., "Wave Variability and Wave Spectra for Wind-Generated Gravity Waves," Beach Erosion Board, Corps of Engineers, Technical Memo No. 118, 1959, pp. 146- 180.**

- A.3 **Report of Committee 1, "Environmental Conditions," Proceedings Second International Ship Structures Congress, Delft, Netherlands, July 1964, Vol. 1, pp. 1:5-1:13.**

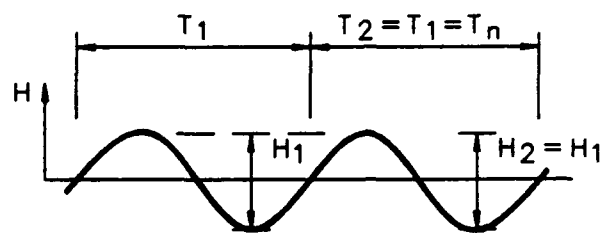
- A.4 **Pierson, W.J. and Moskowitz, L., "A Proposed Spectral Form for Fully Developed Wind Seas Based on the Similarity Theory of S.A. Kitaigorodsky," Journal of Geophysical Research, Vol. 69, No. 24, Dec 1964.**

- A.5 **Rye, H., Byrd, R., and Torum, A., "Sharply Peaked Wave Energy Spectra in the North Sea," Offshore Technology Conference, 1974, No. OTC 2107, pp. 739-744.**

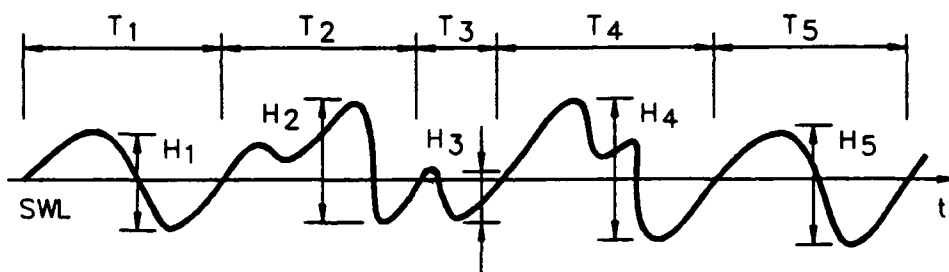
- A.6 **Scott, J.R., "A Sea Spectrum for Model Tests and Long-Term Ship Prediction," Journal of Ship Research, Vol. 9, No. 3, Dec. 1965, pp. 145-152.**

- A.7 **Darbyshire, J., "The One-Dimensional Wave Spectrum in the Atlantic Ocean and in Coastal Waters," Proceedings of Conference on Ocean Wave Spectra, 1961, pp. 27-39.**

- A.8 **Wiegel, R.L., "Design of Offshore Structures Using Wave Spectra," Proceedings Oceanology International, Brighton, England, 1975, pp. 233-243.**



REGULAR WAVES



IRREGULAR WAVES

Figure A-1 Regular and Irregular Waves

APPENDIX B

REVIEW OF LINEAR SYSTEM RESPONSE TO RANDOM EXCITATION

CONTENTS

B. REVIEW OF LINEAR SYSTEM RESPONSE TO RANDOM EXCITATION

B.1 GENERAL

- B.1.1 Introduction
- B.1.2 Abstract
- B.1.3 Purpose

B.2 RESPONSE TO RANDOM WAVES

- B.2.1 Spectrum Analysis Procedure
- B.2.2 Transfer Function
 - B.2.2.1 Equations of Motions
 - B.2.2.2 Response Amplitude Operator
- B.2.3 Wave Spectra
 - B.2.3.1 Wave Slope Spectra
 - B.2.3.2 Wave Spectra for Moving Vessels
 - B.2.3.3 Short-Crested Seas
- B.2.4 Force Spectrum
- B.2.5 White Noise Spectrum

B.3 EXTREME RESPONSE

- B.3.1 Maximum Wave Height Method
- B.3.2 Wave Spectrum Method

B.4 OPERATIONAL RESPONSE

- B.4.1 Special Family Method
- B.4.2 Wave Spectrum Method

B. REVIEW OF LINEAR SYSTEM RESPONSE TO RANDOM EXCITATION

B.1 GENERAL

B.1.1 Introduction

Spectral analysis is used to determine the response of linear systems to random excitation. In the case of offshore structures, the random excitation comes from either irregular waves or winds. Typical offshore systems subjected to spectral analysis include ships, semisubmersibles, jack-ups, tension-leg platforms and bottom-supported fixed platforms. Responses of interest include motions, accelerations, and member internal forces, moments, and stresses.

Floating units are evaluated by spectral analysis for motions in random seas. The strength and structural fatigue integrity are often assessed with spectral analysis.

B.1.2 Abstract

A spectral analysis combines a set of regular wave response amplitude operators, RAOs, with a sea spectrum to produce a response spectrum. Characteristics of the response may be calculated from the response spectrum, and a random sea transfer function can be derived.

For certain spectral analyses, the sea spectrum must be modified to produce a wave slope spectrum or to adjust the sea spectrum for vessel speed. A spreading function can be applied to the sea spectrum to model a short-crested random sea.

A wave force spectrum can be created directly from force RAOs and the sea spectrum.

A regular wave transfer function is found as the solution to the equations of motion. The regular wave transfer function can be expressed in terms of RAO and a phase angle.

A white noise function may be used to represent a very broad banded input spectrum, if the response spectrum is narrow banded.

The extreme response can be calculated from a given extreme wave, or the extreme response may be statistically derived from a set of spectral analyses.

The sea spectra used in the computation of random sea response can be reduced in number by selecting a smaller family of representative spectra, or by creating a set of mean spectra.

B.1.3 Purpose

The purpose of this appendix is to provide a background of the spectral analysis method and to clarify the concept of a response spectrum and how its properties are derived.

B.2 RESPONSE TO RANDOM WAVES

The spectral analysis method is a means of taking the known response of an offshore structure to regular waves and determining the structure's response to a random sea. The input to the spectral analysis method is the response amplitude per unit wave amplitude (or equally, the response double amplitude per unit wave height) for a range of periods or frequencies of regular waves. These ratios of response amplitude to wave amplitude are known as "Response Amplitude Operators" or just "RAOs." The response of the offshore structure is first obtained for a set of unit amplitude, regular, sinusoidal waves. The regular wave response may be obtained either from model tests or from empirical or theoretical analyses.

A wave energy spectrum is selected to represent the random sea. Wave spectra are described in Appendix A. The wave spectrum represents the distribution of the random sea's energy among an infinite set of regular waves that when added together create the random character of

the sea. By assuming that the response is linear, the response of the offshore structure to a regular wave is equal to the RAO times the regular wave amplitude. By assuming that the response to one wave does not affect the response to another wave, the response of the offshore structure to a random sea is the sum of its responses to each of the constituent regular waves in the random sea. The response is therefore a collection of responses each with a different amplitude, frequency, and phase.

The energy of each constituent wave is proportional to the wave amplitude squared. The energy of the response to a constituent wave of the random sea is proportional to the response squared, or is proportional to the RAO squared times the wave amplitude squared. The response energy may also be represented by a spectrum from which characteristics of the response may be derived. From the response spectrum characteristics and the wave spectrum characteristics, a "transfer function" can be obtained which relates the response and wave characteristics.

8.2.1 Spectrum Analysis Procedure

The spectral analysis procedure involves four steps: 1) obtaining the response amplitude operators, 2) multiplying the wave spectrum ordinates by the RAOs squared to get the response spectrum, 3) calculating the response spectrum characteristics, and 4) using the response spectrum characteristics to compute the random sea response transfer function.

The RAOs are usually calculated for a discrete set of wave frequencies, and the discrete RAOs are then fit with a curve to produce a continuous function. The singular term "RAO" is used both to signify a single response amplitude to wave amplitude ratio and to signify the continuous function through all of the RAOs. Any response that is linearly related (proportional) to wave amplitude may be reduced to an RAO function. Typical responses are motions, accelerations, bending moments, shears, stresses, etc.

Multiplication of the wave spectrum ordinates by the RAO squared is simple. The two underlying assumptions are that the response varies linearly with wave amplitude and the assumption that the response to a wave of one frequency is independent of the response to waves of other frequencies.

Response spectrum characteristics are taken from the shape of the spectrum or are calculated from the area under the response spectrum and the area moments of the response spectrum. Typical characteristics are significant response amplitude, maximum response amplitude, mean period of the response, and peak period of the response spectrum.

The random sea transfer function is the ratio of a response spectrum characteristic to a wave spectrum characteristic. A random sea transfer function is usually presented as a function of the random sea characteristic period. A typical transfer function might be the ratio of maximum bending moment amplitude per unit significant wave height. The transfer function is useful for estimating the response to another wave spectrum with similar form but different amplitude.

B.2.2 Transfer Function

A transfer function converts input to output for linear systems. A transfer function is graphically represented in Figure 8-1. A transfer function can relate motion response to the height of incident waves directly, or a transfer function can relate motion response to wave force, or a transfer function can relate member stresses to wave or wind force.

For typical applications to the design of offshore structures, the input energy forms are waves, current and wind. The desired output forms are static displacements, dynamic displacements, and member stresses.

B.2.2.1 Equation of Motions

By assuming that the motions are small enough that the inertial, damping and spring forces can be summed linearly, the equation of motion can be formulated.

$$M\ddot{X} + D\dot{X} + KX = F(x,t)$$

where M is the mass matrix which includes the structure mass properties plus the hydrodynamic added mass effects,

D is the linearized damping matrix which includes the viscous damping, the wave damping, and the structural damping effects,

K is the stiffness matrix which includes the waterplane spring properties, the restoring properties of moorings or tendons, and the stiffness properties of the structure and any foundation,

X is the system displacement vector,

\dot{X} is the system velocity vector = (dx/dt) ,

\ddot{X} is the system acceleration vector, = (d^2x/dt^2) , and

F is the force vector which may be calculated from empirical methods such as Morrison's equation or from diffraction theory methods.

The equations of motion can be solved with frequency domain or time domain techniques. The frequency domain solution involves the methods of harmonic analysis or the methods of Laplace and Fourier transforms. The time domain solution involves the numerical solution by a time step simulation of the motion.

B.2.2.2 Response Amplitude Operator

The solution of the equations of motion result in a transfer function. The motion transfer function has an in-phase component and an out-of-phase component. The transfer function is usually represented in complex form,

$$X(\omega) = A[XI(\omega) + iXO(\omega)]$$

or in angular form,

$$X(\omega) = A[XI \cos(\omega t) + XO \sin(\omega t)]$$

where

X is the total response,

A is the wave height,

XI is the in-phase component of the response for unit wave height, and

XO is the out-of-phase component of the response for unit wave height.

From this equation, the response amplitude operator (amplitude per unit wave height), is found to be,

$$RAO = \text{SQRT} (XI^2 + XO^2),$$

and the phase of the harmonic response relative to the wave is,

$$\phi = \text{ATAN} (XO/XI).$$

The response can be written in terms of the RAO and phase as,

$$X(\omega) = A \cdot \text{RAO}(\omega) \cdot \cos(\omega t + \phi(\omega)).$$

When a spectral analysis is applied to the transfer function the wave amplitudes, A, become a function of wave frequency, ω , and the $X(\omega)$ is replaced by the differential slice of the response power density spectrum.

$$S_R(\omega) \cdot d\omega = [A(\omega) \cdot \text{RAO}(\omega)]^2$$

or

$$S_R(\omega) \cdot d\omega = A^2(\omega) \cdot \text{RAO}^2(\omega)$$

or

$$S_R(\omega) \cdot d\omega = S(\omega) \cdot d\omega \cdot \text{RAO}^2(\omega)$$

$$\text{Thus, } S_f(\omega) = S(\omega) \cdot \text{RAO}^2(\omega)$$

The response spectrum $S(\omega)$ is therefore just the sea spectrum times the RAO squared.

For multiple-degree-of-freedom systems, there is coupling between some of the motions, such as pitch and heave. For example, to obtain the motion or motion RAO for heave of a point distant from the center of pitch rotation, the pitch times rotation arm must be added to the structure heave. This addition must be added with proper consideration of the relative phase angles of the pitch and heave motions, and therefore, such addition must be performed at the regular wave analysis stage. The combined heave (w/pitch) RAO can then be used in a spectral analysis to obtain the heave spectrum and heave response characteristics at the point.

B.2.3 Wave Spectra

The wave spectrum used in the spectral analysis may be an idealized mathematical spectrum or a set of data points derived from the measurement of real waves. When a set of data points are used, a linear or higher order curve fit is employed to create a continuous function. Custom wave spectra for specific regions are often provided as one of the conventional idealized spectra with parameter values selected to match a set of measured wave data. For areas where there is little wave data, wave height characteristics are estimated from wind speed records from the general area.

B.2.3.1 Wave Slope Spectra

For certain responses, particularly the angular motions of pitch and roll, the RAO is often presented as response angle per unit wave slope angle. For these cases the wave spectrum in amplitude squared must be converted to a wave slope spectrum. The maximum slope of any constituent wave of the spectrum is assumed to be small enough that the wave slope angle in radians is approximately equal to the tangent of the wave slope. The water depth is assumed to be deep enough (at least one-half the longest wave length) that the wave length is approximately equal to:

$$(g/2\pi)*T^2 \text{ or } 2\pi g/\omega^2.$$

By using the Fourier series representation of the wave spectrum, selecting one constituent wave, and expressing the wave equation in spatial terms instead of temporal terms, the wave slope is derived as follows.

$$\eta = a*\cos(2\pi x/L) = a*\cos(x\omega^2/g)$$

$$d\eta/dx = -(a\omega^2/g)*\sin(x\omega^2/g)$$

$$[dn/dx]_{\max} = a\omega^2/g$$

Squaring the equation to get the slope squared,

$$[dn/dx]^2 = a^2(\omega^4/g^2)$$

Therefore, the wave spectrum equation must be multiplied by (ω^4/g^2) to obtain the slope spectrum. The wave slope angle spectrum is the wave slope spectrum converted to degrees squared, i.e., multiplied by $(180/\pi)^2$.

8.2.3.2 Wave Spectra for Moving Vessels

For self-propelled vessels or structures under tow, the forward speed of the vessel or structure will have an effect upon the apparent frequency of the waves. The apparent frequency of the waves is usually referred to as the encounter frequency. For a vessel heading into the waves the encounter frequency is higher than the wave frequency seen by a stationary structure. For a vessel moving in the same direction as the waves, the encounter frequency is less than the wave frequency seen by a fixed structure, and if the vessel's speed is great enough it may be overrunning some of the shorter waves which will give the appearance that these shorter waves are coming from ahead instead of from behind.

The encounter frequency for a regular wave is given by the following relationship.

$$\omega_e = \omega + V\omega^2/g$$

where ω is the wave frequency in radians per second as seen from a stationary observer,

V is the velocity component parallel to and opposite in direction to the wave direction, and

g is the acceleration of gravity in units compatible with the velocity units.

The energy of, or area under the curve of the sea spectrum must remain constant.

$$\int S_e(\omega_e) * d\omega_e = \int S(\omega) * d\omega$$

Taking the derivative of the encounter frequency equation gives the following.

$$d\omega_e = [1 + 2V\omega/g] * d\omega$$

Substituting the derivative into the area integral gives the following.

$$\int S_e(\omega_e) * [1 + 2V\omega/g] * d\omega = \int S(\omega) * d\omega$$

Therefore, equating the integrands gives the relationship between the encounter spectrum and the stationary sea spectrum.

$$S_e(\omega_e) = S(\omega) / [1 + 2V\omega/g]$$

This equation is required to transform a stationary sea spectrum to an encounter spectrum for the purpose of integrating the responses.

$$m_0 = \int r_e^2 * S_e * d\omega_e$$

However, if only the response statistics are desired, and not the actual response spectrum, then the same substitutions as above can be made.

$$S_e = S / [1 + 2V\omega/g]$$

$$d\omega_e = [1 + 2V\omega /g] * d\omega$$

$$\int r_e^2 S_e d\omega_e = \int r_e^2 S d\omega$$

Therefore, the encounter frequency need only be used to select the response amplitude operator and the integration is still over the stationary frequency, ω .

$$\text{i.e., } r_e = r(\omega_e) = r(\omega + V\omega^2/g)$$

B.2.3.3 Short-Crested Seas

The usual mathematical representation of a sea spectrum is one-dimensional with the random waves traveling in a single direction with the crests and troughs of the waves extending to infinity on either side of the direction of wave travel. A one-dimensional irregular sea is also referred to as a long-crested irregular sea. In the real ocean the waves tend to be short-crested due to the interaction of waves from different directions.

A two-dimensional spectrum (short-crested sea) is created from a standard one-dimensional mathematical spectrum by multiplying the spectrum by a "spreading function." The most commonly used spreading function is the "cosine-squared" function.

$$f(\psi) = (2/\pi) \cos^2 \psi$$

where ψ is the angle away from the general wave heading,
 $(-\pi/2 < \psi < \pi/2)$

The cosine-squared spreading function spreads the sea spectrum over an angle ± 90 degrees from the general wave heading.

To incorporate multi-directional or short-crested irregular seas into a spectral analysis, the RAOs for a range of wave headings must be obtained. A spectral analysis is performed for each heading using the one-dimensional sea spectrum. The results of the one-dimensional analyses are then multiplied by integration factors and summed.

The following is a sample of a set of heading angles and the integration factors for a cosine squared spreading function.

<u>ψ</u>	<u>Factor</u>
0°	0.2200
±20°	0.1945
±40°	0.1300
±60°	0.0567
±80°	0.0088

B.2.4 Force Spectrum

For simple single-degree-of-freedom systems, a force spectrum can be generated directly from the calculated or measured regular wave forces.

The force on the structure is calculated by empirical or theoretical methods, or is derived by analyzing measured strain records from tests on the structure or on a model of the structure. This force is the right hand side of the equation of motion as described in Section B.2.2.1.

The force itself has an in-phase and an out-of-phase component relative to the regular wave which generates the force. The force can be written in complex form,

$$F(\omega) = A*[FI(\omega) + i*FO(\omega)]$$

or in force RAO and phase form,

$$F(\omega) = A*RAO_f(\omega)*\cos(\omega t + \phi(\omega))$$

where $RAO_f = \text{SQRT}(FI^2 + FO^2)$, and

$$\phi = \text{ATAN}(FO/FI).$$

The force spectrum can be created by multiplying a selected wave spectrum times the force RAO squared.

$$S_f(\omega) = S(\omega) * RAO_f^2(\omega)$$

B.2.5 White Noise Spectrum

Most sea spectra have a well defined peak of energy and the energy trails off to near zero away from the peak. Other environmental inputs that are described by spectra, such as wind force, may not have a definite peak and may even appear constant over a wide range (broad band) of frequencies.

Often the response RAO is narrow banded, that is, the structure tends to respond at a narrow range of frequencies, centered about a resonant frequency. When the combination of a broad banded excitation spectrum and a narrow banded RAO exist, the spectral analysis can be greatly simplified.

A broad banded spectrum can be approximated by a "white noise spectrum" which has constant energy over the whole frequency range of the spectrum.

For a single degree of freedom system, the response can be defined in terms of a "dynamic amplification function" times an expected static displacement. The dynamic amplification function is as follows,

$$|H(\omega)| = 1 / [(1 - \omega/\omega_n)^2]^2 + (2\xi\omega/\omega_n)^2]^{1/2}$$

where

ω is radial frequency,

ω_n is the undamped "natural frequency",

$$\omega_n = (k/m)^{1/2},$$

ξ is the damping ratio, the ratio of the actual damping to the critical damping. $\xi = c/(4km)^{1/2}$,

k is the spring constant,

m is the mass that is in motion, and

c is the actual damping.

The expected static displacement is simply force divided by the spring constant, or the expected static displacement spectrum is as follows,

$$S_{\delta}(\omega) = S_f(\omega)/k^2$$

From these equations, the response spectrum is found to be,

$$R(\omega) = (1/k^2) * |H(\omega)|^2 * S_f(\omega),$$

and the mean squared response is,

$$\overline{y^2(t)} = \int_0^{\infty} (1/k)^2 * |H(\omega)|^2 * S_f(\omega) * d\omega.$$

The $(1/k)^2$ is constant, and by approximating the force spectrum by a white noise spectrum with magnitude $S_f(\omega_n)$, the mean squared response is simplified to,

$$\overline{y^2(t)} = (S_f(\omega_n)/k^2) * \int_0^{\infty} |H(\omega)|^2 * d\omega.$$

For lightly damped systems, ($\xi \ll 1$), the integral may be evaluated to yield,

$$\overline{y^2(t)} = [\pi * \omega_n * S_f(\omega_n)] / (2 * \xi * k^2)$$

B.3 EXTREME RESPONSE

The extreme response of an offshore structure may be determined in two ways. An extreme environmental event may be selected, and the responses to the extreme event then calculated. A set of environmental spectra can be selected; the response spectra to each environmental spectra calculated; and the extreme responses derived by statistical analysis of the response spectra. The first method is often called a "deterministic" method, and the second method is referred to as a "probabilistic" method. In actual design practice the two methods are often intermixed or combined in order to confirm that the extreme response has been found.

B.3.1 Maximum Wave Height Method

In deterministic design, a set of extreme conditions is supplied by oceanographers or meteorologists. The extreme conditions are of course derived from statistical analyses of wave and weather records, but the design engineer is usually not involved in that stage of the calculations.

The given extreme conditions are applied to the offshore structure to determine the various responses. Unfortunately, the given extreme conditions may not always produce the extreme responses. For example, the prying and racking loads governing the design of many structural members of semisubmersibles are typically maximized in waves with lower heights and shorter lengths than the maximum height wave. Tendon loads on tension leg platforms (TLPs) are also often maximized in waves that are lower and shorter than the maximum wave.

Since the oceanographer or meteorologist who produced the set of extreme conditions does not have information about the characteristics of the offshore structure, he/she is unable to select an extreme or near extreme condition that will produce the greatest response. Conversely, the design engineer usually has little or no information about the wave and weather data that was used to derive

the set of extreme conditions, and thus, he/she is unable to create alternate conditions to check for greater response.

The design engineer may request a range of extreme conditions, such as: the maximum height wave with a period of 9 sec, the maximum height wave with a period of 10 sec, etc. The increased number of conditions increases the number of analyses required, but allows the design engineer to confirm which conditions produce the extreme responses.

The maximum wave height method is best used when the response is highly nonlinear and the spectral analysis method is therefore not appropriate.

B.3.2 Wave Spectrum Method

A full probabilistic analysis involves calculating responses to the entire suite of possible environmental conditions. Statistical analysis of these responses is then performed in order to predict a suitable extreme for each response. This requires far fewer assumptions on the part of those who supply environmental criteria, but a much more extensive set of environmental data.

With the wave spectrum method, a set of wave spectra are provided by oceanographers or meteorologists. The RAOs for the response of interest are squared and multiplied by the wave spectrum. A wave spectrum is assumed to represent a Gaussian random distribution. Since the response spectrum is created by a linear multiplication, the response spectrum also represents a Gaussian random distribution. The significant response, maximum response, etc. can be calculated using the equations for calculating the significant, maximum, etc. wave heights.

The equations for maximum wave height are summarized here in terms of response:

Significant response, (DA):

$$R_s = 4.00 \cdot (m_0)^{1/2}$$

Maximum response in 1000 cycles, (DA):

$$R_{1/1000} = 7.43 \cdot (m_0)^{1/2} = 1.86 \cdot R_s$$

Maximum response is t hours, (DA):

$$R_{\max} = 2 \cdot [2 \cdot m_0 \cdot \ln(3600 \cdot t / T_z)]^{1/2}$$

where m_0 is the area under the response spectrum,

T_z is the zero-up-crossing period of the response as found from the equation,

$$T_z = 2\pi \cdot (m_0 / m_2)^{1/2}, \text{ and}$$

m_2 is the second radial frequency moment of the response spectrum.

B.4 OPERATIONAL RESPONSE

In order to determine the normal day-to-day motions and stresses to assess motion related downtime and fatigue damage, the distribution of wave heights versus wave periods are considered. A wave scatter diagram condenses and summarizes wave height and wave period statistics. It is a two-parameter probability density function. Typically a wave scatter diagram is presented as a grid of boxes, with one axis of the grid being average zero-up-crossing periods and the other axis being significant wave heights. Within the boxes of the wave scatter diagram are numbers which represent the percentage of the sea records having the corresponding characteristics of H_s and T_z see Figure A-2.

A response scatter diagram could be generated by taking the wave spectrum for each sample used to create the wave scatter diagram and performing a spectral analysis for the response. The computed characteristics are then used to assign the percentage of occurrence to the appropriate box in the response scatter diagram. This entails considerable work and can be simplified by reducing the number of sea spectra considered, as described below.

B.4.1 Special Family Method

All of the original sea spectra used to define the wave scatter diagram must be available, in order to select a special family of sea spectra to represent the whole population.

The sea spectra are first grouped by wave height bands, such as 0 to 2 ft significant wave height, 2 ft to 4 ft H_s , etc. The average properties of the spectra within a group are computed. Within each group, which may contain thousands of sample sea spectra, a small set of sea spectra are selected to represent all of the spectra in the group. The small set will typically contain 4 to 10 spectra.

The spectra of a representative set are selected by a Monte Carlo (Shotgun) process which randomly picks, say 8, spectra from the group. The mean spectrum and the standard deviation of the spectral ordinates about the mean spectrum are computed for the 8 spectra. A weighted sum of differences in properties between the 8 spectra and the total population of the group represent the "goodness of fit" of that set of 8 spectra.

A second representative set of 8 spectra is then selected from the group, and the "goodness of fit" of the second set is computed. The better set (first or second) is retained and compared to a third sample of 8, etc. The process is repeated many times, say 1000, within each wave group.

From this process, the original number of sea spectra, which may have been thousands, is reduced to the number of wave height bands times the number of spectra in each representative set.

B.4.2 Wave Spectrum Method

A reduced set of sea spectra can be generated to represent the variation of H_s and T_z as given in a wave scatter diagram.

If the original sea spectra are not available, a set of sea spectra can be created directly from the wave scatter diagram. In this case the shape of the spectrum must be assumed. For various areas of the world's oceans, preferred mathematical spectrum equations exist. For the North Sea, the mean JONSWAP spectrum is preferred. For open ocean, the Bretschneider (ISSC) spectrum is preferred. For the Gulf of Mexico, the Scott spectrum has been recommended.

Using the H_s and T_z for each populated box in the wave scatter diagram, and the selected sea spectrum equation, a set of wave spectra are defined. With this method the number of sea spectra is reduced to the number of populated boxes in the wave scatter diagram, but no more than the number of wave height bands times the number of wave period band.

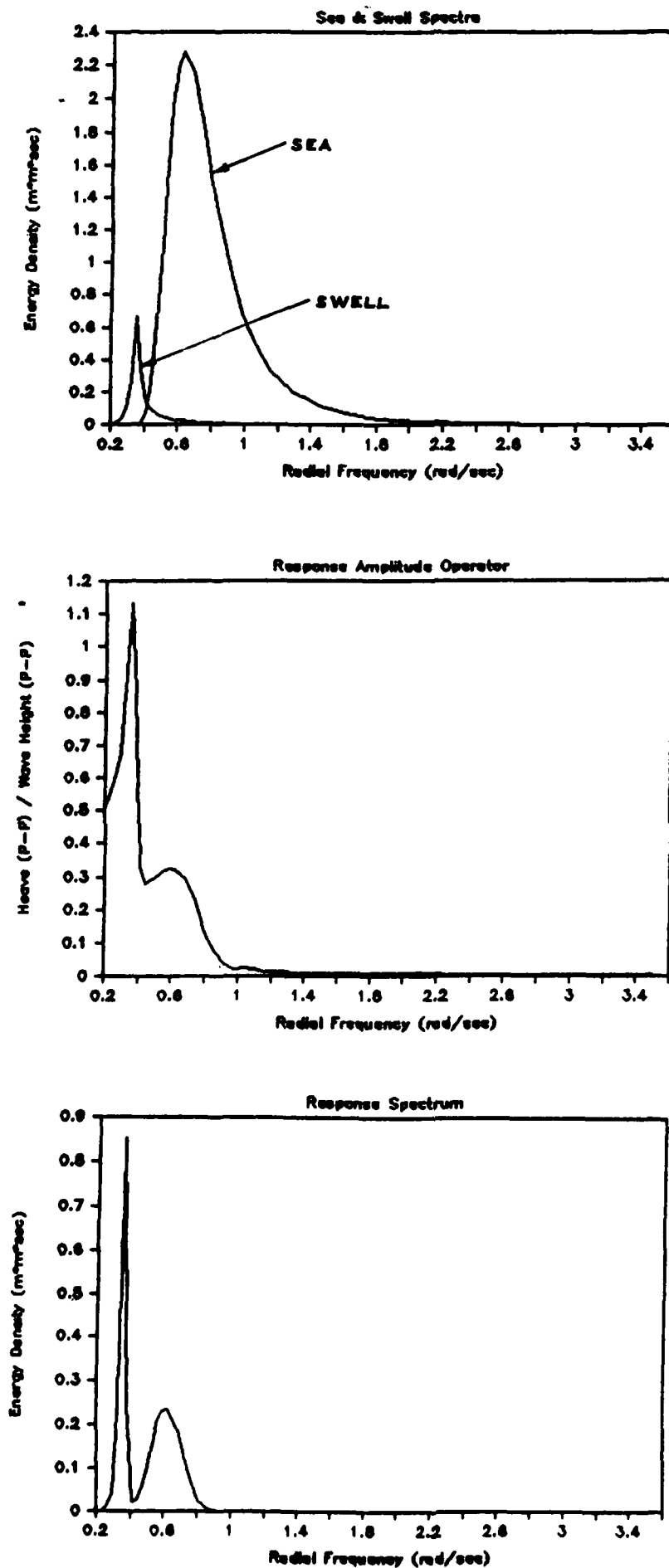


**Figure B-1 Sea Spectra, Response Amplitude Operator (RAO)
and Response Spectrum**

APPENDIX C

STRESS CONCENTRATION FACTORS

CONTENTS

- C. STRESS CONCENTRATION FACTORS**
- C.1 OVERVIEW**
 - C.1.1 Objectives and Scope**
 - C.1.2 Current Technology**
- C.2 STRESS CONCENTRATION FACTOR EQUATIONS**
 - C.2.1 Kuang with Marshall Reduction**
 - C.2.2 Smedley-Wordsworth**
- C.3 PARAMETRIC STUDY RESULTS**
 - C.3.1 Figures**
 - C.3.2 Tables**
- C.4 FINITE ELEMENT ANALYSES RESULTS**
 - C.4.1 Column-Girder Connection**
- C.5 REFERENCES**

C. STRESS CONCENTRATION FACTORS

C.1 OVERVIEW

C.1.1 Objectives and Scope

A comprehensive document on stress Concentration factors (SCF) would include assessment of test results, detailed review of empirical equations, evaluation of finite element studies, and presentation of parametric studies showing the sensitivities of parameters affecting SCFs.

The objective of this appendix is limited. Following a brief discussion of empirical equations, parametric study results are presented to assist the engineer in avoiding undesirable joint details. The sensitivity and interaction of variables shown in tables and figures also allow quick assessment of steps necessary to improve other geometries.

Empirical formulations are applicable to a limited range of simple joint geometries. A complex joint often requires carrying out of a finite element analyses (FEA) to determine the SCFs. The results of a FEA is also presented to illustrate the applicable SCFs for a given geometry.

C1.2 Current Technology

The SCF values can be computed through the use of a number of alternative equations. These equations have been mostly based on analytical (finite element) and small-scale experimental (acrylic model test) work. The tests carried out on joints that reflect those in-service (i.e. both in size and fabrication methods) are few and limited to several simple joint configurations. Thus, the equations available should be reviewed carefully to ascertain their range of validity and overall reliability prior to their use in design. Considering the simple joint configurations of T, Y, DT, K and X, the equations available for use in design are:

- o Kuang (Reference C.1)
- o Wordsworth (References C.2, C.3)
- o Gibstein (References C.4, C.5)
- o Efthymiou (Reference C.6)
- o Marshall (Reference C.7)
- o UEG (Reference C.8)

There are significant differences in the validity ranges of these equations. The SCFs computed based on different equations also often vary considerably. The Kuang equations are applicable to T, Y, and K joints for various load types. Wordsworth and Woodsworth/Smedley equations are applicable to all simple joints. Gibstein equations are applicable to T joints while the Efthymiou equations cover T/Y joints and simple/overlapping K/YT joints. The equations proposed by Marshall are applicable to simple joints, based on those equations by Kellogg (Reference C.9), and were incorporated into API RP 2A.

Substantial work has been carried out to validate the applicability of various SCF equations. Although some of the work carried out by major oil companies are unpublished, such work still influence ongoing analytical and experimental research. Delft von D.R.V. et al. (Reference C.10) indicate that the UEG equations offer a good combination of accuracy and conservatism while the Efthymiou (i.e., Shell-SIPM) equations show a good comparison with experimental data.

Ma and Tebbet (Reference C.11) report that there is no consensus on whether a design SCF should represent a mean, lower bound or some other level of confidence. Tebbett and Lalani's (Reference C.12) work on reliability aspects of SCF equations indicate that SCF equations underpredicting the SCF values in less than 16% of the cases can be considered reliable. Thus, when presenting the findings of 45 elastic tests carried out on 15 tubular joints representing typical construction, Ma and Tebbet report that Wordsworth, UEG and Efthymiou equations meet this criteria and offer the best reliability.

Ma and Tebbett also state that while both UEG and Wordsworth equations overpredict X joint SCFs, none of the equations overpredict the K joint SCFs. The comparative data indicate that the SCFs computed using Kuang and Gibstein equations for T/Y joints subjected to axial loading under predict the measured data in more than 16% of the cases. (See Figure C.1-1).

Tolloczko and Lalani (Reference C.13) have reviewed all available new test data and conclude that reliability trends described earlier for simple joints remain valid and also state that Efthymiou equations accurately predict the SCFs for overlapping joints.

C.2 STRESS CONCENTRATION FACTOR EQUATIONS

C.2.1 Kuang with Marshall Reduction

The Kuang stress Concentration factor equations for simple unstiffened joints are shown on the following page. The brace stress Concentration factor equations include Marshall reduction factor, Q^r . The validity ranges for the Kuang stress Concentration factor equations are:

<u>Term</u>	<u>Validity Range</u>
d/D	0.13 - 1.0
T/D	0.015 - 0.06
t/T	0.20 - 0.80
g/D	0.04 - 1.0
D/L	0.05 - 0.3
θ	25 - 90

where, D = chord diameter
T = chord thickness
d = brace diameter
t = brace thickness
g = gap between adjacent braces
L = chord length
 θ = angle between brace and chord

C.2.2 Smedley-Wordsworth

The Smedley-Wordsworth stress Concentration factor equations for simple unstiffened joints are shown on the following pages. The notes for the equations shown on the following pages include the Shell d/D limitation of 0.95. This interpretation is open to a project-by-project review.

The validity ranges for the Smedley-Wordsworth equations are:

<u>Term</u>	<u>Validity Range</u>
d/D	0.13 - 1.0
$D/2T$	12.0 - 32.0
t/T	0.25 - 1.0
g/D	0.05 - 1.0
$2L/D$	8.0 - 40
	30 - 90

where, D = chord diameter
 T = chord thickness
 d = brace diameter
 t = brace thickness
 g = gap between adjacent braces
 L = chord length
 = angle between brace and chord

C.3 PARAMETRIC STUDY RESULTS

C.3.1 Figures

The Kuang and Smedley-Wordsworth chord stress Concentration factors for T joints are shown in Section C.3.1(a) and C.3.1(b), respectively. The Kuang and Smedley-Wordsworth chord stress Concentration factors for K joints are shown in Section C.3.1(c) and C.3.1(d), respectively. The Smedley-Wordsworth chord stress Concentration factors for X joints are shown in Section C.3.1(e). Since the chord side of the weld stress Concentration factor is generally higher than the brace side of the weld stress Concentration factor, only the chord side of the weld stress Concentration factors are shown.

C.3.1(a) Kuang Chord SCF's for T-Joints

The Kuang chord SCF's for T-joints are shown on the following pages. The following parameters are assumed for the Kuang figures:

- 1) $\gamma = D/2T = 12.0$
- 2) $\theta = \quad = 30.0 \text{ degrees}$
- 3) $\alpha = D/L = 0.0571$

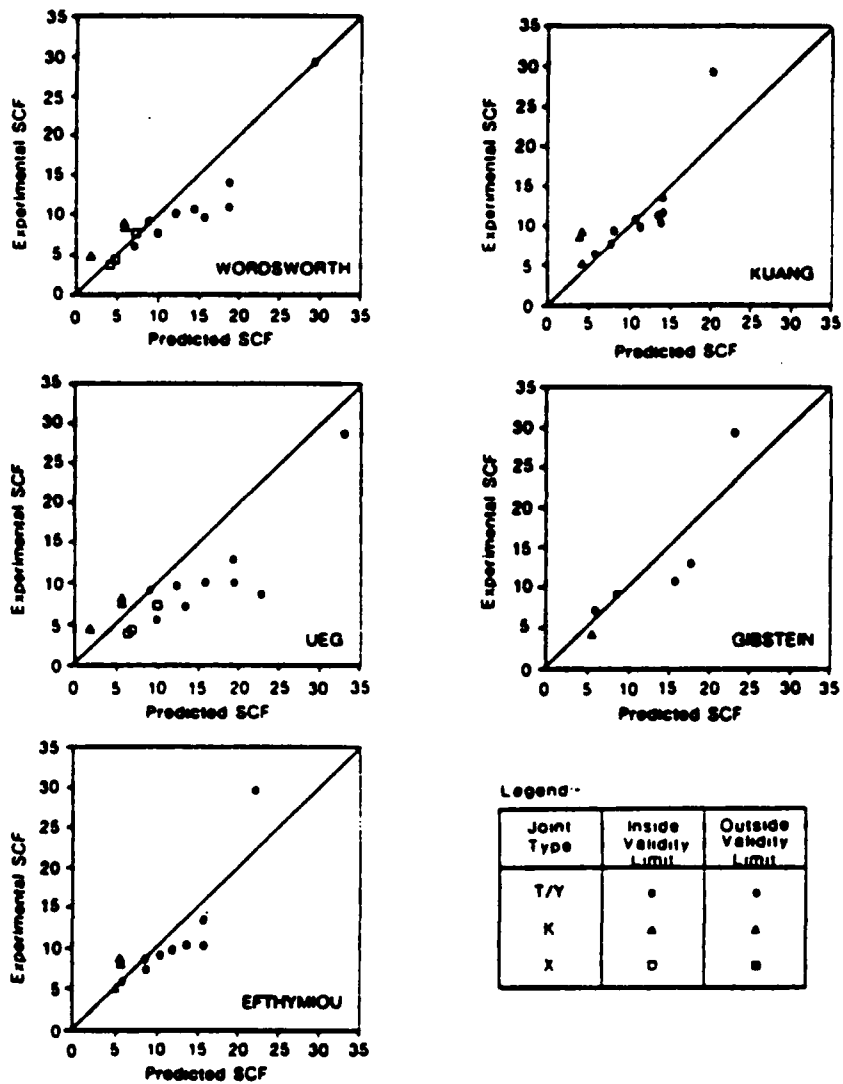


Fig. 6—Results of comparison—axial loading.

Side of Weir of Interest	Stud Type	Axial SCF	Inplane Bending SCF	Out of Plane Bending SCF
Chord	T and Y	$\frac{(1.177)(\frac{d}{b})^{1.333} (\sin \theta)^{1.694}}{(\frac{d}{b})^{.806} (\frac{d}{b})^{.057} \exp \left[(1.21)(\frac{d}{b}) \right]}$	$\frac{(1.163)(\frac{d}{b})^{.86} (\sin \theta)^{.57}}{(\frac{d}{b})^{.6} (\frac{d}{b})^{.04}}$	$\frac{(1.50)(\frac{d}{b})^{.889} (\frac{d}{b})^{.787} (\sin \theta)^{1.567}}{(\frac{d}{b})^{1.014}} \text{ for } \frac{d}{b} < .55$ $\frac{(1.229)(\frac{d}{b})^{.889} (\sin \theta)^{1.567}}{(\frac{d}{b})^{1.014} (\frac{d}{b})^{.619}} \text{ for } \frac{d}{b} > .55$
Chord	K1	$\frac{(1.949)(\frac{d}{b})^{1.104} (\frac{d}{b})^{.067} (\sin \theta)^{1.521}}{(\frac{d}{b})^{.666} (\frac{d}{b})^{.059}}$	$\frac{(11.400)(\frac{d}{b})^{.94} (\frac{d}{b})^{.06} (\sin \theta)^{.9}}{(\frac{d}{b})^{.38}}$	As for Chord Side T and Y
Chord	K2 and K3	$\frac{(11.261)(\frac{d}{b})^{1.066} (\frac{d}{b})^{.12} (\sin \theta)}{(\frac{d}{b})^{.56}}$	As for Chord Side K1	As for Chord Side T and Y
Brace	T and Y	$1.0 \cdot (Q_b) \left[\frac{(2.784)(\frac{d}{b})^{1.34} (\sin \theta)^{1.94}}{(\frac{d}{b})^{.55} (\frac{d}{b})^{.12} \exp \left[(1.35)(\frac{d}{b}) \right]} - 1.0 \right]$	$1.0 \cdot (Q_b) \left[\frac{(11.109)(\frac{d}{b})^{.38} (\sin \theta)^{.21}}{(\frac{d}{b})^{.23} (\frac{d}{b})^{.38}} - 1.0 \right]$	$1.0 \cdot (Q_b) \left[\frac{(.943)(\frac{d}{b})^{.543} (\frac{d}{b})^{.801} (\sin \theta)^{2.033}}{(\frac{d}{b})^{.852}} - 1.0 \right] \text{ for } \frac{d}{b} < .55$ $1.0 \cdot (Q_b) \left[\frac{(.441)(\frac{d}{b})^{.543} (\sin \theta)^{2.033}}{(\frac{d}{b})^{.852} (\frac{d}{b})^{.781}} - 1.0 \right] \text{ for } \frac{d}{b} > .55$
Brace	K1	$1.0 \cdot (Q_b) \left[\frac{(1.825)(\frac{d}{b})^{.56} (\frac{d}{b})^{.058} \exp(1.448 \sin \theta)}{(\frac{d}{b})^{.157} (\frac{d}{b})^{.441}} - 1.0 \right]$	$1.0 \cdot (Q_b) \left[\frac{(2.827)(\frac{d}{b})^{.35} (\sin \theta)^{.5}}{(\frac{d}{b})^{.35}} - 1.0 \right]$	As for Brace Side T and Y
Brace	K2	$1.0 \cdot (Q_b) \left[\frac{(5.651)(\frac{d}{b})^{.68} (\frac{d}{b})^{.126} (\sin \theta)^{.5}}{(\frac{d}{b})^{.1} (\frac{d}{b})^{.36}} - 1.0 \right] \text{ for } \theta < 45^\circ$ $1.0 \cdot (Q_b) \left[\frac{(12.801)(\frac{d}{b})^{.68} (\frac{d}{b})^{.126} (\sin \theta)^{2.88}}{(\frac{d}{b})^{.1} (\frac{d}{b})^{.36}} - 1.0 \right] \text{ for } \theta > 45^\circ$	As for Brace Side K1	As for Brace Side T and Y
Brace	K3	$1.0 \cdot (Q_b) \left[\frac{(4.491)(\frac{d}{b})^{.672} (\frac{d}{b})^{.159} (\sin \theta)^{2.267}}{(\frac{d}{b})^{.123} (\frac{d}{b})^{.396}} - 1.0 \right]$	As for Brace Side K1	As for Brace Side T and Y

NOTES: $Q_b = \exp - (1.51 + 0.115 \sin \theta)$ $Q_b > 0.7$

Chord SideBrace SideK-Joints

$$SCF_{cx} = 0.949 \gamma^{-0.666} \beta^{-0.059} \tau^{1.104} \eta^{0.067} \sin 1.521 \theta$$

$$SCF_{bx} = 0.825 \gamma^{-0.157} \beta^{-0.441} \tau^{0.500} \eta^{0.068} \omega^{1.448} \sin$$

$$SCF_{cy} = 1.400 \gamma^{-0.38} \beta^{0.06} \tau^{0.94} \sin 0.9 \theta$$

$$SCF_{by} = 2.827 \beta^{-0.36} \tau^{0.36} \sin 0.5 \theta$$

T-Joints

$$SCF_{cx} = 1.177 \gamma^{-0.808} \omega^{-1.2\beta^3} \tau^{1.333} \alpha^{-0.057} \sin 1.694 \theta$$

$$SCF_{bx} = 2.784 \gamma^{-0.55} \omega^{-1.36\beta^3} \tau \alpha^{-0.12} \sin 1.94 \theta$$

$$SCF_{cy} = 0.463 \gamma^{-0.6} \beta^{-0.04} \tau^{0.86} \sin 0.57 \theta$$

$$SCF_{by} = 1.109 \gamma^{-0.23} \beta^{-0.38} \tau^{0.38} \sin 0.21 \theta$$

$$SCF_{cz} = 0.507 \gamma^{-1.014} \tau^{0.889} \beta^{0.787} \sin 1.557 \theta$$

$$SCF_{bz} = 0.843 \gamma^{-0.852} \tau^{0.543} \beta^{0.801} \sin 2.033 \theta$$

$$\text{for } 0.3 \leq \beta \leq 0.55$$

$$\text{for } 0.3 \leq \beta \leq 0.55$$

$$SCF_{cz} = 0.229 \gamma^{-1.014} \tau^{0.889} \beta^{-0.619} \sin 1.557 \theta$$

$$SCF_{bz} = 0.441 \gamma^{-0.852} \tau^{0.543} \beta^{-0.281} \sin 2.033 \theta$$

$$\text{for } 0.55 < \beta \leq 0.75$$

$$\text{for } 0.55 < \beta \leq 0.75$$

TK-Joints

$$SCF_{cx} = 1.26 \gamma^{-0.54} \beta^{0.12} \tau^{1.088} \sin \theta$$

$$SCF_{bx} = 5.65 \gamma^{-0.1} \beta^{-0.36} \tau^{0.68} \omega^{0.126} \sin 0.5 \theta$$

$$\text{for } 0^\circ < \theta \leq 45^\circ$$

$$SCF_{bx} = 12.88 \gamma^{-0.1} \beta^{-0.36} \tau^{0.68} \omega^{0.126} \sin 2.88 \theta$$

$$\text{for } 45^\circ < \theta < 90^\circ$$

$$SCF_{bx(\text{central})} = 4.4918 \gamma^{-0.123} \beta^{-0.396} \tau^{0.672} \omega^{0.159} \sin 2.267 \theta$$

Where

γ = chord thickness/chord diameter

θ = angle between brace and chord

τ = brace thickness/chord thickness

α = chord diameter/chord length between supports

η = separation distance between braces/chord diameter

ω = separation distance between braces for TK joints/chord diameter

β = brace diameter/chord diameter

Chord SideBrace SideK-Joints

$$SCF_{cx} = 1.8 (\tau \sin \theta \sqrt{\gamma})$$

$$SCF_{cy} = 1.2 (\tau \sin \theta \sqrt{\gamma})$$

$$SCF_{cz} = 2.7 (\tau \sin \theta \sqrt{\gamma})$$

$$SCF_{bx} = 1.0 + 0.6 Q_r [1.0 + \sqrt{\frac{\tau}{\beta}} \cdot SCF_{cx}] \geq 1.8$$

$$SCF_{by} = 1.0 + 0.6 Q_r [1.0 + \sqrt{\frac{\tau}{\beta}} \cdot SCF_{cy}] \geq 1.8$$

$$SCF_{bz} = 1.0 + 0.6 Q_r [1.0 + \sqrt{\frac{\tau}{\beta}} \cdot SCF_{cz}] \geq 1.8$$

Y-Branch Joints

$$SCF_{Kuang} = 2.06 \gamma^{0.808} e^{-1.2\beta^3} (\sin \theta)^{1.694} \tau^{1.333}$$

$$SCF_{AWS} = 14 \tau \sin \theta \quad \text{for } \gamma \leq 25$$

$$= 1.5 \tau \sin \theta \gamma^{0.7} \quad \text{for } \gamma > 25$$

$$SCF_{cxmod} = SCF_{cx} + \tau \cos \theta$$

$$SCF_{Tc} = SCF_{Kuang} < SCF_{AWS}$$

$$> SCF_{cxmod}$$

$$SCF_y = \text{same as for K}$$

$$SCF_z = \text{same as for K}$$

$$SCF_{Tb} = 1.0 + 0.6 Q_r [1.0 + \sqrt{\frac{\tau}{\beta}} \cdot SCF_{Tc}] \geq 1.8$$

$$> SCF_{bx}$$

$$SCF_y = \text{same as for K}$$

$$SCF_z = \text{same as for K}$$

Unreinforced Cross Joints

$$SCF_x = 1.333 (SCF_{Tc})_{y\text{-branch}} + \frac{t_c}{T}$$

$$SCF_y = 1.333 (SCF_{cy})$$

$$SCF_z = 1.333 (SCF_{cz})$$

$$SCF_{bx} = 1.0 + 0.6 Q_r [1.0 + \sqrt{\frac{\tau}{\beta}} \cdot SCF_x] \geq 1.8$$

$$SCF_{by} = 1.0 + 0.6 Q_r [1.0 + \sqrt{\frac{\tau}{\beta}} \cdot SCF_y] \geq 1.8$$

$$SCF_{bz} = 1.0 + 0.6 Q_r [1.0 + \sqrt{\frac{\tau}{\beta}} \cdot SCF_z] \geq 1.8$$

Where

θ = angle between brace and chord

D = can diameter

T = can thickness

t_c = nominal chord thickness

d = brace diameter

t = stub thickness

$\tau = t/T$

$\gamma = (D-T)/2T$

$\beta = d/D$

$Q_r = \exp [-(0.5 T + t)/\sqrt{0.5 d^2}]$

Chord Side

$$SCF_{cx} = 1.7\gamma\tau\beta(2.42 - 2.28\beta^{2.2})\sin\beta^2(15 - 14.4\beta)\theta$$

$$SCF_{cy} = 0.75\gamma^{0.6}\tau^{0.8}(1.6\beta^{1/4} - 0.7\beta^2)\sin(1.5 - 1.6\beta)\theta$$

$$SCF_{cz} = \gamma\tau\beta(1.56 - 1.46\beta^5)\sin\beta^2(15 - 14.4\beta)\theta$$

Brace Side

$$SCF_{bx} = 1 + 0.63 SCF_{cx}$$

$$SCF_{by} = 1 + 0.63 SCF_{cy}$$

$$SCF_{bz} = 1 + 0.63 SCF_{cz}$$

Where

- β = Brace Diameter/Chord Diameter
- γ = Chord Radius/Chord Thickness
- τ = Brace Thickness/Chord Thickness
- θ = Acute Angle Between Brace and Chord

Smedley Formulas Used for Computing Stress Concentration Factors
for Unreinforced Cross Joints

Definition of Parameters, Validity Ranges and Notes on Tables

Definition of Tubular Joint Parameters

$\alpha = 2L/D$ where D = chord outside diameter
 $\beta = d/D$ T = chord wall thickness
 $\gamma = D/2T$ L = chord length (distance between points of contraflexure)
 $\tau = t/T$ d = brace outside diameter
 t = brace wall thickness
 $\zeta = g/D$ g = gap between adjacent braces

Validity Ranges for Parametric Equations

$8 \leq \alpha \leq 40$
 $0.13 \leq \beta \leq 1.0$
 $12 \leq \gamma \leq 32$
 $0.25 \leq \tau \leq 1.0$
 $0.01 \leq \zeta \leq 1.0$ (Tables 1 and 2) $-0.4 \leq \zeta \leq 0.01$ (Table 3)
 $30^\circ \leq \theta \leq 90^\circ$
 $\theta_1 \geq \theta_2$
 $\theta_3 \leq 90^\circ$

Notes on Tables

(1) Tables 1 to 3

(1) $SCF \text{ (brace)} = 1 + 0.63 \text{ SCF (chord)}$

(2) SCFs are limited to a minimum value of 1.6

(3) For joints outside specified validity ranges calculate SCF with actual joint parameters and with parameters set to nearest validity limit. The greater SCF value obtained should be used in analysis. See also notes B(1) and C(1) below.

(2) Table 1 only

(1) If $0.98 \leq \beta \leq 1.0$ then use $\beta = 0.98$.

(2) The K and KT joint equations are based on nominal stress in brace 1.

(3) For KT joints where the load in brace 3 is smaller than 10% of the maximum load in adjacent braces 1 and 2 the joint type should be re-categorised as K with g the gap between braces 1 and 2.

(4) The equations indicated for K and KT joints apply only to balanced axial load.

(3) Table 2 only

(1) If $\beta \geq 0.95$ for out-of-plane bending then use $\beta = 0.95$.

(2) The equations indicated for K and KT joints apply only to loading on all braces in the same direction for out-of-plane bending.

(4) Table 3 only

(1) For K joints in out-of-plane bending replace the constant 0.9 by the term $1 - (0.1 \sqrt{1+4\zeta})$ when $\zeta \geq 0$.

(2) For KT joints in out-of-plane bending replace the constant 0.8 by the term $(1 - 0.1 \sqrt{1+4\zeta})^2$ when $\zeta \geq 0$.

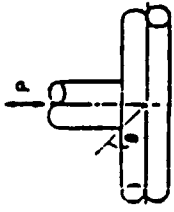
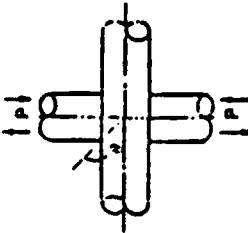
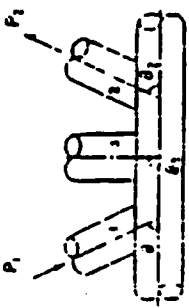


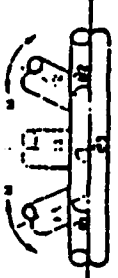
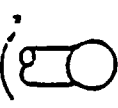
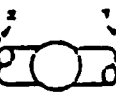
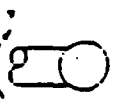
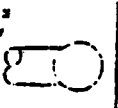
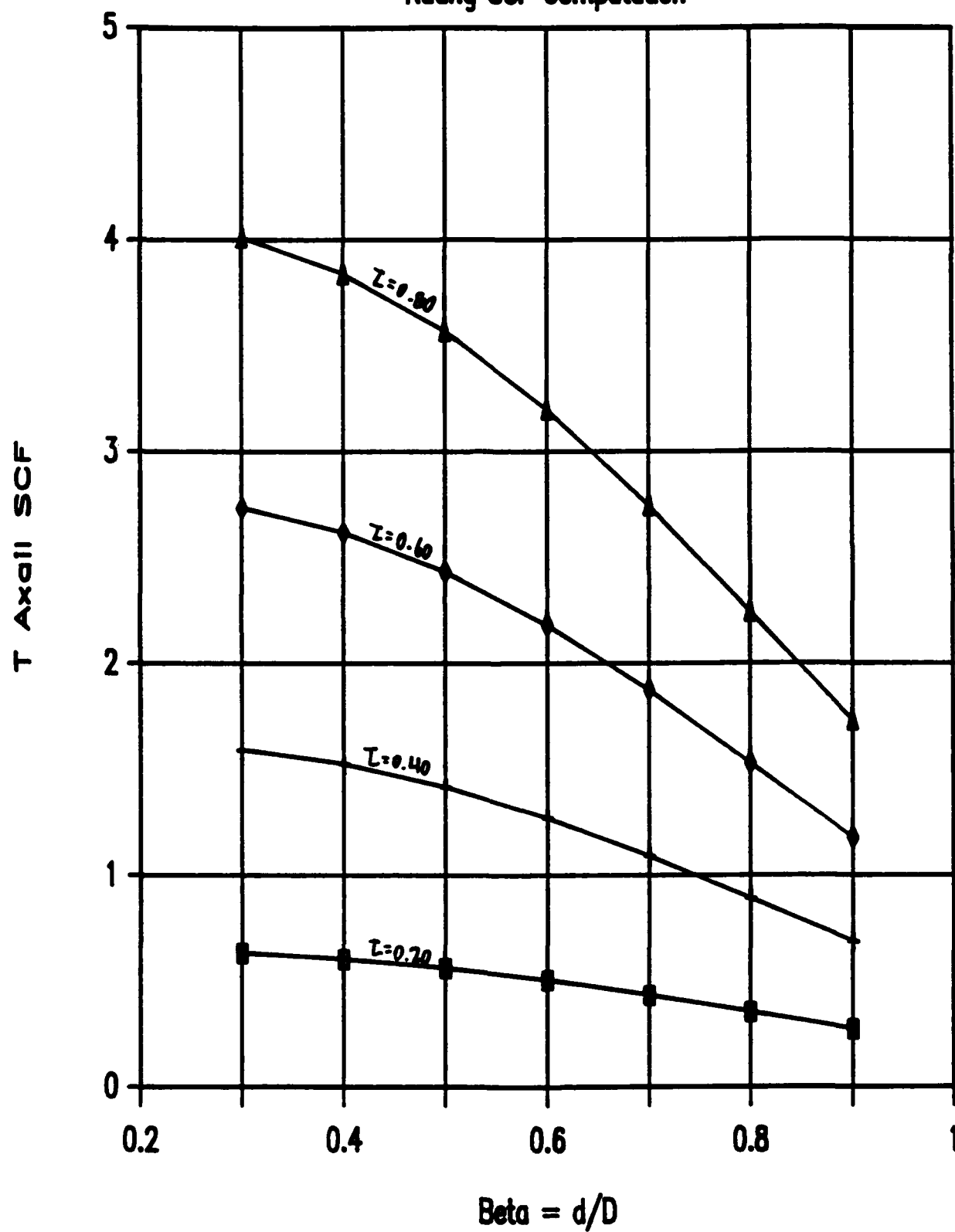
JOINT TYPE AND LOADING	CHORD, SADDLE SCF	CHORD, CROWN SCF
<p><u>Axial</u></p> <p>T, T Joints</p> 	$1.7 \beta (6.78 - 6.12 \beta^{2.5}) \sin^{1.7+0.7\beta^3} \theta$	$\left[0.7 + 1.37 \gamma^{0.5} r (1-\beta) \right] \left[2 \sin^{0.5} \theta - \sin^3 \theta \right] +$ $\left[\frac{r(2\gamma\beta - 1)(\alpha/2 - \beta \sin \theta) \sin \theta}{2\gamma - 3} \right] \times$ $\left[1.05 + \frac{30r^{1.5}(1.2-\beta)(\cos^4 \theta + 0.15)}{\gamma} \right]$
<p>DT, X Joints</p> 	$1.7 \gamma \tau \beta (2.42 - 2.28 \beta^{2.2}) \sin^2 (\beta^2 (15 - 14.4 \beta)) \theta$	<p>No information available on SCF</p>
<p>K, KT Joints</p> 	$\left[\gamma \tau \beta (6.78 - 6.42 \beta^{0.5}) \right] \times$ $\left[\left(\sin^{1.7+0.7\beta^3} \theta_1 \right) - \left(\sin^{1.7+0.7\beta^3} \theta_2 \right) \right] \left(\frac{\sin \theta_1}{\sin \theta_2} \right)^{1.8} \sin^{1.7+0.7\beta^3} \theta_2$	$1.1 \gamma^{0.65} r \left(\frac{\sin \theta_1}{\sin^{0.5} \theta_2} \right) (2r)^{0.05/\beta} (1.5 \beta^{0.25} - \beta^2)$

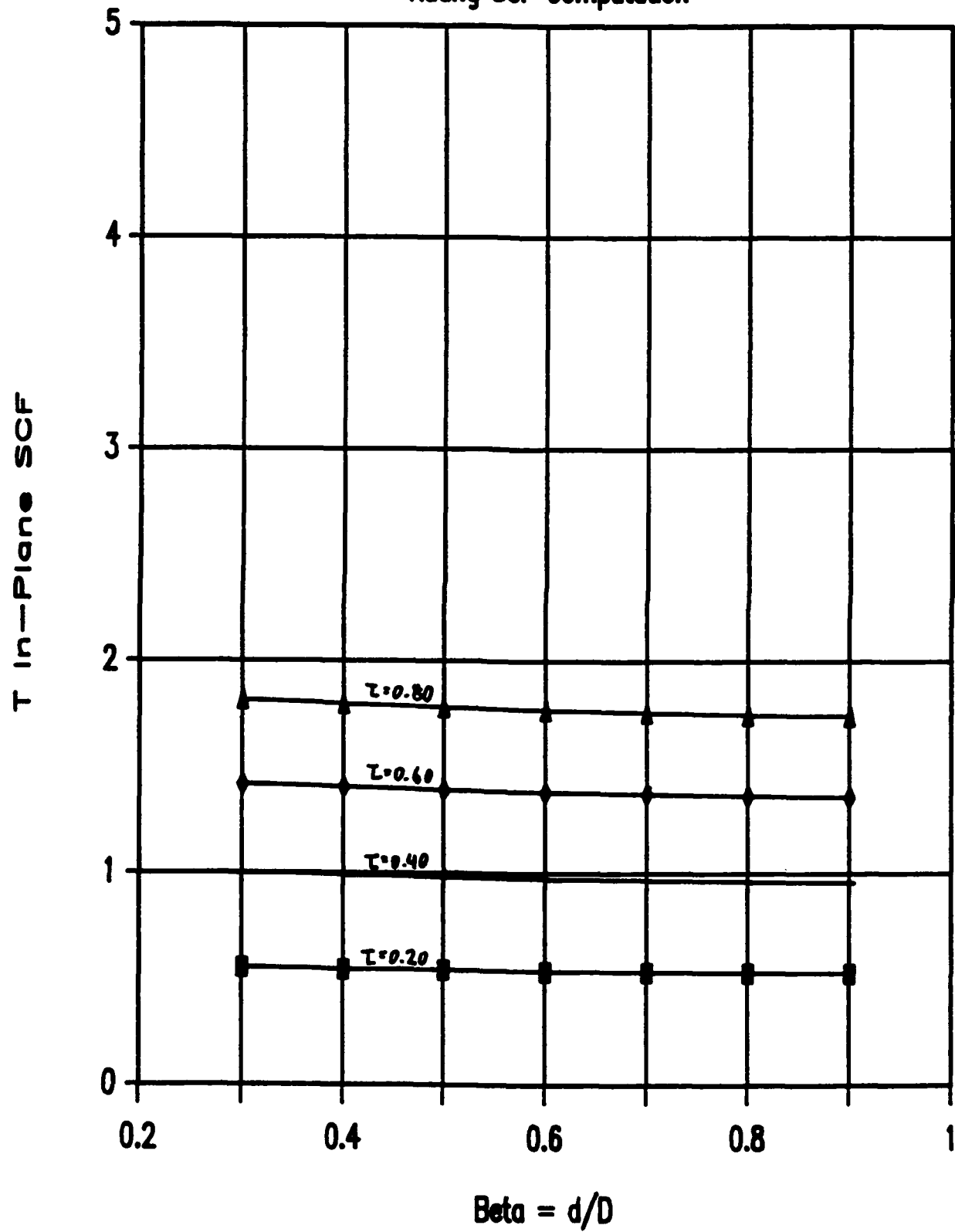
Table 1. Parametric Equations for SCF's of Unstiffened, Non-overlapped Tubular Joints - Axial Loading in Brace

JOINT TYPE AND LOADING	CHORD, SADDLE SCF	CHORD, CROWN SCF
Non-Overlapped 		
DT, X Joints 	SCF = 0	$0.75 \gamma^{0.6} r^{0.8} (1.6 \beta^{0.25} - 0.7 \beta^2) \sin^{(1.5 - 1.6 \beta)} \theta$
K, KT Joints 		
Out-of-Plane Bending 	$\gamma r \beta (1.6 - 1.15 \beta^2) \sin^{(1.35 + \beta^2)} \theta$	
DT, > Joints 	$\gamma r \beta (1.56 - 1.46 \beta^2) \sin^{(\beta^2(15 - 14.4 \beta))} \theta$	SCF = 0
K Joints 	$\left[\gamma r \beta (1.6 - 1.15 \beta^2) \right] \times$ $\left[(\sin^{(1.35 + \beta^2)} \theta_1) + (\sin^{(1.35 + \beta^2)} \theta_2) \right] \times$ $\left[(0.016 \beta \gamma) (r + 0.45) \right]^{0.3} (\theta_1 / \theta_2) \left[1 - 0.1 (1 + r) \right]$	
KT Joints 	$\left[\gamma r \beta (1.6 - 1.15 \beta^2) \right] \times$ $\left[(\sin^{(1.35 + \beta^2)} \theta_1) + (\sin^{(1.35 + \beta^2)} \theta_2) \right] \times$ $\left[(0.016 \beta \gamma) (r + 0.45) \right]^{0.3} 2 (\theta_1 / \theta_2) \left[1 - 0.1 (1 + r) \right]^2$	
Table 2. Parametric Equations for SCF's of Uninflamed, Non-Overlapped Tubular Joints - Moment Loading in Brace		

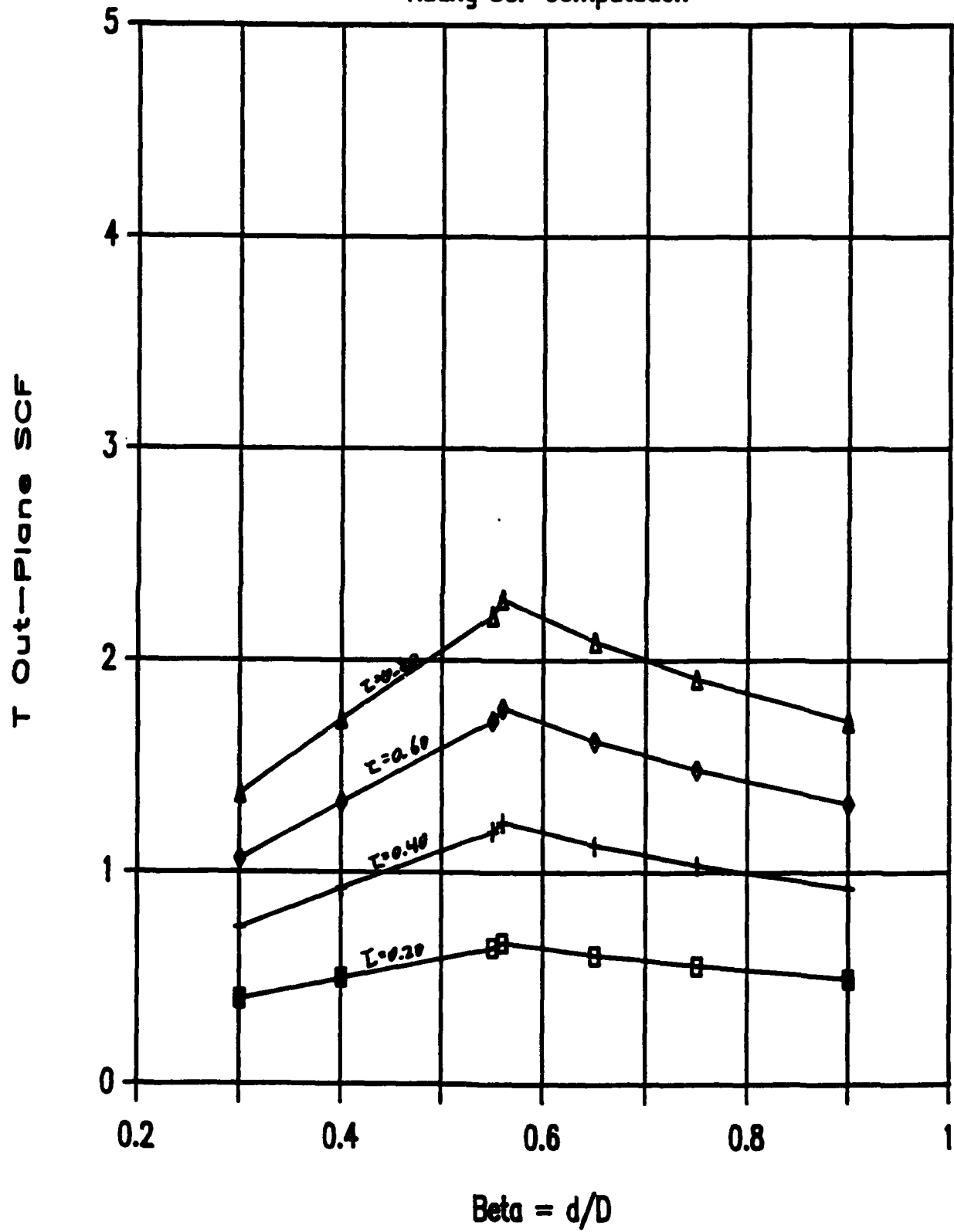
Kuang SCF Computation



Kuang SCF Computation



Kuang SCF Computation



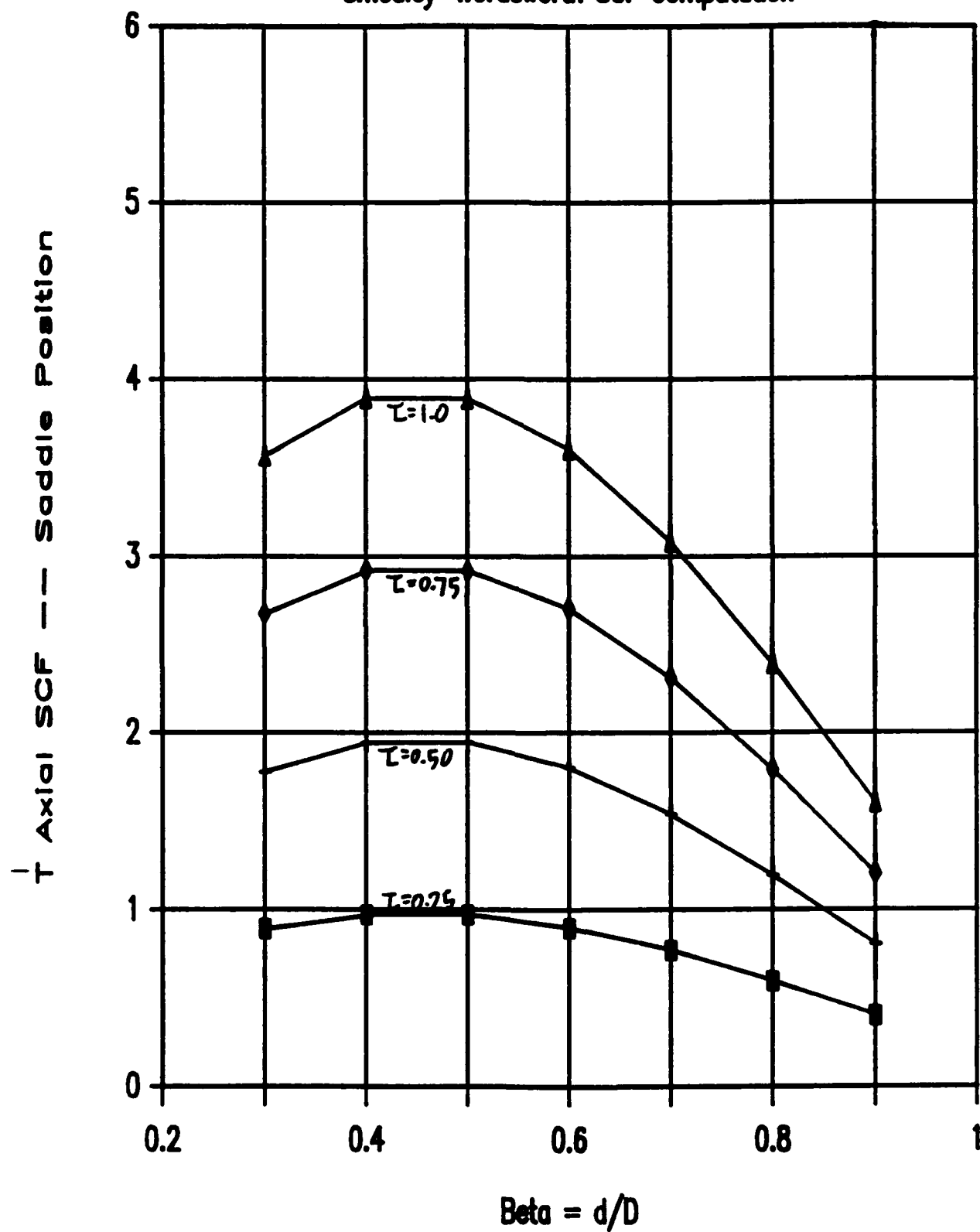
C.3.1(b) Smedley-Wordsworth Chord SCF's for T-Joints

The Smedley-Wordsworth chord SCF's for T-joints are shown on the following pages. The following parameters are assumed for the Smedley-Wordsworth figures:

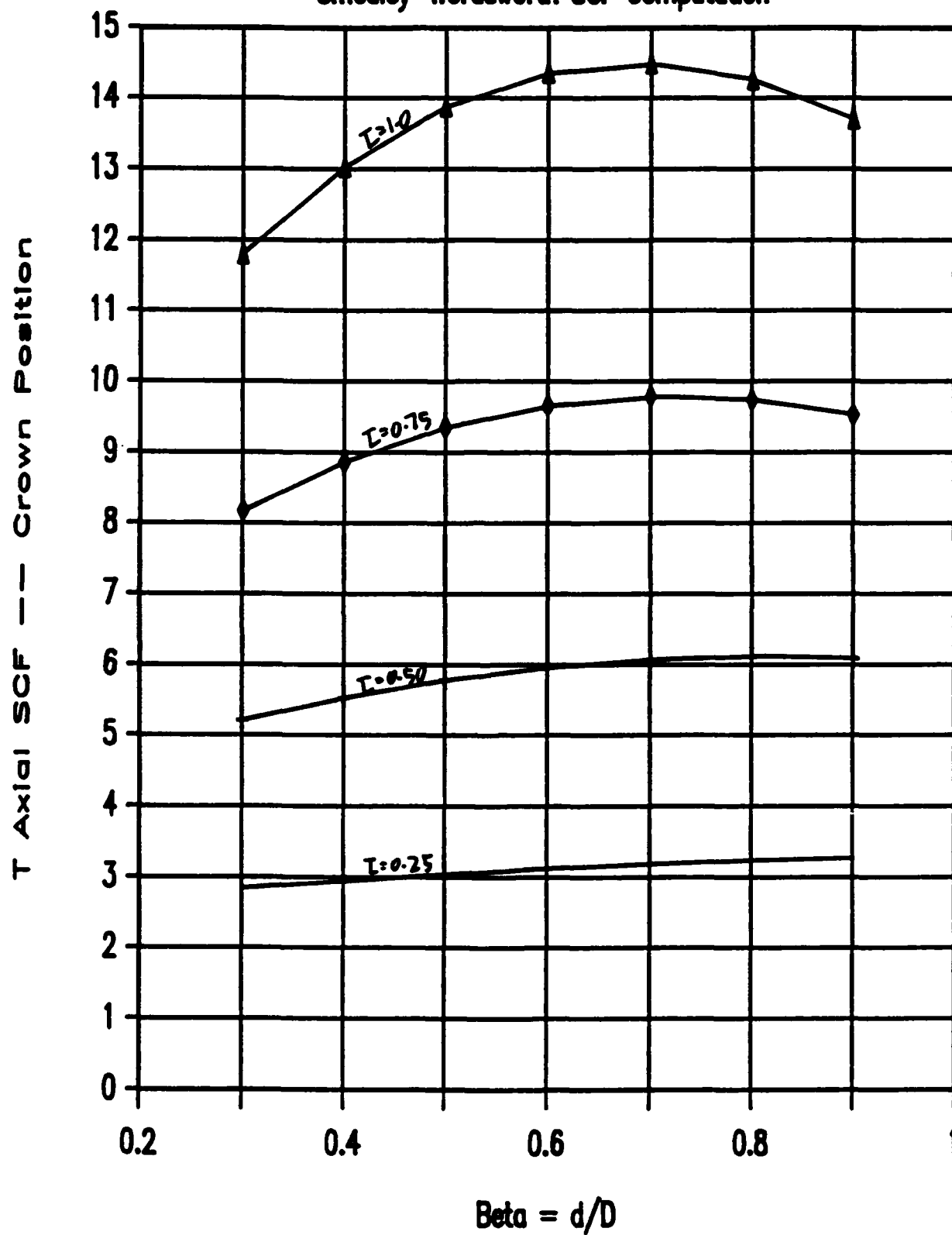
- 1) $\gamma = D/2T = 12.0$
- 2) $\theta = \quad = 30.0 \text{ degrees}$
- 3) $\alpha = 2L/D = 35.0$

The Shell d/D limitations have not been imposed for the SCF calculation.

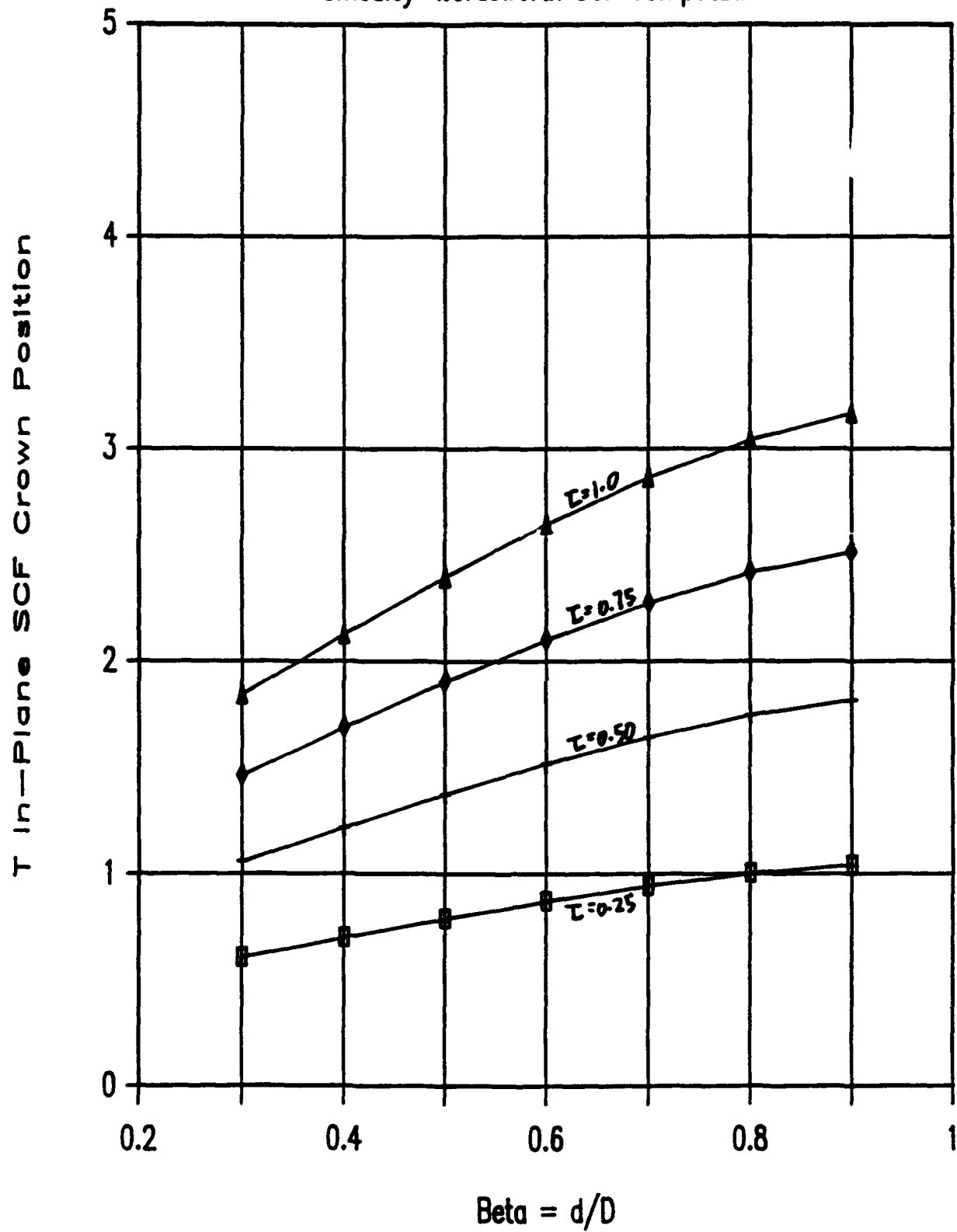
Smedley-Wordsworth SCF Computation



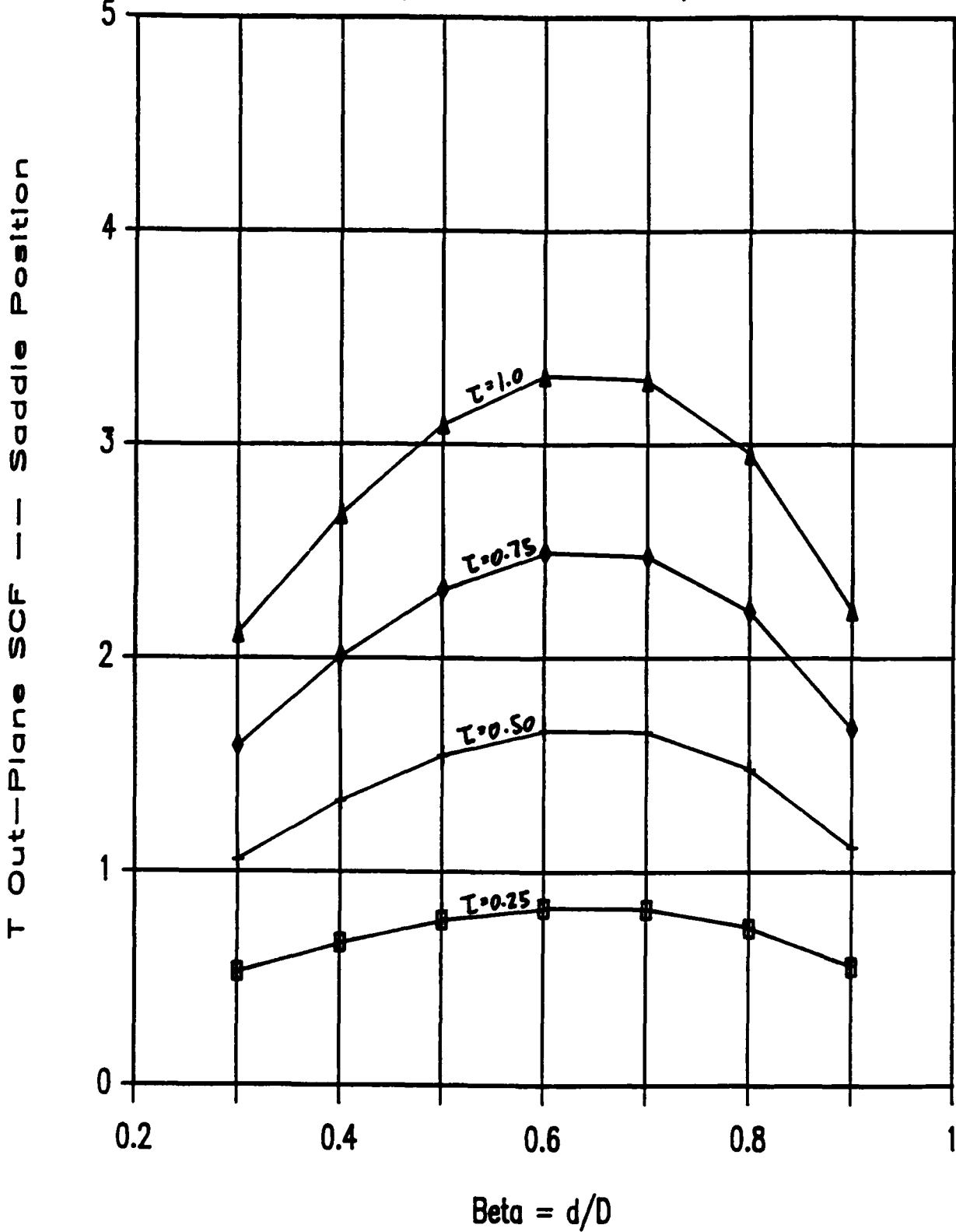
Smedley-Wordsworth SCF Computation



Smedley-Wordsworth SCF Computation



Smedley-Wordsworth SCF Computation

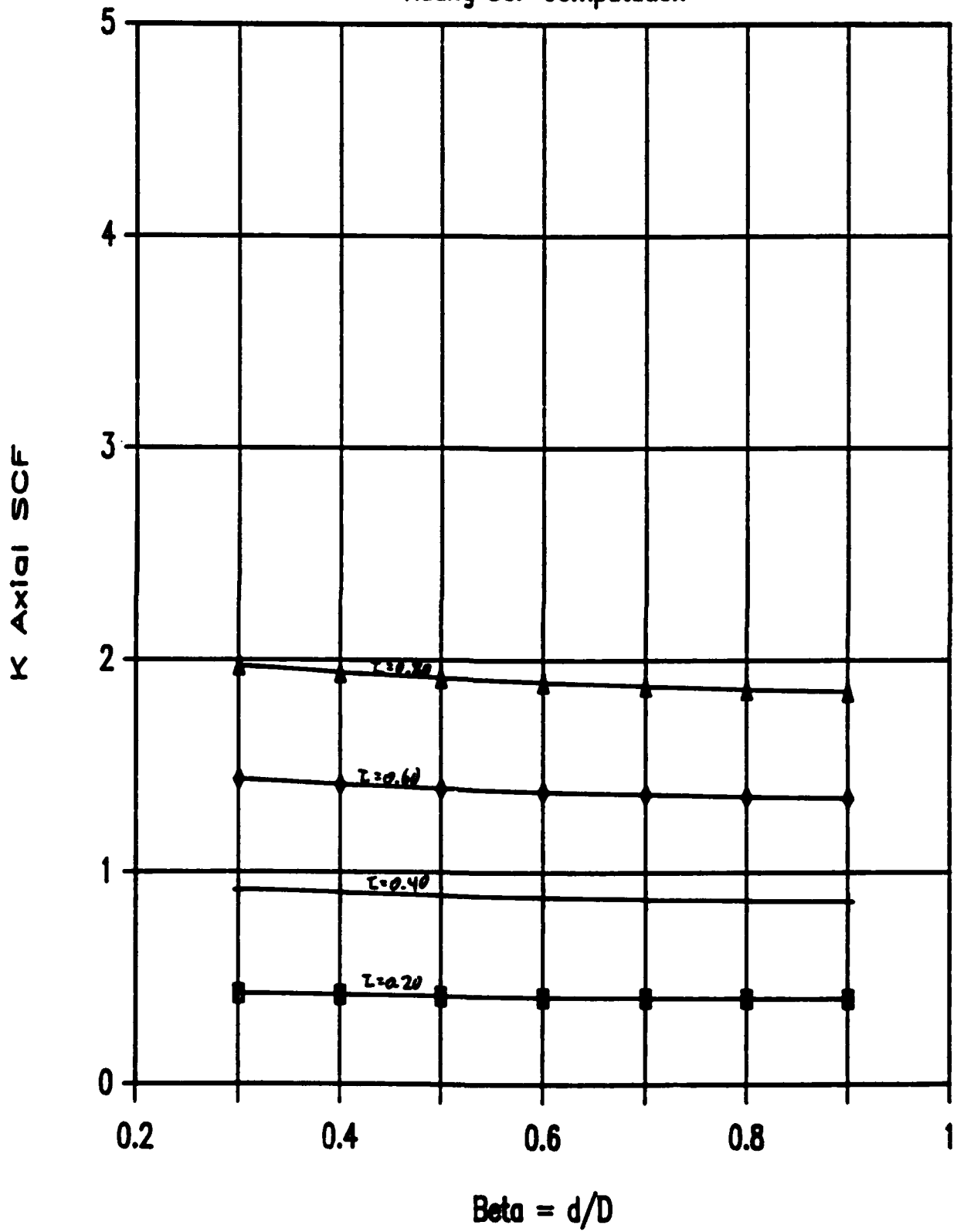


C.3.1(c) Kuang Chord SCF's for T-Joints

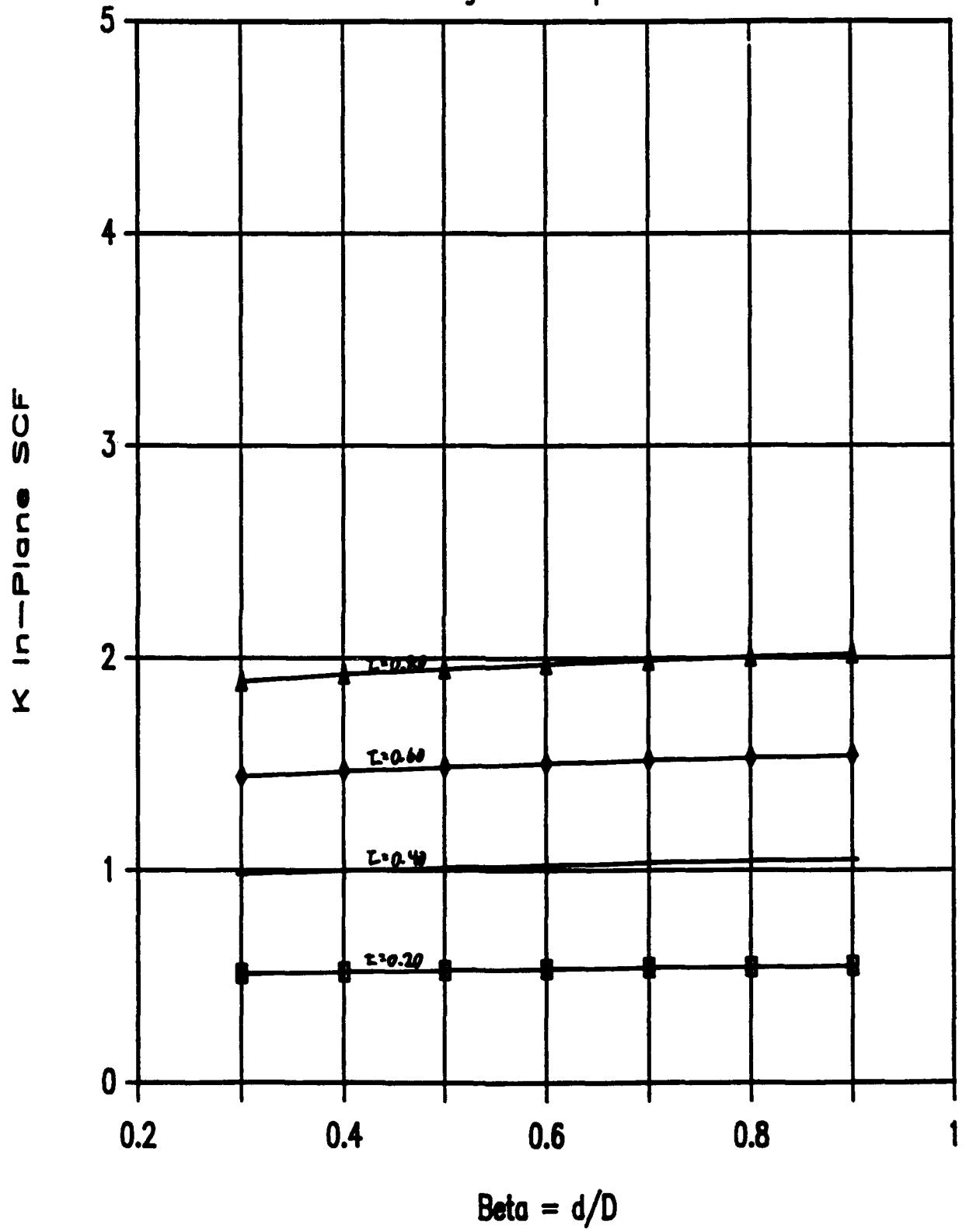
The Kuang chord SCF's for K-joints are shown on the following pages. The following parameters are assumed for the Kuang figures:

- 1) $\gamma = D/2T = 12.0$
- 2) $\theta = \quad = 30.0 \text{ degrees}$
- 3) $\alpha = D/L = 0.0571$

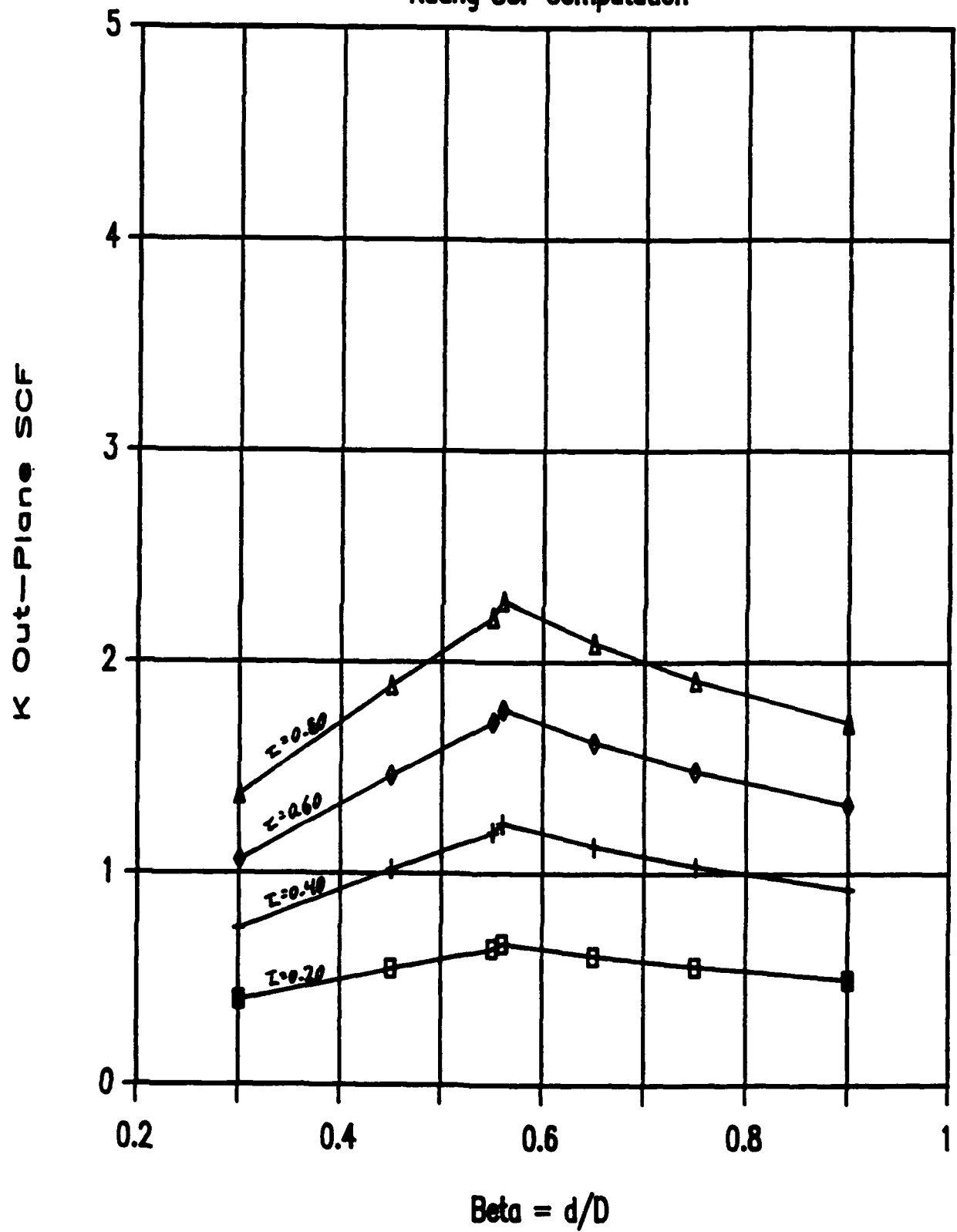
Kuang SCF Computation



Kuang SCF Computation



Kuang SCF Computation



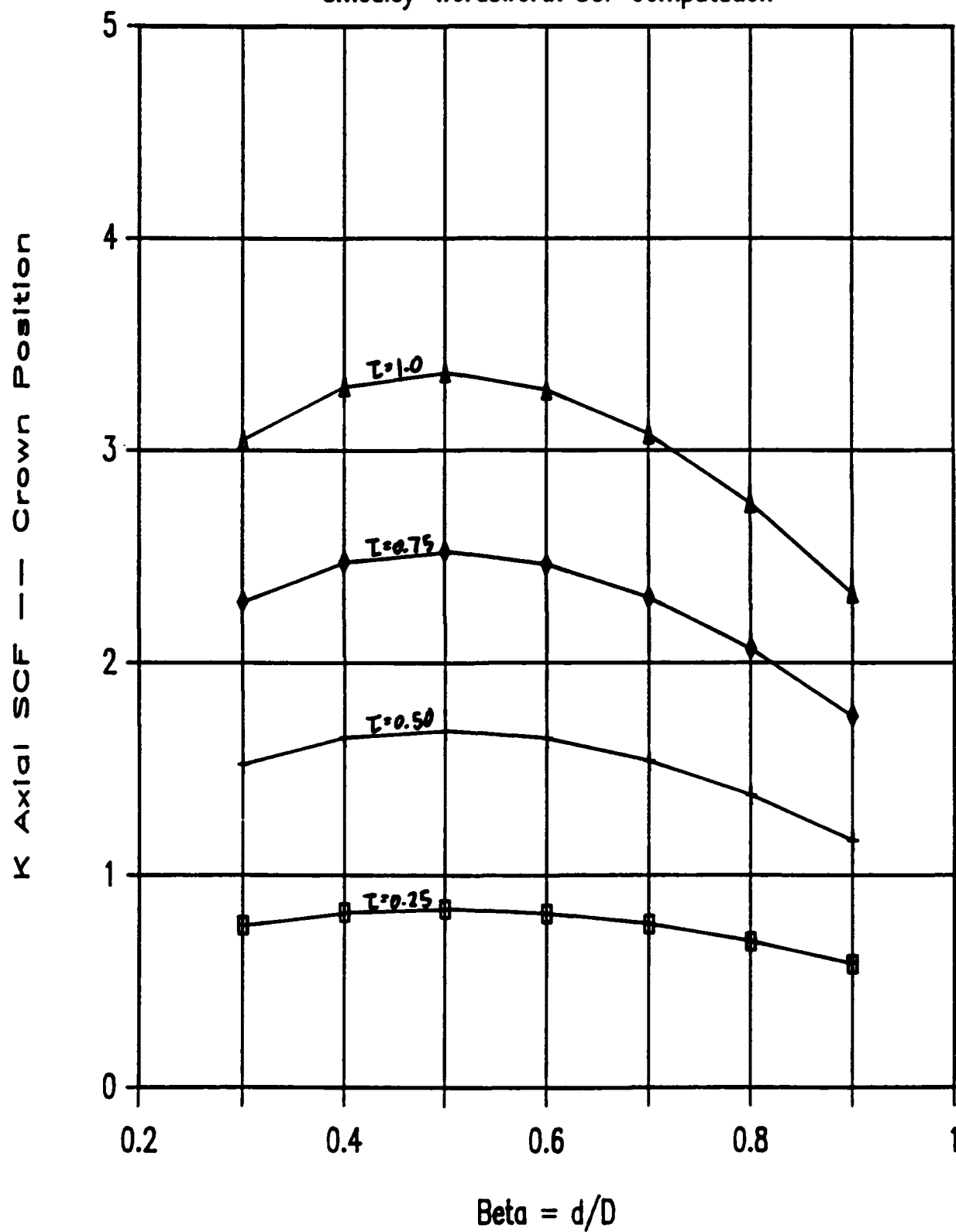
C.3.1(d) Smedley-Wordsworth Chord SCF's for K-Joints

The Smedley-Wordsworth chord SCF's for K-joints are shown on the following pages. The following parameters are assumed for the Smedley-Wordsworth figures:

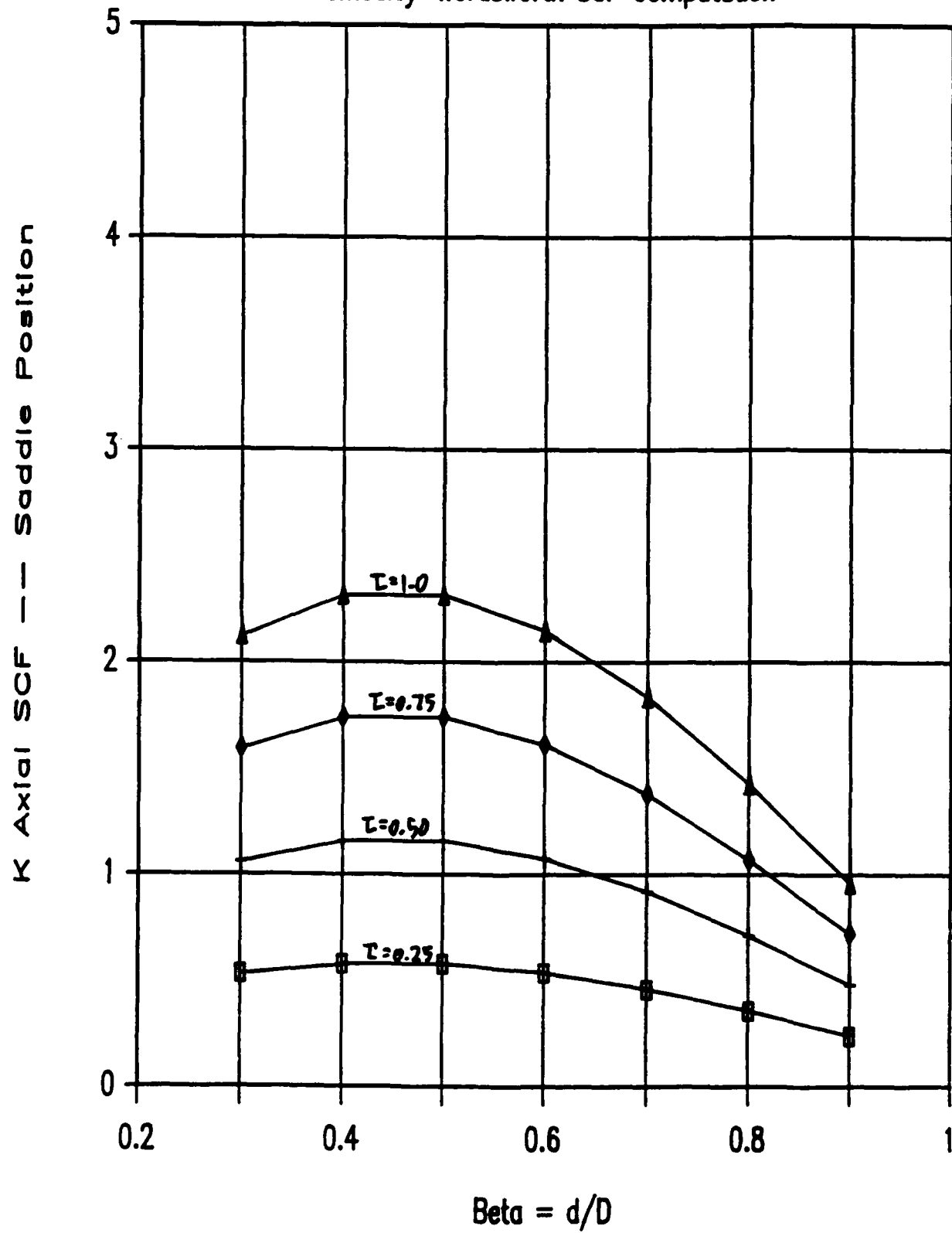
- 1) $\gamma = D/2T = 12.0$
- 2) $\theta = \theta_2 = 30.0$ degrees
- 3) $\alpha = 2L/D = 35.0$

The Shell d/D limitations have not been imposed for the SCF calculation.

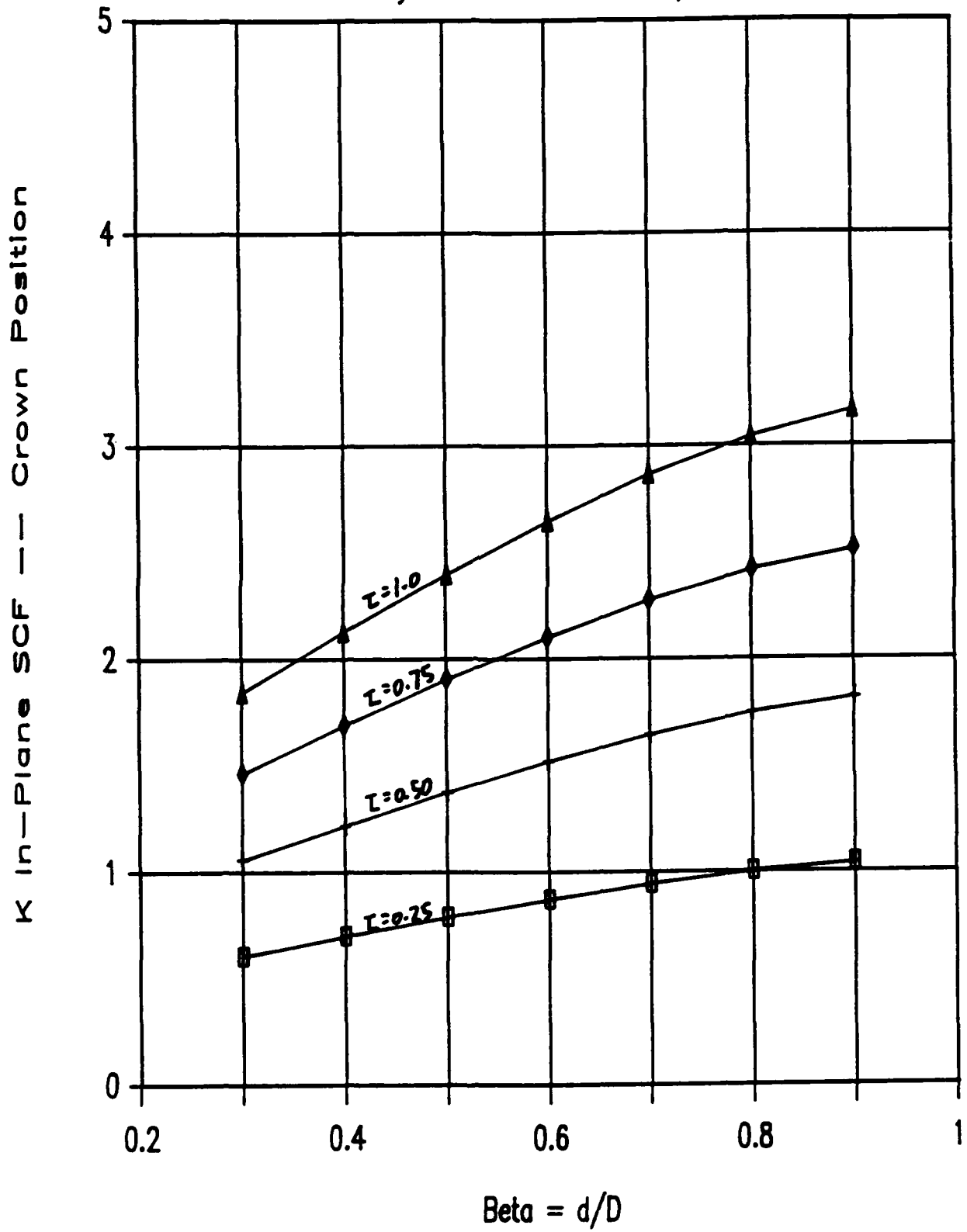
Smedley-Wordsworth SCF Computation



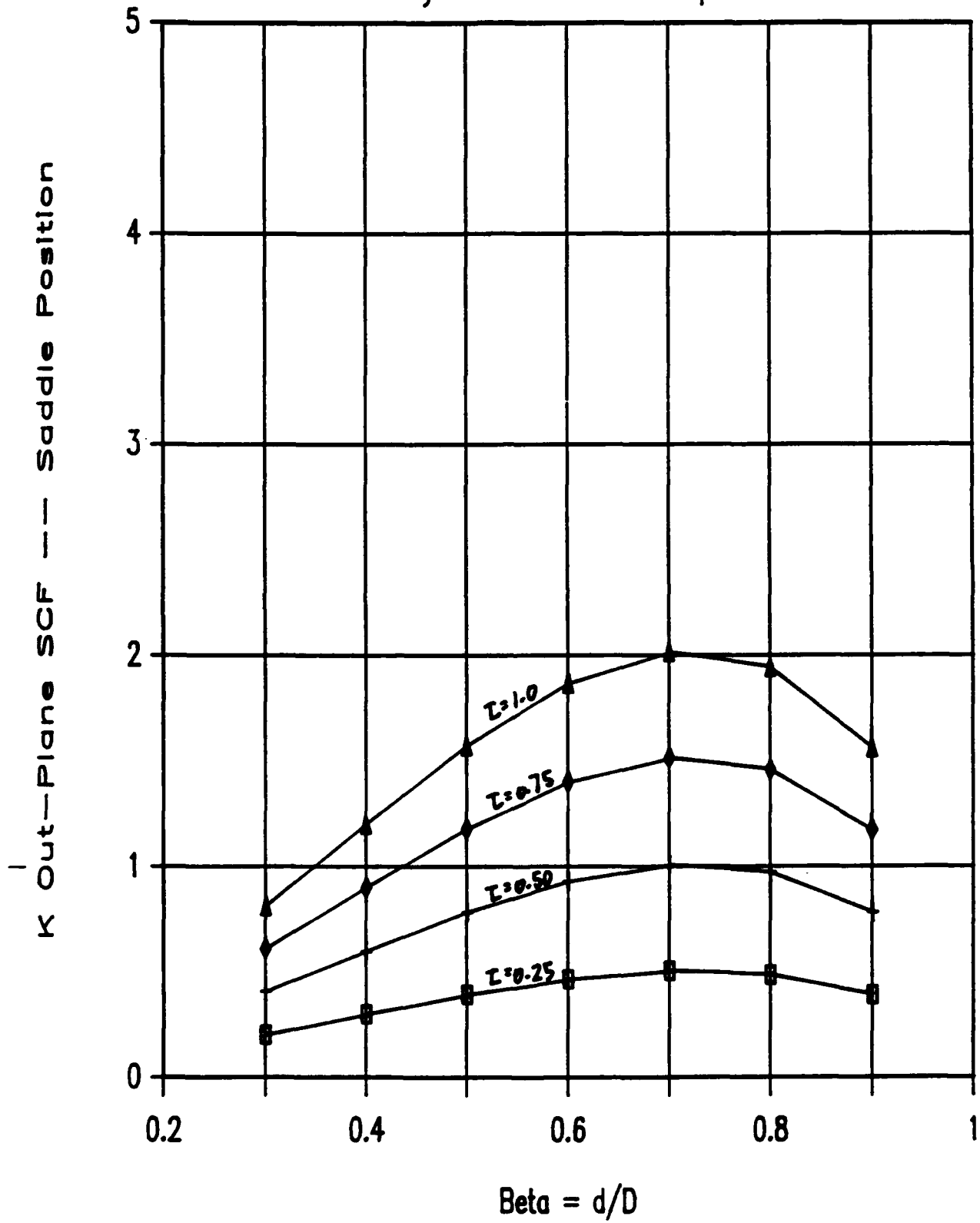
Smedley-Wordsworth SCF Computation



Smedley-Wordsworth SCF Computation



Smedley-Wordsworth SCF Computation



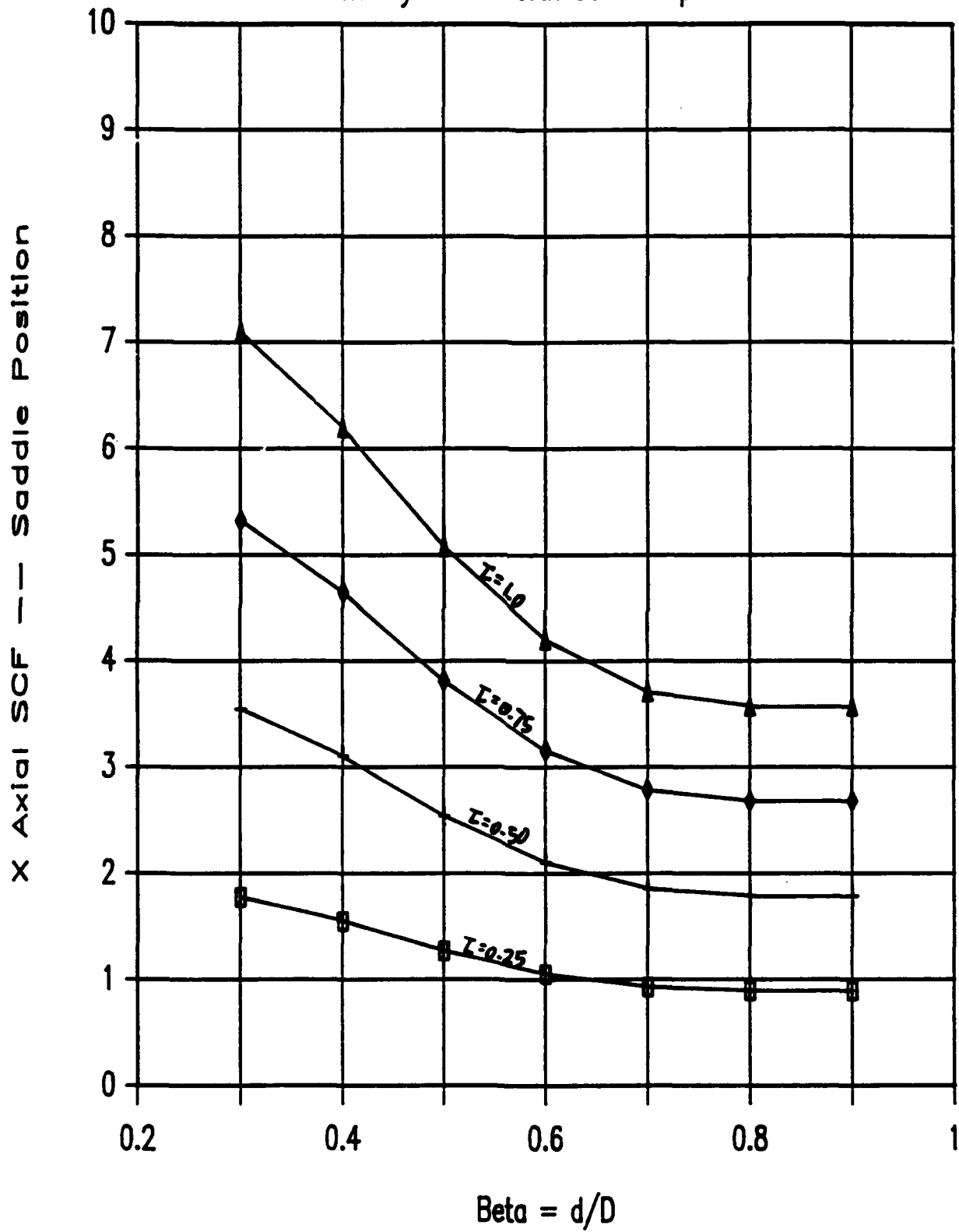
C.3.1(e) Smedley-Wordsworth Chord SCF's for X-Joints

The Smedley-Wordsworth chord SCF's for X-joints are shown on the following pages. The following parameters are assumed for the Smedley-Wordsworth figures:

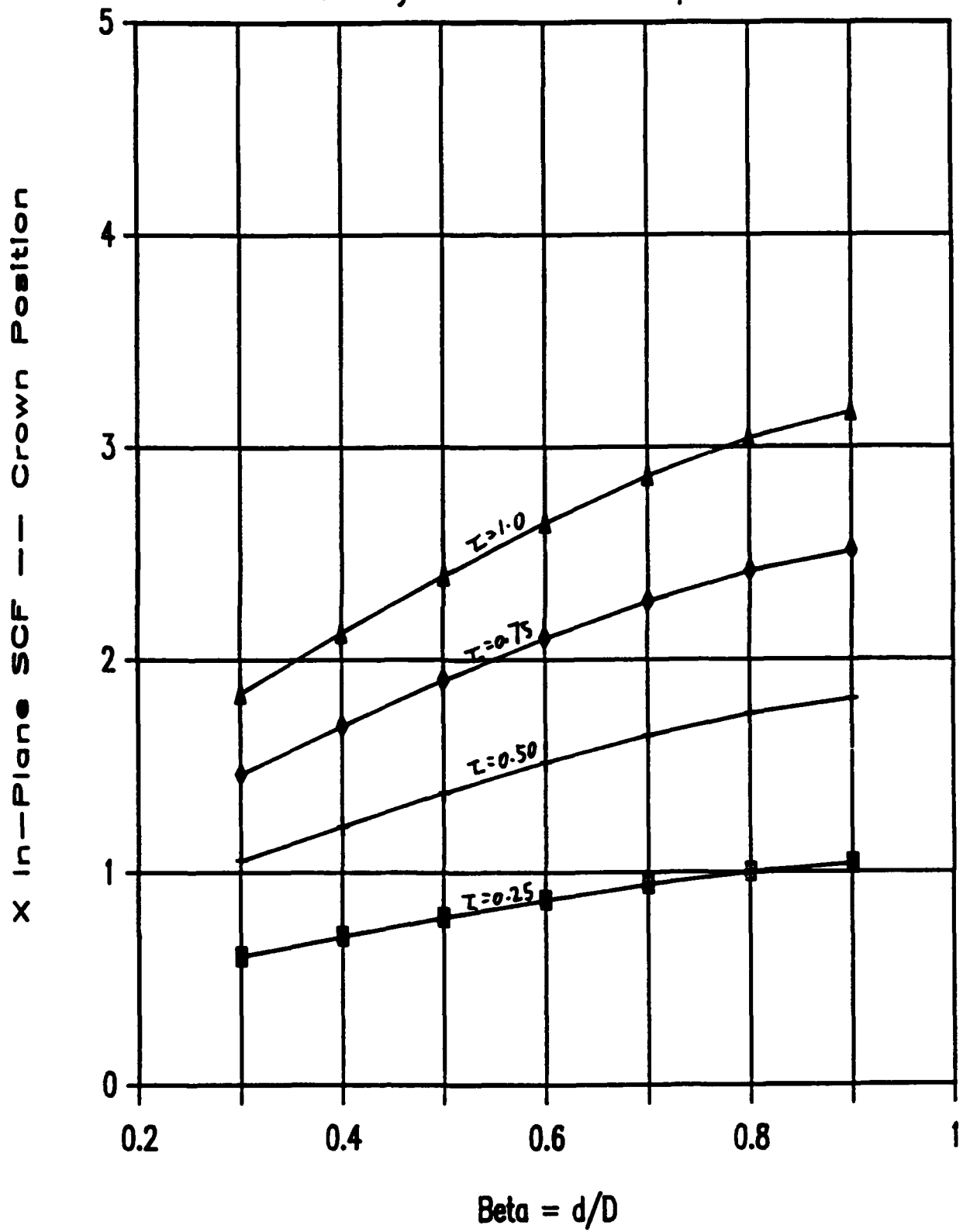
- 1) $\gamma = D/2T = 12.0$
- 2) $\theta = \quad = 30.0$ degrees
- 3) $\alpha = D/L = 35.0$

The Shell d/D limitations have not been imposed for the SCF calculation.

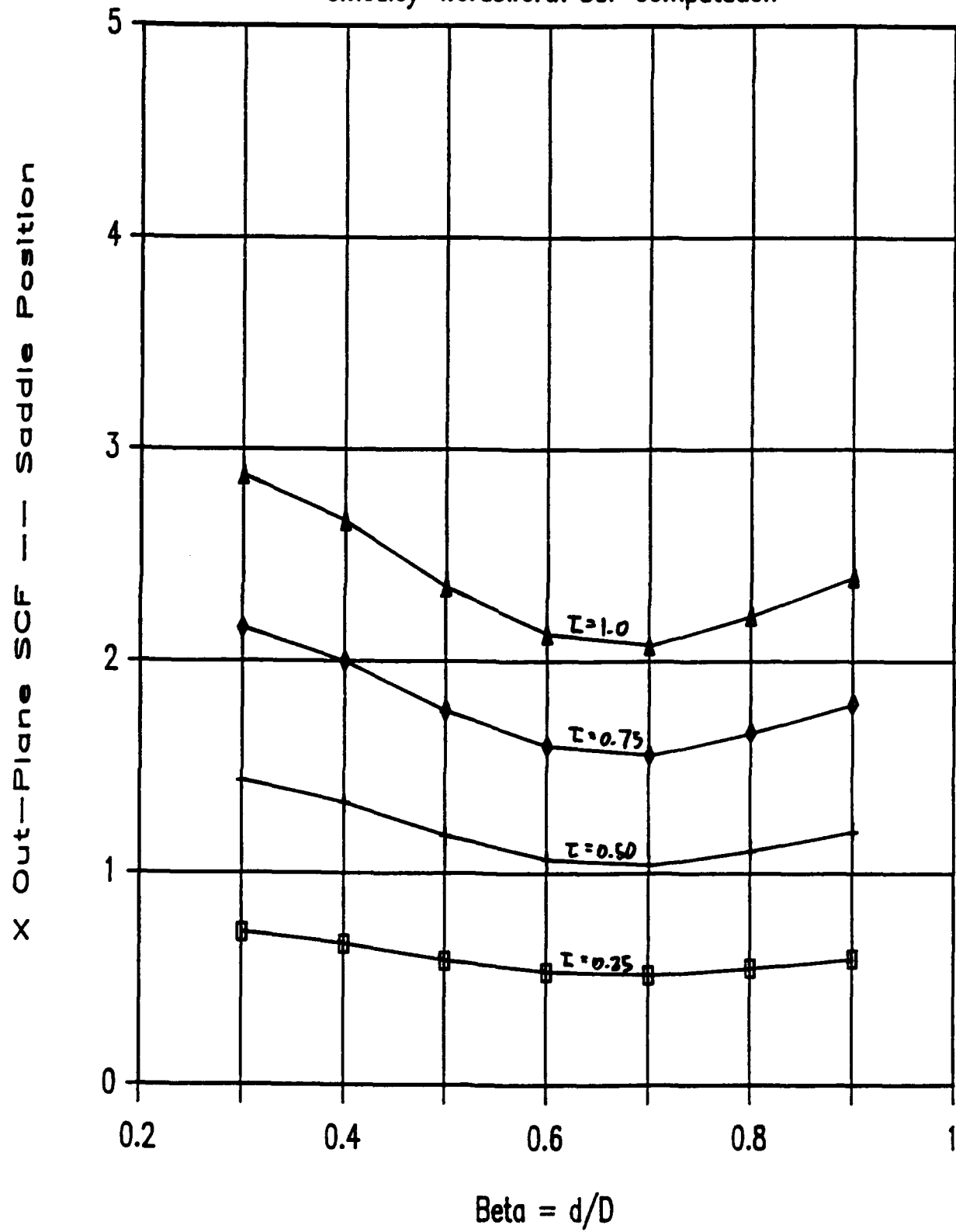
Smedley-Wordsworth SCF Computation



Smedley-Wordsworth SCF Computation



Smedley-Wordsworth SCF Computation



C.3.2 Tables

The Kuang and Smedley-Wordsworth chord stress Concentration factors for T joints are shown in Section C.3.2(a) and C.3.2(b), respectively. Since the chord side of the weld stress Concentration factor is generally higher than the brace side of the weld stress Concentration factor, only the chord side of the weld stress Concentration factors are shown.

C.3.2(a) Kuang Chord SCF's for T-Joints

The Kuang chord SCF's for T-joints are shown on the following pages. The following parameters are assumed for the Kuang figures:

$$1) \quad \alpha = D/L = 0.0571$$

Kusog SCF Computation

T-joint Axial SCF Chord Side of Weld

Theta =	Tan = t/T	Gamma = 12.0				Gamma = 15.0				Gamma = 20.0				Gamma = 25.0			
		Beta = d/B				Beta = d/B				Beta = d/B				Beta = d/B			
		0.3	0.5	0.7	0.9	0.3	0.5	0.7	0.9	0.3	0.5	0.7	0.9	0.3	0.5	0.7	0.9
	0.20	10.632	0.562	0.432	0.272	10.757	0.673	0.518	0.326	10.935	0.849	0.654	0.411	11.144	1.017	0.783	0.492
30.0 deg 0.524 rad	0.40	11.593	1.416	1.090	0.686	11.908	1.696	1.306	0.821	12.407	2.140	1.648	1.037	12.883	2.563	1.973	1.241
	0.60	12.736	2.432	1.872	1.178	13.276	2.913	2.242	1.411	14.134	3.675	2.829	1.780	14.930	4.401	3.388	2.132
	0.80	14.014	3.569	2.747	1.729	14.808	4.274	3.290	2.070	16.066	5.393	4.151	2.612	17.264	6.458	4.972	3.128
	0.20	11.137	1.011	0.778	0.490	11.362	1.211	0.932	0.586	11.719	1.528	1.176	0.740	12.058	1.830	1.409	0.885
45.0 deg 0.785 rad	0.40	12.866	2.548	1.961	1.234	13.432	3.052	2.349	1.478	14.331	3.850	2.964	1.865	15.187	4.611	3.550	2.233
	0.60	14.921	4.375	3.368	2.119	15.893	5.239	4.033	2.538	17.436	6.611	5.089	3.202	18.905	7.917	6.094	3.835
	0.80	17.221	6.420	4.942	3.110	18.648	7.688	5.919	3.724	19.91	9.700	7.467	4.699	21.306	11.61	8.943	5.627
	0.20	11.604	1.426	1.097	0.690	11.921	1.707	1.314	0.827	12.423	2.154	1.658	1.043	12.902	2.580	1.986	1.230
60.0 deg 1.047 rad	0.40	14.041	3.592	2.765	1.740	14.839	4.302	3.312	2.084	16.106	5.428	4.179	2.629	17.312	6.501	5.004	3.149
	0.60	16.938	6.168	4.748	2.988	18.308	7.387	5.686	3.578	19.48	9.320	7.174	4.514	21.25	11.16	8.592	5.406
	0.80	19.18	9.051	6.967	4.384	21.219	10.83	8.344	5.250	21.538	13.67	10.52	6.625	23.42	16.37	12.60	7.933
	0.20	12.046	1.819	1.400	0.881	12.451	2.179	1.677	1.035	13.092	2.749	2.116	1.331	13.703	3.292	2.534	1.595
90.0 deg 1.571 rad	0.40	15.156	4.584	3.528	2.220	16.175	5.489	4.226	2.639	17.790	6.926	5.332	3.335	19.330	8.295	6.385	4.018
	0.60	18.852	7.870	6.058	3.812	20.60	9.425	7.255	4.565	21.37	11.89	9.154	5.760	23.01	14.24	10.96	6.898
	0.80	22.98	11.54	8.890	5.594	24.55	13.83	10.64	6.699	24.62	17.44	13.43	8.452	27.50	20.89	16.08	10.12

Kennedy SCF Computation

T-joint In-Plane SCF Chord Side of Weld

Theta =	Tau = t/T	Gamma = 12.0				Gamma = 15.0				Gamma = 20.0				Gamma = 25.0			
		Beta = d/B				Beta = d/B				Beta = d/B				Beta = d/B			
		0.3	0.5	0.7	0.9	0.3	0.5	0.7	0.9	0.3	0.5	0.7	0.9	0.3	0.5	0.7	0.9
	0.20	10.551	0.540	0.533	0.528	10.631	0.618	0.610	0.603	10.749	0.734	0.724	0.717	10.857	0.840	0.828	0.820
30.0 deg	0.40	11.001	0.981	0.968	0.958	11.145	1.122	1.107	1.096	11.361	1.333	1.315	1.302	11.556	1.524	1.504	1.489
0.524 rad	0.60	11.419	1.391	1.372	1.358	11.623	1.590	1.569	1.553	11.929	1.890	1.864	1.846	12.205	2.160	2.131	2.110
	0.80	11.818	1.781	1.757	1.740	12.078	2.036	2.009	1.989	12.470	2.420	2.388	2.364	12.824	2.767	2.730	2.703
	0.20	10.672	0.658	0.650	0.643	10.768	0.753	0.743	0.735	10.913	0.895	0.883	0.874	11.044	1.023	1.009	0.999
45.0 deg	0.40	11.220	1.195	1.179	1.168	11.395	1.367	1.349	1.335	11.658	1.624	1.603	1.587	11.896	1.857	1.832	1.814
0.785 rad	0.60	11.729	1.694	1.672	1.655	11.977	1.937	1.911	1.892	12.350	2.302	2.272	2.249	12.687	2.632	2.597	2.571
	0.80	12.215	2.170	2.141	2.120	12.532	2.481	2.448	2.424	13.010	2.949	2.909	2.880	13.441	3.371	3.326	3.293
	0.20	10.754	0.739	0.729	0.722	10.863	0.845	0.834	0.825	11.025	1.004	0.991	0.981	11.172	1.148	1.133	1.122
60.0 deg	0.40	11.370	1.342	1.324	1.311	11.566	1.534	1.514	1.499	11.861	1.823	1.799	1.781	12.128	2.085	2.057	2.036
1.047 rad	0.60	11.941	1.902	1.877	1.858	12.220	2.175	2.146	2.124	12.638	2.585	2.550	2.524	13.016	2.935	2.915	2.886
	0.80	12.486	2.436	2.404	2.380	12.843	2.785	2.748	2.721	13.378	3.310	3.266	3.233	13.863	3.784	3.734	3.696
	0.20	10.819	0.802	0.792	0.784	10.936	0.917	0.905	0.896	11.113	1.090	1.076	1.065	11.272	1.247	1.230	1.218
90.0 deg	0.40	11.487	1.457	1.437	1.423	11.700	1.665	1.643	1.627	12.020	1.979	1.953	1.933	12.310	2.263	2.233	2.210
1.571 rad	0.60	12.107	2.065	2.037	2.017	12.409	2.361	2.329	2.306	12.863	2.805	2.768	2.740	13.274	3.207	3.164	3.133
	0.80	12.699	2.644	2.609	2.583	13.086	3.023	2.983	2.953	13.667	3.593	3.545	3.509	14.193	4.108	4.053	4.012

Kuang SCF Computation

T-joint Out-of-Plane SCF Chord Side of Weld

		Gamma = 12.0				Gamma = 15.0				Gamma = 20.0				Gamma = 25.0			
Theta =	Tau = t/T	Beta = d/B				Beta = d/B				Beta = d/B				Beta = d/B			
		0.3	0.55	0.56	0.75	0.3	0.55	0.56	0.75	0.3	0.55	0.56	0.75	0.3	0.55	0.56	0.75
	0.20	10.098	0.158	0.668	0.357	10.502	0.809	0.838	0.699	10.672	1.084	1.122	0.936	10.843	1.359	1.407	1.174
30.0 deg	0.40	10.182	0.293	1.238	1.033	10.930	1.499	1.552	1.295	11.246	2.007	2.078	1.734	11.562	2.517	2.606	2.174
0.524 rad	0.60	10.260	0.420	1.775	1.481	11.334	2.150	2.226	1.858	11.786	2.878	2.980	2.487	12.240	3.609	3.737	3.118
	0.80	10.337	0.543	2.292	1.913	11.723	2.777	2.875	2.399	12.307	3.717	3.848	3.212	12.893	4.662	4.826	4.027
	0.20	10.168	0.271	1.146	0.957	10.862	1.389	1.438	1.200	11.154	1.859	1.925	1.606	11.447	2.331	2.413	2.014
45.0 deg	0.40	10.312	0.503	2.123	1.772	11.596	2.572	2.663	2.222	12.137	3.443	3.565	2.975	12.680	4.318	4.470	3.730
0.785 rad	0.60	10.447	0.721	3.045	2.541	12.289	3.688	3.818	3.187	13.064	4.938	5.112	4.266	13.843	6.192	6.410	5.349
	0.80	10.578	0.931	3.933	3.282	12.956	4.763	4.931	4.115	13.958	6.377	6.602	5.510	14.963	7.996	8.278	6.909
	0.20	10.231	0.372	1.572	1.312	11.182	1.904	1.971	1.645	11.582	2.549	2.639	2.202	11.984	3.197	3.309	2.762
60.0 deg	0.40	10.428	0.689	2.912	2.430	12.189	3.527	3.651	3.047	12.930	4.722	4.888	4.079	13.674	5.921	6.129	5.115
1.047 rad	0.60	10.613	0.989	4.175	3.485	13.139	5.058	5.236	4.370	14.202	6.771	7.009	5.850	15.269	8.490	8.789	7.335
	0.80	10.792	1.277	5.392	4.500	14.054	6.332	6.762	5.643	15.427	8.744	9.052	7.535	16.805	10.96	11.35	9.673
	0.20	10.289	0.465	1.967	1.641	11.478	2.382	2.466	2.058	11.979	3.189	3.302	2.735	12.482	3.999	4.140	3.435
90.0 deg	0.40	10.535	0.862	3.643	3.040	12.738	4.412	4.568	3.812	13.666	5.907	6.115	5.103	14.597	7.407	7.668	6.399
1.571 rad	0.60	10.767	1.257	5.224	4.359	13.927	6.327	6.550	5.467	15.257	8.471	8.769	7.318	16.592	10.62	10.99	9.177
	0.80	10.991	1.597	6.746	5.630	15.071	8.171	8.459	7.060	16.789	10.93	11.32	9.451	18.513	13.71	14.20	11.85

C.3.2(b) Smedley-Wordsworth Chord SCF's for T-Joints

The Smedley-Wordsworth chord SCF's for T-joints are shown on the following pages. The following parameters are assumed for the Smedley-Wordsworth figures:

$$1) \quad \alpha = 2L/D = 35.0$$

The Shell d/D limitations have not been imposed for the SCF calculation.

Wordsworth-Sawley SCF Computation

T-joint Axial SCF Crown Position

Theta =	Tau = t/T	Gamma = 12.0				Gamma = 15.0				Gamma = 20.0				Gamma = 25.0			
		Beta = d/D				Beta = d/D				Beta = d/D				Beta = d/D			
		0.3	0.5	0.7	0.9	0.3	0.5	0.7	0.9	0.3	0.5	0.7	0.9	0.3	0.5	0.7	0.9
	0.25	12.847	3.058	3.203	3.283	12.928	3.081	3.177	3.218	13.049	3.148	3.180	3.166	13.207	3.228	3.206	3.145
30.0 deg 0.524 rad	0.50	15.223	5.799	6.084	6.094	15.296	5.719	5.907	5.871	15.492	5.734	5.793	5.678	15.716	5.823	5.775	5.583
	0.75	18.185	9.361	9.793	9.527	18.140	9.012	9.291	9.015	18.276	8.808	8.891	8.552	18.516	8.807	8.730	8.308
	1.00	111.80	13.88	14.49	13.71	111.53	13.08	13.46	12.75	111.48	12.46	12.57	11.87	111.66	12.26	12.15	11.38
	0.25	13.194	3.607	3.961	4.258	13.278	3.627	3.925	4.175	13.425	3.694	3.920	4.105	13.567	3.774	3.942	4.074
45.0 deg 0.785 rad	0.50	15.771	6.724	7.433	7.909	15.875	6.670	7.267	7.672	16.106	6.714	7.165	7.466	16.354	6.821	7.157	7.364
	0.75	18.785	10.47	11.54	12.03	18.829	10.21	11.11	11.54	19.059	10.11	10.78	11.10	19.359	10.16	10.67	10.87
	1.00	112.29	14.96	16.43	16.75	112.19	14.36	15.58	15.88	112.33	13.96	14.87	15.09	112.62	13.88	14.55	14.66
	0.25	13.218	3.814	4.364	4.868	13.294	3.827	4.320	4.772	13.428	3.884	4.304	4.690	13.557	3.954	4.318	4.651
60.0 deg 1.047 rad	0.50	15.749	7.026	8.128	9.058	15.869	7.001	7.986	8.830	16.104	7.063	7.905	8.631	16.345	7.175	7.903	8.531
	0.75	18.523	10.60	12.27	13.52	18.643	10.47	11.95	13.10	18.933	10.46	11.72	12.73	19.256	10.57	11.66	12.54
	1.00	111.57	14.63	16.88	18.33	111.65	14.30	16.29	17.65	111.94	14.14	15.83	17.03	112.32	14.19	15.65	16.71
	0.25	13.084	3.868	4.609	5.308	13.138	3.862	4.547	5.196	13.240	3.892	4.511	5.097	13.343	3.941	4.509	5.046
90.0 deg 1.571 rad	0.50	15.569	7.205	8.690	10.02	15.658	7.158	8.530	9.778	15.842	7.184	8.422	9.558	16.035	7.262	8.397	9.443
	0.75	18.220	10.81	13.05	14.93	18.315	10.67	12.73	14.51	18.550	10.64	12.50	14.13	18.814	10.71	12.41	13.93
	1.00	111.06	14.76	17.76	20.10	111.14	14.45	17.22	19.45	111.39	14.30	16.78	18.86	111.70	14.33	16.60	18.54

Worsworth-Sadlev SCF Computation

T-joint Axial SCF Saddle Position

		Gamma = 12.0				Gamma = 15.0				Gamma = 20.0				Gamma = 25.0			
Theta =	Tau = t/T	Beta =d/D				Beta =d/D				Beta =d/D				Beta =d/D			
		0.3	0.5	0.7	0.9	0.3	0.5	0.7	0.9	0.3	0.5	0.7	0.9	0.3	0.5	0.7	0.9
	0.25	0.992	0.973	0.770	0.402	1.115	1.216	0.963	0.502	1.487	1.622	1.284	0.670	1.858	2.028	1.606	0.838
30.0 deg 0.524 rad	0.50	1.784	1.946	1.541	0.804	2.230	2.433	1.927	1.005	2.974	3.244	2.569	1.340	3.717	4.056	3.212	1.676
	0.75	2.676	2.920	2.312	1.206	3.346	3.650	2.890	1.508	4.461	4.867	3.854	2.011	5.576	6.084	4.818	2.514
	1.00	3.569	3.893	3.083	1.609	4.461	4.867	3.854	2.011	5.948	6.489	5.139	2.681	7.435	8.112	6.424	3.352
	0.25	1.618	1.808	1.510	0.865	2.023	2.260	1.887	1.081	2.698	3.014	2.516	1.442	3.372	3.768	3.146	1.802
45.0 deg 0.785 rad	0.50	3.237	3.617	3.020	1.730	4.047	4.521	3.775	2.163	5.396	6.028	5.033	2.884	6.745	7.536	6.292	3.605
	0.75	4.856	5.426	4.530	2.596	6.070	6.782	5.662	3.245	8.094	9.043	7.550	4.326	10.11	11.30	9.438	5.408
	1.00	6.475	7.234	6.040	3.461	8.094	9.043	7.550	4.326	10.79	12.05	10.06	5.768	13.49	15.07	12.58	7.211
	0.25	2.293	2.598	2.237	1.354	2.867	3.248	2.797	1.693	3.823	4.331	3.729	2.257	4.778	5.413	4.662	2.821
60.0 deg 1.047 rad	0.50	4.587	5.197	4.475	2.709	5.734	6.496	5.594	3.386	7.646	8.662	7.459	4.515	9.557	10.82	9.324	5.643
	0.75	6.881	7.795	6.713	4.063	8.601	9.744	8.391	5.079	11.46	12.99	11.18	6.772	14.33	16.24	13.98	8.465
	1.00	9.175	10.39	8.951	5.418	11.46	12.99	11.18	6.772	15.29	17.32	14.91	9.030	19.11	21.65	18.64	11.28
	0.25	2.937	3.360	2.958	1.661	3.671	4.200	3.697	2.326	4.895	5.600	4.930	3.102	6.119	7.001	6.162	3.878
90.0 deg 1.571 rad	0.50	5.874	6.721	5.916	3.723	7.343	8.401	7.395	4.653	9.790	11.20	9.860	6.205	12.23	14.00	12.32	7.756
	0.75	8.811	10.08	8.874	5.584	11.01	12.60	11.09	6.980	14.68	16.80	14.79	9.307	18.35	21.00	18.48	11.63
	1.00	11.74	13.44	11.83	7.446	14.68	16.80	14.79	9.307	19.58	22.40	19.72	12.41	24.47	28.00	24.65	15.51

COPY AVAILABLE TO DTIC DOES NOT PERMIT FULLY LEGIBLE REPRODUCTION,

Wordsworth-Smedley SCF Computation

T-joint In-Plane SCF Crown Position

Theta =	Tau = t/T	Gamma = 12.0				Gamma = 15.0				Gamma = 20.0				Gamma = 25.0			
		Beta = d/D				Beta = d/D				Beta = d/D				Beta = d/D			
		0.3	0.5	0.7	0.9	0.3	0.5	0.7	0.9	0.3	0.5	0.7	0.9	0.3	0.5	0.7	0.9
	0.25	1.067	0.791	0.946	1.044	1.094	0.905	1.081	1.194	1.025	1.075	1.285	1.419	1.043	1.229	1.469	1.623
30.0 deg	0.50	1.057	1.378	1.647	1.819	1.209	1.575	1.883	2.080	1.437	1.872	2.238	2.471	1.642	2.141	2.558	2.826
0.524 rad	0.75	1.462	1.906	2.278	2.516	1.672	2.179	2.604	2.877	1.987	2.590	3.095	3.419	2.272	2.961	3.539	3.908
	1.00	1.841	2.399	2.868	3.167	2.105	2.743	3.278	3.621	2.501	3.260	3.896	4.303	2.860	3.727	4.455	4.920
	0.25	1.065	1.009	1.079	1.066	1.099	1.153	1.233	1.219	1.175	1.370	1.466	1.449	1.343	1.567	1.676	1.657
45.0 deg	0.50	1.506	1.756	1.879	1.857	1.721	2.008	2.148	2.123	2.046	2.386	2.553	2.523	2.339	2.728	2.918	2.885
0.785 rad	0.75	2.083	2.429	2.599	2.569	2.381	2.778	2.971	2.937	2.830	3.301	3.531	3.490	3.235	3.774	4.037	3.991
	1.00	2.622	3.058	3.271	3.234	2.998	3.497	3.740	3.697	3.562	4.155	4.445	4.394	4.073	4.751	5.082	5.023
	0.25	1.063	1.162	1.165	1.080	1.216	1.329	1.332	1.234	1.445	1.579	1.583	1.467	1.652	1.806	1.810	1.677
60.0 deg	0.50	1.852	2.024	2.029	1.880	2.117	2.314	2.320	2.149	2.516	2.750	2.757	2.554	2.876	3.144	3.152	2.920
1.047 rad	0.75	2.561	2.800	2.807	2.600	2.928	3.201	3.209	2.973	3.480	3.804	3.814	3.533	3.979	4.350	4.360	4.039
	1.00	3.224	3.525	3.533	3.273	3.686	4.030	4.040	3.742	4.381	4.789	4.801	4.448	5.009	5.475	5.489	5.085
	0.25	1.231	1.286	1.231	1.089	1.408	1.470	1.407	1.245	1.673	1.747	1.672	1.480	1.913	1.997	1.912	1.692
90.0 deg	0.50	2.144	2.239	2.143	1.896	2.452	2.559	2.450	2.168	2.914	3.042	2.912	2.576	3.331	3.478	3.329	2.946
1.571 rad	0.75	2.966	3.097	2.965	2.623	3.391	3.540	3.389	2.999	4.030	4.207	4.028	3.564	4.608	4.810	4.605	4.074
	1.00	3.734	3.898	3.732	3.302	4.269	4.457	4.267	3.775	5.075	5.296	5.070	4.486	5.800	6.055	5.797	5.129

Wordsworth-Sadley SCF Computation

T-joint Out-of-Plane SCF Saddle Position

Theta =	Tau = t/T	Gamma = 12.0				Gamma = 15.0				Gamma = 20.0				Gamma = 25.0			
		Beta = d/D				Beta = d/D				Beta = d/D				Beta = d/D			
		0.3	0.5	0.7	0.9	0.3	0.5	0.7	0.9	0.3	0.5	0.7	0.9	0.3	0.5	0.7	0.9
	0.25	10.529	0.773	0.825	0.556	10.662	0.967	1.031	0.695	10.883	1.289	1.375	0.927	11.103	1.612	1.719	1.159
30.0 deg	0.50	11.059	1.547	1.650	1.112	11.324	1.934	2.062	1.390	11.766	2.579	2.750	1.854	12.207	3.224	3.438	2.318
0.524 rad	0.75	11.589	2.321	2.475	1.669	11.986	2.902	3.094	2.086	12.649	3.869	4.125	2.781	13.311	4.837	5.157	3.477
	1.00	12.119	3.095	3.300	2.225	12.649	3.869	4.125	2.781	13.532	5.159	5.500	3.709	14.415	6.449	6.876	4.636
	0.25	10.872	1.347	1.561	1.176	11.090	1.684	1.951	1.470	11.454	2.245	2.602	1.960	11.818	2.807	3.252	2.450
45.0 deg	0.50	11.745	2.694	3.122	2.352	12.181	3.368	3.903	2.940	12.908	4.491	5.204	3.920	13.636	5.614	6.505	4.900
0.785 rad	0.75	12.618	4.042	4.683	3.528	13.272	5.053	5.854	4.410	14.363	6.737	7.806	5.880	15.454	8.421	9.757	7.351
	1.00	13.490	5.389	6.245	4.704	14.363	6.737	7.806	5.880	15.817	8.983	10.40	7.841	17.272	11.22	13.01	9.801
	0.25	11.168	1.863	2.267	1.822	11.460	2.329	2.833	2.278	11.947	3.106	3.778	3.037	12.434	3.882	4.723	3.796
60.0 deg	0.50	12.337	3.727	4.534	3.644	12.921	4.659	5.667	4.556	13.895	6.212	7.557	6.074	14.868	7.765	9.446	7.593
1.047 rad	0.75	13.505	5.591	6.801	5.467	14.382	6.989	8.501	6.834	15.842	9.318	11.33	9.112	17.303	11.64	14.16	11.39
	1.00	14.674	7.455	9.068	7.289	15.842	9.318	11.33	9.112	17.790	12.42	15.11	12.14	19.737	15.53	18.89	15.18
	0.25	11.437	2.346	2.954	2.486	11.796	2.932	3.692	3.108	12.395	3.910	4.923	4.144	12.994	4.887	6.154	5.180
90.0 deg	0.50	12.874	4.692	5.908	4.973	13.593	5.865	7.385	6.216	14.791	7.820	9.847	8.288	15.989	9.775	12.30	10.36
1.571 rad	0.75	14.312	7.038	8.862	7.459	15.390	8.797	11.07	9.324	17.187	11.73	14.77	12.43	18.984	14.66	18.46	15.54
	1.00	15.749	9.384	11.81	9.946	17.187	11.73	14.77	12.43	19.583	15.64	19.69	16.57	111.97	19.55	24.61	20.72

Kuang SCF Computation

K-joint Axial SCF
Chord Side of Weld

		Gamma = 12.0				Gamma = 15.0				Gamma = 20.0				Gamma = 25.0			
Theta =	Tan =	Beta = d/b				Beta = d/b				Beta = d/b				Beta = d/b			
	t/T	0.3	0.5	0.7	0.9	0.3	0.5	0.7	0.9	0.3	0.5	0.7	0.9	0.3	0.5	0.7	0.9
	0.20	10.427	0.414	0.406	0.400	10.495	0.481	0.471	0.464	10.600	0.582	0.571	0.562	10.696	0.676	0.662	0.653
30.0 deg	0.40	10.918	0.891	0.873	0.860	11.065	1.034	1.013	0.998	11.290	1.252	1.227	1.209	11.497	1.453	1.424	1.403
0.524 rad	0.60	11.437	1.394	1.367	1.347	11.667	1.618	1.586	1.562	12.019	1.939	1.921	1.892	12.343	2.273	2.229	2.196
	0.80	11.974	1.915	1.878	1.850	12.290	2.222	2.179	2.147	12.774	2.692	2.639	2.600	13.219	3.123	3.062	3.017
	0.20	10.724	0.702	0.688	0.678	10.840	0.815	0.799	0.787	11.017	0.987	0.967	0.953	11.180	1.145	1.122	1.106
45.0 deg	0.40	11.356	1.510	1.480	1.458	11.805	1.751	1.717	1.692	12.186	2.121	2.080	2.049	12.537	2.461	2.413	2.378
0.785 rad	0.60	12.434	2.362	2.316	2.282	12.825	2.741	2.687	2.647	13.421	3.320	3.254	3.206	13.969	3.852	3.776	3.720
	0.80	13.345	3.245	3.182	3.135	13.881	3.765	3.691	3.637	14.700	4.561	4.471	4.405	15.453	5.291	5.187	5.111
	0.20	10.985	0.956	0.937	0.923	11.143	1.109	1.087	1.071	11.384	1.343	1.317	1.297	11.606	1.539	1.528	1.505
60.0 deg	0.40	12.118	2.055	2.015	1.985	12.457	2.384	2.337	2.303	12.976	2.888	2.831	2.789	13.453	3.351	3.285	3.236
1.047 rad	0.60	13.314	3.215	3.152	3.106	13.845	3.731	3.657	3.604	14.657	4.519	4.430	4.365	15.403	5.243	5.140	5.064
	0.80	14.553	4.418	4.331	4.267	15.282	5.126	5.025	4.951	16.398	6.208	6.086	5.996	17.423	7.203	7.061	6.957
	0.20	11.226	1.190	1.166	1.149	11.423	1.380	1.353	1.333	11.723	1.672	1.639	1.615	11.999	1.940	1.902	1.874
90.0 deg	0.40	12.636	2.558	2.507	2.470	13.058	2.968	2.909	2.866	13.704	3.594	3.524	3.472	14.298	4.170	4.088	4.028
1.571 rad	0.60	14.124	4.002	3.923	3.866	14.785	4.643	4.552	4.485	15.796	5.624	5.513	5.432	16.725	6.525	6.397	6.303
	0.80	15.666	5.498	5.390	5.311	16.574	6.379	6.254	6.162	17.963	7.726	7.575	7.463	19.239	8.965	8.788	8.659

Kanag SCF Computation

K-joint In-Plane SCF Chord Side of Weld

Theta =	Tau = t/T	Gamma = 12.0				Gamma = 15.0				Gamma = 20.0				Gamma = 25.0			
		Beta = d/b				Beta = d/b				Beta = d/b				Beta = d/b			
		0.3	0.5	0.7	0.9	0.3	0.5	0.7	0.9	0.3	0.5	0.7	0.9	0.3	0.5	0.7	0.9
	0.20	10.514	0.530	0.541	0.549	10.539	0.577	0.589	0.598	10.624	0.644	0.657	0.667	10.679	0.700	0.715	0.726
30.0 deg 0.524 rad	0.40	10.986	1.017	1.038	1.054	11.074	1.107	1.130	1.147	11.198	1.235	1.260	1.279	11.304	1.344	1.372	1.393
	0.60	11.444	1.489	1.520	1.543	11.572	1.621	1.654	1.679	11.754	1.808	1.845	1.873	11.909	1.968	2.008	2.039
	0.80	11.893	1.952	1.992	2.022	12.060	2.124	2.168	2.201	12.298	2.370	2.418	2.455	12.502	2.580	2.632	2.672
	0.20	10.702	0.724	0.739	0.750	10.764	0.788	0.804	0.816	10.853	0.879	0.897	0.911	10.928	0.957	0.977	0.991
45.0 deg 0.785 rad	0.40	11.348	1.390	1.418	1.439	11.467	1.513	1.543	1.567	11.636	1.687	1.722	1.748	11.781	1.837	1.874	1.903
	0.60	11.973	2.034	2.076	2.107	12.148	2.214	2.260	2.294	12.396	2.470	2.521	2.559	12.608	2.689	2.744	2.786
	0.80	12.586	2.666	2.721	2.762	12.815	2.902	2.961	3.006	13.100	3.238	3.304	3.354	13.418	3.524	3.596	3.651
	0.20	10.843	0.869	0.887	0.900	10.917	0.946	0.965	0.980	11.023	1.035	1.077	1.093	11.114	1.149	1.172	1.190
60.0 deg 1.047 rad	0.40	11.617	1.668	1.702	1.728	11.761	1.815	1.852	1.881	11.964	2.025	2.066	2.098	12.138	2.204	2.249	2.284
	0.60	12.368	2.442	2.492	2.529	12.578	2.658	2.712	2.753	12.875	2.965	3.025	3.071	13.130	3.227	3.293	3.343
	0.80	13.103	3.200	3.265	3.315	13.378	3.483	3.554	3.608	13.768	3.886	3.965	4.025	14.102	4.230	4.316	4.382
	0.20	10.959	0.989	1.009	1.025	11.044	1.077	1.099	1.115	11.165	1.201	1.226	1.244	11.268	1.308	1.334	1.355
90.0 deg 1.571 rad	0.40	11.841	1.898	1.937	1.966	12.004	2.066	2.108	2.141	12.236	2.305	2.352	2.388	12.433	2.509	2.560	2.599
	0.60	12.695	2.779	2.836	2.879	12.934	3.025	3.087	3.134	13.273	3.375	3.444	3.496	13.563	3.673	3.748	3.805
	0.80	13.532	3.642	3.717	3.773	13.845	3.965	4.046	4.107	14.289	4.423	4.513	4.582	14.669	4.814	4.913	4.987

Kuang SCF Computation

K-joint Out-of-Plane SCF
Chord Side of Weld

		Gamma = 12.0				Gamma = 15.0				Gamma = 20.0				Gamma = 25.0			
Theta =	Tau = t/T	Beta = d/b				Beta = d/b				Beta = d/b				Beta = d/b			
		0.3	0.55	0.56	0.75	0.3	0.55	0.56	0.75	0.3	0.55	0.56	0.75	0.3	0.55	0.56	0.75
	0.20	0.400	0.645	0.668	0.557	0.502	0.809	0.838	0.699	0.672	1.084	1.122	0.936	0.843	1.359	1.407	1.174
30.0 deg	0.40	0.742	1.196	1.238	1.033	0.930	1.499	1.552	1.295	1.246	2.007	2.078	1.734	1.562	2.517	2.606	2.174
0.524 rad	0.60	1.064	1.715	1.775	1.481	1.334	2.150	2.226	1.858	1.786	2.878	2.980	2.487	2.240	3.609	3.737	3.118
	0.80	1.374	2.214	2.292	1.913	1.723	2.777	2.875	2.399	2.307	3.717	3.848	3.212	2.893	4.662	4.826	4.027
	0.20	0.687	1.107	1.146	0.957	0.862	1.389	1.438	1.200	1.154	1.859	1.925	1.606	1.447	2.331	2.413	2.014
45.0 deg	0.40	1.273	2.051	2.123	1.772	1.596	2.572	2.663	2.222	2.137	3.443	3.565	2.975	2.680	4.318	4.470	3.730
0.785 rad	0.60	1.825	2.941	3.045	2.541	2.289	3.688	3.818	3.187	3.064	4.938	5.112	4.266	3.843	6.192	6.410	5.349
	0.80	2.357	3.799	3.933	3.282	2.956	4.763	4.931	4.115	3.958	6.377	6.602	5.510	4.963	7.996	8.278	6.909
	0.20	0.942	1.519	1.572	1.312	1.182	1.904	1.971	1.645	1.582	2.549	2.639	2.202	1.984	3.197	3.309	2.762
60.0 deg	0.40	1.745	2.813	2.912	2.430	2.189	3.527	3.651	3.047	2.930	4.722	4.888	4.079	3.674	5.921	6.129	5.115
1.047 rad	0.60	2.503	4.033	4.175	3.485	3.139	5.058	5.236	4.370	4.202	6.771	7.009	5.850	5.269	8.490	8.789	7.335
	0.80	3.233	5.209	5.392	4.500	4.054	6.532	6.762	5.643	5.427	8.744	9.052	7.555	6.805	10.96	11.35	9.473
	0.20	1.179	1.900	1.967	1.641	1.478	2.382	2.466	2.058	1.979	3.189	3.302	2.755	2.482	3.999	4.140	3.455
90.0 deg	0.40	2.184	3.519	3.643	3.040	2.738	4.412	4.568	3.812	3.666	5.907	6.115	5.103	4.597	7.407	7.668	6.399
1.571 rad	0.60	3.131	5.046	5.224	4.359	3.927	6.327	6.550	5.467	5.257	8.471	8.769	7.318	6.592	10.62	10.99	9.177
	0.80	4.044	6.517	6.746	5.630	5.071	8.171	8.459	7.060	6.789	10.93	11.32	9.531	8.513	13.71	14.20	11.85

Northworth-Sandley SCF Computation

K-joint Axial SCF Crown Position

Theta =	Tau = t/T	Gamma = 12.0				Gamma = 15.0				Gamma = 20.0				Gamma = 25.0			
		Beta = d/D				Beta = d/D				Beta = d/D				Beta = d/D			
		0.3	0.5	0.7	0.9	0.3	0.5	0.7	0.9	0.3	0.5	0.7	0.9	0.3	0.5	0.7	0.9
	0.25	0.762	0.841	0.768	0.582	0.881	0.973	0.888	0.673	1.063	1.173	1.071	0.811	1.229	1.356	1.238	0.938
30.0 deg	0.50	1.525	1.683	1.537	1.164	1.763	1.946	1.777	1.346	2.126	2.347	2.143	1.622	2.458	2.713	2.477	1.876
0.524 rad	0.75	2.288	2.525	2.306	1.746	2.645	2.920	2.666	2.019	3.189	3.520	3.214	2.434	3.667	4.070	3.716	2.814
30.0 deg	1.00	3.051	3.367	3.075	2.328	3.527	3.893	3.555	2.692	4.253	4.694	4.286	3.245	4.916	5.426	4.955	3.752
	0.25	0.907	1.001	0.914	0.692	1.048	1.157	1.057	0.800	1.264	1.395	1.274	0.964	1.461	1.613	1.473	1.115
45.0 deg	0.50	1.814	2.002	1.828	1.384	2.097	2.315	2.114	1.600	2.528	2.791	2.548	1.929	2.923	3.226	2.946	2.231
0.785 rad	0.75	2.721	3.003	2.742	2.076	3.146	3.472	3.171	2.401	3.793	4.186	3.823	2.994	4.385	4.840	4.419	3.346
45.0 deg	1.00	3.628	4.005	3.657	2.769	4.195	4.630	4.228	3.201	5.057	5.582	5.097	3.859	5.847	6.453	5.893	4.462
	0.25	1.321	1.458	1.331	1.008	1.527	1.685	1.539	1.165	1.841	2.032	1.856	1.405	2.129	2.349	2.145	1.624
60.0 deg	0.50	2.642	2.916	2.663	2.016	3.055	3.371	3.079	2.331	3.683	4.065	3.712	2.810	4.258	4.699	4.291	3.249
1.047 rad	0.75	3.963	4.374	3.995	3.024	4.582	5.057	4.618	3.497	5.524	6.097	5.568	4.216	6.387	7.049	6.437	4.874
30.0 deg	1.00	5.285	5.833	5.326	4.033	6.110	6.743	6.158	4.662	7.366	8.130	7.424	5.621	8.516	9.399	8.533	6.499
	0.25	1.282	1.415	1.293	0.979	1.483	1.637	1.494	1.131	1.788	1.973	1.802	1.364	2.067	2.281	2.083	1.577
90.0 deg	0.50	2.565	2.831	2.586	1.958	2.966	3.274	2.989	2.263	3.576	3.947	3.604	2.729	4.134	4.563	4.167	3.155
1.571 rad	0.75	3.848	4.247	3.879	2.937	4.449	4.911	4.484	3.395	5.364	5.920	5.406	4.093	6.201	6.845	6.250	4.732
45.0 deg	1.00	5.131	5.663	5.172	3.916	5.932	6.548	5.979	4.527	7.152	7.894	7.209	5.458	8.269	9.125	8.334	6.310

Worsworth-Sandley SCF Computation

K-joint Axial SCF Saddle Position

Theta =	Tau = t/T	Gamma = 12.0				Gamma = 15.0				Gamma = 20.0				Gamma = 25.0			
		Beta = d/D				Beta = d/D				Beta = d/D				Beta = d/D			
		0.3	0.5	0.7	0.9	0.3	0.5	0.7	0.9	0.3	0.5	0.7	0.9	0.3	0.5	0.7	0.9
	0.25	10.531	0.579	0.458	0.239	10.614	0.670	0.530	0.276	10.723	0.788	0.624	0.325	10.799	0.871	0.690	0.360
30.0 deg	0.50	11.062	1.158	0.917	0.478	11.228	1.340	1.061	0.533	11.446	1.577	1.249	0.651	11.598	1.743	1.380	0.720
0.524 rad	—	—	—	—	—	—	—	—	—	—	—	—	—	—	—	—	—
30.0 deg	0.75	11.593	1.738	1.376	0.718	11.842	2.010	1.592	0.830	12.169	2.366	1.874	0.977	12.397	2.615	2.071	1.080
0.524 rad	—	—	—	—	—	—	—	—	—	—	—	—	—	—	—	—	—
	1.00	12.124	2.317	1.835	0.957	12.457	2.680	2.122	1.107	12.892	3.155	2.498	1.363	13.196	3.487	2.761	1.440
	0.25	10.963	1.076	0.898	0.515	11.114	1.245	1.039	0.595	11.311	1.465	1.223	0.701	11.449	1.619	1.352	0.774
45.0 deg	0.50	11.927	2.153	1.797	1.030	12.229	2.490	2.079	1.191	12.623	2.931	2.447	1.402	12.899	3.239	2.704	1.549
0.785 rad	—	—	—	—	—	—	—	—	—	—	—	—	—	—	—	—	—
45.0 deg	0.75	12.890	3.229	2.696	1.545	13.343	3.735	3.118	1.787	13.935	4.397	3.671	2.103	14.349	4.859	4.056	2.324
0.785 rad	—	—	—	—	—	—	—	—	—	—	—	—	—	—	—	—	—
	1.00	13.854	4.306	3.595	2.060	14.458	4.980	4.158	2.383	15.247	5.863	4.895	2.805	15.799	6.478	5.409	3.099
	0.25	11.323	1.539	1.399	0.916	11.520	1.779	1.633	1.086	11.769	2.090	1.955	1.331	11.930	2.305	2.200	1.537
60.0 deg	0.50	12.646	3.078	2.798	1.833	13.041	3.558	3.267	2.172	13.538	4.181	3.710	2.663	13.860	4.611	4.401	3.075
1.047 rad	—	—	—	—	—	—	—	—	—	—	—	—	—	—	—	—	—
30.0 deg	0.75	13.969	4.618	4.197	2.750	14.561	5.337	4.901	3.258	15.308	6.271	5.866	3.795	15.790	6.917	6.602	4.613
0.524 rad	—	—	—	—	—	—	—	—	—	—	—	—	—	—	—	—	—
	1.00	15.292	6.157	5.596	3.667	16.082	7.116	6.534	4.344	17.077	8.362	7.821	5.327	17.720	9.223	8.803	6.150
	0.25	11.714	1.994	1.817	1.207	11.975	2.305	2.115	1.420	12.308	2.710	2.517	1.719	12.530	2.992	2.815	1.960
90.0 deg	0.50	13.428	3.988	3.634	2.415	13.950	4.610	4.230	2.940	14.617	5.421	5.034	3.439	15.061	5.984	5.631	3.920
1.571 rad	—	—	—	—	—	—	—	—	—	—	—	—	—	—	—	—	—
45.0 deg	0.75	15.143	5.982	5.452	3.623	15.925	6.916	6.346	4.260	16.925	8.132	7.551	5.159	17.592	8.976	8.446	5.380
0.785 rad	—	—	—	—	—	—	—	—	—	—	—	—	—	—	—	—	—
	1.00	16.857	7.977	7.269	4.831	17.900	9.221	8.461	5.680	19.234	10.84	10.06	6.879	10.12	11.96	11.26	7.840

COPY AVAILABLE TO DTIC DOES NOT PERMIT FULLY LEGIBLE REPRODUCTION

Wordsworth-Seadley SCF Computation

K-joint In-Plane SCF Crown Position

		Gamma = 12.0				Gamma = 15.0				Gamma = 20.0				Gamma = 25.0			
Theta =	Tau = t/T	Beta =d/D				Beta =d/D				Beta =d/D				Beta =d/D			
		0.3	0.5	0.7	0.9	0.3	0.5	0.7	0.9	0.3	0.5	0.7	0.9	0.3	0.5	0.7	0.9
	0.25	0.607	0.791	0.946	1.044	0.694	0.905	1.081	1.194	0.825	1.075	1.285	1.419	0.943	1.229	1.469	1.623
30.0 deg	0.50	1.057	1.378	1.647	1.819	1.209	1.575	1.883	2.080	1.437	1.872	2.238	2.471	1.642	2.141	2.558	2.826
0.524 rad	0.75	1.462	1.906	2.278	2.516	1.672	2.179	2.604	2.977	1.987	2.590	3.095	3.419	2.272	2.961	3.539	3.908
	1.00	1.841	2.399	2.868	3.167	2.105	2.743	3.278	3.621	2.501	3.260	3.896	4.303	2.860	3.727	4.455	4.920
	0.25	0.865	1.009	1.079	1.066	0.989	1.153	1.233	1.219	1.175	1.370	1.466	1.449	1.343	1.567	1.676	1.657
45.0 deg	0.50	1.506	1.756	1.879	1.857	1.721	2.008	2.148	2.123	2.046	2.386	2.553	2.523	2.339	2.728	2.918	2.885
0.785 rad	0.75	2.083	2.429	2.599	2.569	2.381	2.778	2.971	2.937	2.830	3.301	3.531	3.490	3.235	3.774	4.037	3.991
	1.00	2.622	3.058	3.271	3.234	2.998	3.497	3.740	3.677	3.562	4.155	4.445	4.394	4.073	4.751	5.082	5.023
	0.25	1.063	1.162	1.165	1.080	1.216	1.329	1.332	1.234	1.445	1.579	1.583	1.467	1.652	1.806	1.810	1.677
60.0 deg	0.50	1.852	2.024	2.029	1.880	2.117	2.314	2.320	2.149	2.516	2.750	2.757	2.554	2.876	3.144	3.152	2.920
1.047 rad	0.75	2.561	2.800	2.807	2.600	2.928	3.201	3.209	2.973	3.480	3.804	3.814	3.533	3.979	4.350	4.360	4.039
	1.00	3.224	3.525	3.533	3.273	3.686	4.030	4.040	3.742	4.361	4.789	4.801	4.448	5.009	5.475	5.489	5.085
	0.25	1.231	1.286	1.231	1.089	1.408	1.470	1.407	1.245	1.673	1.747	1.672	1.480	1.913	1.997	1.912	1.692
70.0 deg	0.50	2.144	2.239	2.143	1.896	2.452	2.539	2.450	2.168	2.914	3.042	2.912	2.576	3.331	3.478	3.329	2.946
1.571 rad	0.75	2.966	3.097	2.965	2.623	3.391	3.540	3.389	2.999	4.030	4.207	4.028	3.564	4.608	4.810	4.605	4.074
	1.00	3.734	3.898	3.732	3.302	4.269	4.457	4.267	3.775	5.073	5.296	5.070	4.486	5.800	6.055	5.797	5.129

COPY AVAILABLE TO DTIC DOES NOT PERMIT FULLY LEGIBLE REPRODUCTION

Wordsworth-Sandley SCF Computation

K-joint Out-of-Plane SCF Saddle Position

		Gamma = 12.0				Gamma = 15.0				Gamma = 20.0				Gamma = 25.0			
Theta =	Tau =	Beta = d/D				Beta = d/D				Beta = d/D				Beta = d/D			
	t/T	0.3	0.5	0.7	0.9	0.3	0.5	0.7	0.9	0.3	0.5	0.7	0.9	0.3	0.5	0.7	0.9
	0.25	10.203	0.393	0.504	0.390	10.287	0.555	0.713	0.552	10.448	0.868	1.113	0.862	10.634	1.226	1.573	1.218
30.0 deg	0.50	10.406	0.786	1.009	0.781	10.574	1.111	1.426	1.104	10.897	1.736	2.227	1.724	11.268	2.453	3.147	2.437
0.524 rad	—	—	—	—	—	—	—	—	—	—	—	—	—	—	—	—	—
30.0 deg	0.75	10.609	1.179	1.513	1.171	10.861	1.667	2.139	1.656	11.246	2.604	3.341	2.586	11.902	3.680	4.721	3.655
0.524 rad	—	—	—	—	—	—	—	—	—	—	—	—	—	—	—	—	—
	1.00	10.813	1.573	2.018	1.562	11.149	2.223	2.852	2.208	11.794	3.472	4.454	3.448	12.536	4.907	6.295	4.874
	0.25	10.334	0.684	0.954	0.825	10.473	0.967	1.349	1.167	10.739	1.511	2.107	1.822	11.044	2.135	2.977	2.576
45.0 deg	0.50	10.669	1.369	1.909	1.651	10.946	1.935	2.698	2.334	11.478	3.022	4.214	3.645	12.089	4.271	5.955	5.152
0.785 rad	—	—	—	—	—	—	—	—	—	—	—	—	—	—	—	—	—
45.0 deg	0.75	11.004	2.054	2.863	2.477	11.419	2.902	4.047	3.501	12.217	4.534	6.321	5.468	13.133	6.407	8.933	7.728
0.785 rad	—	—	—	—	—	—	—	—	—	—	—	—	—	—	—	—	—
	1.00	11.339	2.738	3.818	3.303	11.892	3.870	5.396	4.668	12.956	6.045	8.428	7.291	14.178	8.543	11.91	10.30
	0.25	12.606	5.361	7.563	6.680	13.683	7.576	10.68	9.441	15.753	11.83	16.69	14.74	18.130	16.72	23.59	20.83
60.0 deg	0.50	15.213	10.72	15.12	13.36	17.367	15.15	21.37	18.88	111.50	23.66	33.38	29.49	116.26	33.44	47.18	41.67
1.047 rad	—	—	—	—	—	—	—	—	—	—	—	—	—	—	—	—	—
70.0 deg	0.75	17.819	16.08	22.68	20.04	111.05	22.73	32.06	28.32	117.26	35.50	50.08	44.23	124.39	50.17	70.77	62.51
0.524 rad	—	—	—	—	—	—	—	—	—	—	—	—	—	—	—	—	—
	1.00	110.42	21.44	30.25	26.72	124.73	30.30	42.75	37.76	123.91	47.33	66.77	58.98	132.52	66.89	94.37	83.35
	0.25	13.545	7.507	11.04	10.28	15.010	10.60	15.60	14.53	17.826	16.57	24.37	22.70	111.06	23.41	34.45	32.98
90.0 deg	0.50	17.091	15.01	22.08	20.57	110.02	21.21	31.21	29.07	115.65	33.14	48.75	45.41	122.12	46.83	68.90	64.17
1.571 rad	—	—	—	—	—	—	—	—	—	—	—	—	—	—	—	—	—
45.0 deg	0.75	110.63	22.52	33.13	30.85	115.03	31.82	46.82	43.61	123.47	49.71	73.13	68.11	133.18	70.23	103.3	96.26
0.785 rad	—	—	—	—	—	—	—	—	—	—	—	—	—	—	—	—	—
	1.00	114.18	30.03	44.17	41.14	120.04	42.43	62.42	58.14	131.30	66.28	97.50	90.82	144.24	93.67	137.8	128.3

Wordsworth-Seadley SCF Computation

X-joint Axial SCF Saddle Position

Theta =	Tau = t/T	Gamma = 12.0				Gamma = 15.0				Gamma = 20.0				Gamma = 25.0			
		Beta = d/D				Beta = d/D				Beta = d/D				Beta = d/D			
		0.3	0.5	0.7	0.9	0.3	0.5	0.7	0.9	0.3	0.5	0.7	0.9	0.3	0.5	0.7	0.9
	0.25	1.775	1.269	0.926	0.893	12.218	1.587	1.157	1.116	12.958	2.116	1.543	1.488	13.697	2.645	1.929	1.860
30.0 deg	0.50	13.550	2.539	1.852	1.786	14.437	3.174	2.315	2.232	15.916	4.232	3.087	2.977	17.395	5.290	3.859	3.721
0.524 rad	0.75	15.325	3.808	2.778	2.679	16.656	4.761	3.473	3.349	18.875	6.348	4.631	4.465	11.09	7.935	5.789	5.582
	1.00	17.100	5.078	3.705	3.572	18.975	6.348	4.631	4.465	11.83	8.464	6.175	5.954	14.79	10.58	7.718	7.443
	0.25	12.476	2.495	2.135	1.583	13.095	3.119	2.669	1.979	14.127	4.159	3.559	2.639	15.159	5.199	4.449	3.299
45.0 deg	0.50	14.953	4.991	4.271	3.167	16.191	6.239	5.339	3.959	18.255	8.319	7.119	5.278	10.31	10.39	9.899	6.598
0.785 rad	0.75	17.430	7.487	6.407	4.750	19.287	9.358	8.009	5.938	12.38	12.47	10.67	7.918	15.47	15.59	13.34	9.897
	1.00	19.906	9.982	8.543	6.334	12.38	12.47	10.67	7.918	16.51	16.63	14.23	10.55	20.63	20.79	17.79	13.19
	0.25	13.009	3.705	3.482	2.213	13.761	4.632	4.352	2.767	15.015	6.176	5.803	3.689	16.269	7.720	7.254	4.612
60.0 deg	0.50	16.019	7.411	6.964	4.427	17.523	9.264	8.705	5.534	10.03	12.35	11.60	7.379	12.53	15.44	14.50	9.224
1.047 rad	0.75	19.028	11.11	10.44	6.641	11.28	13.89	13.05	8.501	15.04	18.52	17.41	11.06	18.80	23.16	21.76	13.33
	1.00	112.03	14.82	13.92	8.655	15.04	18.52	17.41	11.06	20.06	24.70	23.21	14.75	25.07	30.88	29.01	18.44

COPY AVAILABLE TO DTIC DOES NOT PERMIT FULLY LEGIBLE REPRODUCTION

Wordsworth-Smedley SCF Computation

X-joint In-Plane SCF Crown Position

Theta =	Tau = t/T	Gamma = 12.0				Gamma = 15.0				Gamma = 20.0				Gamma = 25.0			
		Beta = d/D				Beta = d/D				Beta = d/D				Beta = d/D			
		0.3	0.5	0.7	0.9	0.3	0.5	0.7	0.9	0.3	0.5	0.7	0.9	0.3	0.5	0.7	0.9
	0.25	10.607	0.791	0.946	1.044	10.694	0.905	1.081	1.194	10.825	1.075	1.285	1.419	10.743	1.229	1.469	1.623
30.0 deg	0.50	11.057	1.378	1.647	1.819	11.209	1.575	1.983	2.080	11.437	1.872	2.238	2.471	11.642	2.141	2.558	2.826
0.524 rad	0.75	11.462	1.906	2.278	2.516	11.672	2.179	2.604	2.877	11.987	2.590	3.095	3.419	12.272	2.961	3.539	3.908
	1.00	11.941	2.399	2.868	3.167	12.105	2.743	3.278	3.621	12.501	3.260	3.896	4.303	12.860	3.727	4.455	4.920
	0.25	10.865	1.009	1.079	1.066	10.989	1.153	1.233	1.219	11.175	1.370	1.466	1.449	11.343	1.567	1.676	1.657
45.0 deg	0.50	11.506	1.756	1.879	1.857	11.721	2.008	2.148	2.123	12.046	2.386	2.533	2.523	12.339	2.728	2.918	2.885
0.785 rad	0.75	12.083	2.429	2.599	2.569	12.381	2.778	2.971	2.937	12.830	3.301	3.531	3.490	13.235	3.774	4.037	3.991
	1.00	12.622	3.058	3.271	3.234	12.998	3.497	3.740	3.697	13.562	4.135	4.445	4.394	14.073	4.751	5.082	5.023
	0.25	11.063	1.162	1.165	1.080	11.216	1.329	1.332	1.234	11.445	1.579	1.583	1.467	11.652	1.806	1.810	1.677
60.0 deg	0.50	11.852	2.024	2.029	1.980	12.117	2.314	2.320	2.149	12.516	2.750	2.757	2.584	12.976	3.144	3.152	2.920
1.047 rad	0.75	12.561	2.800	2.807	2.600	12.928	3.201	3.209	2.973	13.480	3.804	3.814	3.533	13.979	4.350	4.360	4.039
	1.00	13.224	3.525	3.533	3.273	13.686	4.030	4.040	3.742	14.381	4.789	4.801	4.448	15.009	5.475	5.489	5.085

Wordsworth-Sadley SCF Computation

X-joint Out-of-Plane SCF Saddle Position

Theta =	Tau = t/T	Gamma = 12.0				Gamma = 15.0				Gamma = 20.0				Gamma = 25.0			
		Beta =d/D				Beta =d/D				Beta =d/D				Beta =d/D			
		0.3	0.5	0.7	0.9	0.3	0.5	0.7	0.9	0.3	0.5	0.7	0.9	0.3	0.5	0.7	0.9
	0.25	0.719	0.587	0.519	0.599	0.899	0.734	0.648	0.749	1.199	0.979	0.865	0.999	1.498	1.224	1.081	1.248
30.0 deg	0.50	1.438	1.175	1.038	1.198	1.798	1.469	1.297	1.498	2.398	1.959	1.730	1.998	2.997	2.449	2.163	2.497
0.524 rad	0.75	2.158	1.763	1.557	1.798	2.698	2.204	1.946	2.247	3.597	2.939	2.595	2.997	4.496	3.674	3.244	3.746
	1.00	2.877	2.351	2.076	2.597	3.597	2.939	2.595	2.997	4.796	3.719	3.461	3.996	5.995	4.899	4.326	4.995
	0.25	1.003	1.153	1.197	1.062	1.254	1.444	1.496	1.328	1.673	1.926	1.995	1.771	2.091	2.407	2.494	2.214
45.0 deg	0.50	2.007	2.311	2.394	2.125	2.509	2.889	2.992	2.656	3.346	3.852	3.990	3.542	4.183	4.815	4.968	4.428
0.785 rad	0.75	3.011	3.466	3.591	3.188	3.764	4.333	4.489	3.985	5.019	5.778	5.985	5.313	6.274	7.222	7.482	6.642
	1.00	4.015	4.622	4.788	4.251	5.019	5.778	5.985	5.313	6.692	7.704	7.981	7.085	8.366	9.630	9.976	8.856
	0.25	1.219	1.715	1.951	1.485	1.524	2.144	2.439	1.857	2.033	2.859	3.252	2.476	2.541	3.574	4.066	3.095
60.0 deg	0.50	2.439	3.431	3.903	2.771	3.049	4.289	4.879	3.714	4.066	5.719	6.505	4.952	5.083	7.149	8.132	6.190
1.047 rad	0.75	3.659	5.147	5.855	4.457	4.574	6.434	7.318	5.571	6.099	8.579	9.758	7.428	7.624	10.72	12.19	9.285
	1.00	4.879	6.863	7.806	5.942	6.099	8.579	9.758	7.428	8.132	11.43	13.01	9.904	10.16	14.29	16.26	12.38

C.4 FINITE ELEMENT ANALYSES RESULTS

Finite element analyses were performed on the connections between the column tops and upper hull girders and between the corner columns and tubular bracing of the column-stabilized, twin-hulled semisubmersible. The overall geometry and locations of the two connections are indicated in Figures C.4-1 and C.4-2. Longitudinal and transverse girders (8.2 m deep) coincide with the column faces. The columns are 10.6 by 10.6 m in cross section.

Some dimensions of interest are:

Overall length	96.0 m
Overall width	65.0 m

Lower Hulls (two)

Length	96.0 m
Width	16.5 m
Depth	8.0 m

Stability Columns (six)

Size (square w/ rounded corners)	10.6x10.6 m
Transverse spacing (center-to-center)	54.0 m
Longitudinal spacing	33.0 m

Upper Hull

Length	77.0 m
Width	65.0 m
Depth	8.2 m

C.4.1 Column-Girder Connection

The location of the connection is shown in Figure C.4-1. The joint dimensions are given in Figure C.4-3. The loading analyzed was a combined axial, shear and moment load. The SCF is defined as:

MAXIMUM PRINCIPAL STRESS

$$SCF = \frac{\text{MAXIMUM PRINCIPAL STRESS}}{\text{NOMINAL STRESS IN GIRDER (P/A + M/S)}}$$

The moment M is due to a combination of moment and shear load.

The maximum SCF was found in the gusset plate connecting the transverse girder and column top, at the edge of the gusset plate in the weld between the gusset web and flange. It was equal to 1.66. The SCF in the longitudinal girder at the windlass cutouts reached a value of 1.87. Figure C.4-4 shows the equivalent stress variation over the entire connection. The maximum stress, as already noted, occurs in the crotch region. Figure C.4-5 shows an equivalent stress contour plot of the windlass holes. Table C.4-1 summarizes the SCFs.

MEMBER	LOCATION	DIRECTION TO WELD	SCF
Center Column Transverse	Middle of Gusset	Parallel	1.66
Girder-Column Connection	Gusset-Girder Connection	Perpendicular	1.37
2.3x2.3x1.1 m Gusset	Gusset-Column Connection	Perpendicular	1.10
	Girder Flange	Parallel	1.05
Longitudinal Girder-Column Connection	Middle of Gusset	Parallel	1.52
	Gusset-Girder Connection	Perpendicular	1.14
1.1x1.1x.55 m	Gusset-Column Connection	Perpendicular	1.05
	Girder Flange	Parallel	1.01
Exterior Longitudinal Girder	Bottom Right Corner of Exterior Hole	Parallel	1.87
@ Windlass Holes	Upper Left Corner of Interior Hole	Parallel	1.73

Table C.4-1 Summary of SCFs for a Column - Girder Connection

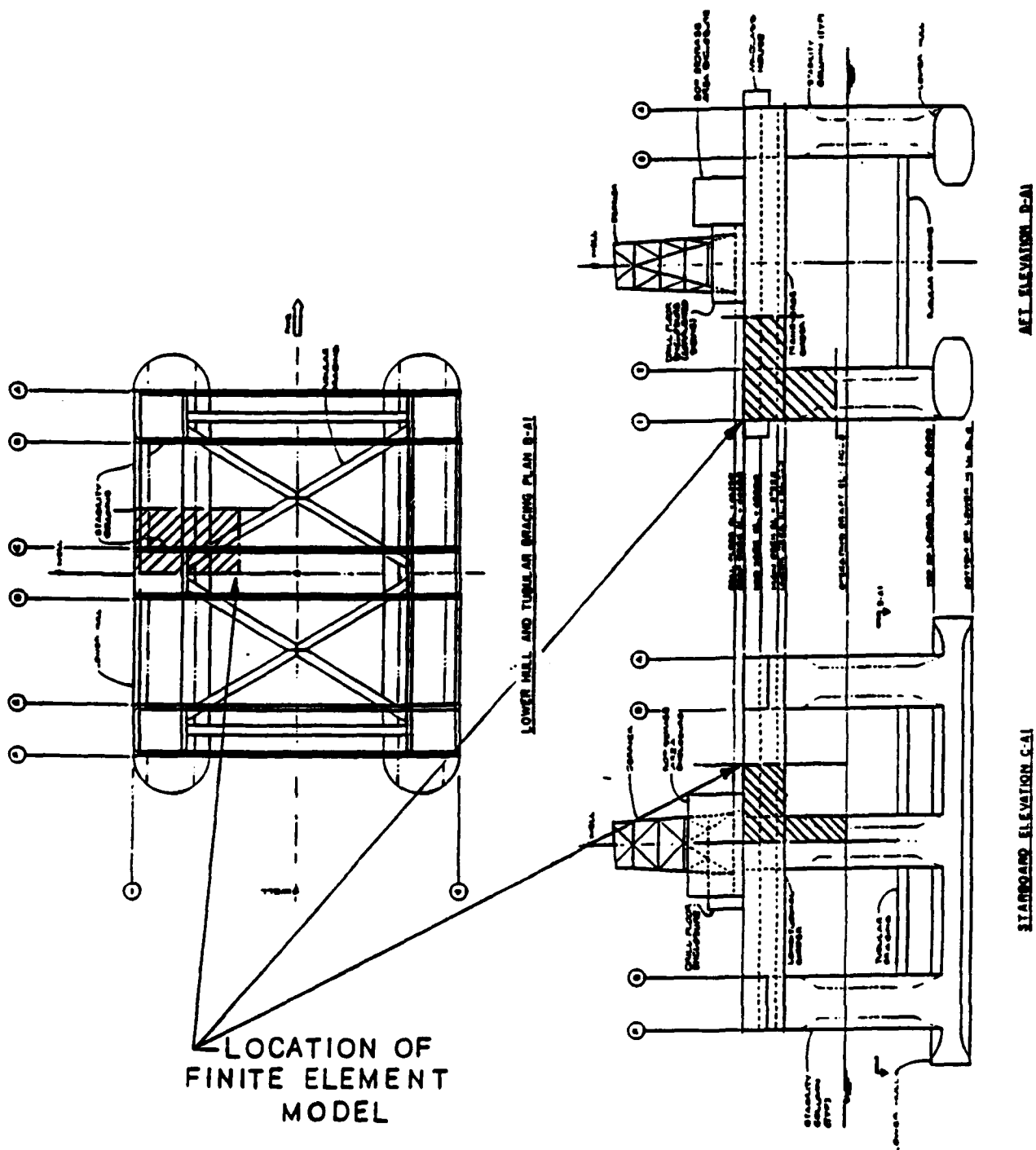


Figure C.4-1 Overall Geometry of Vessel and Location of Column-to-Girder Connection

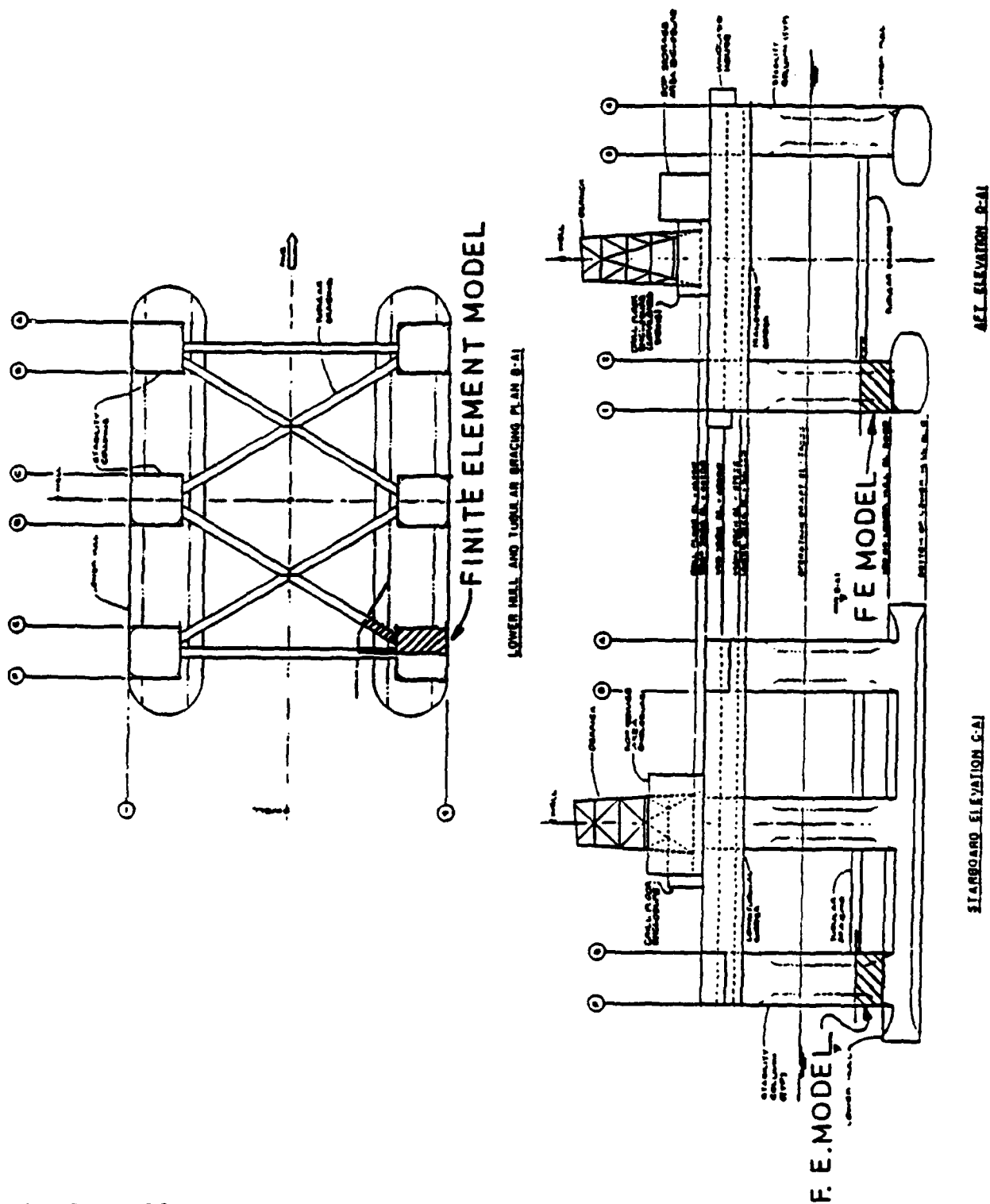


Figure C.4-2 Overall Geometry of Vessel and Location of Corner Column Tubular Connection

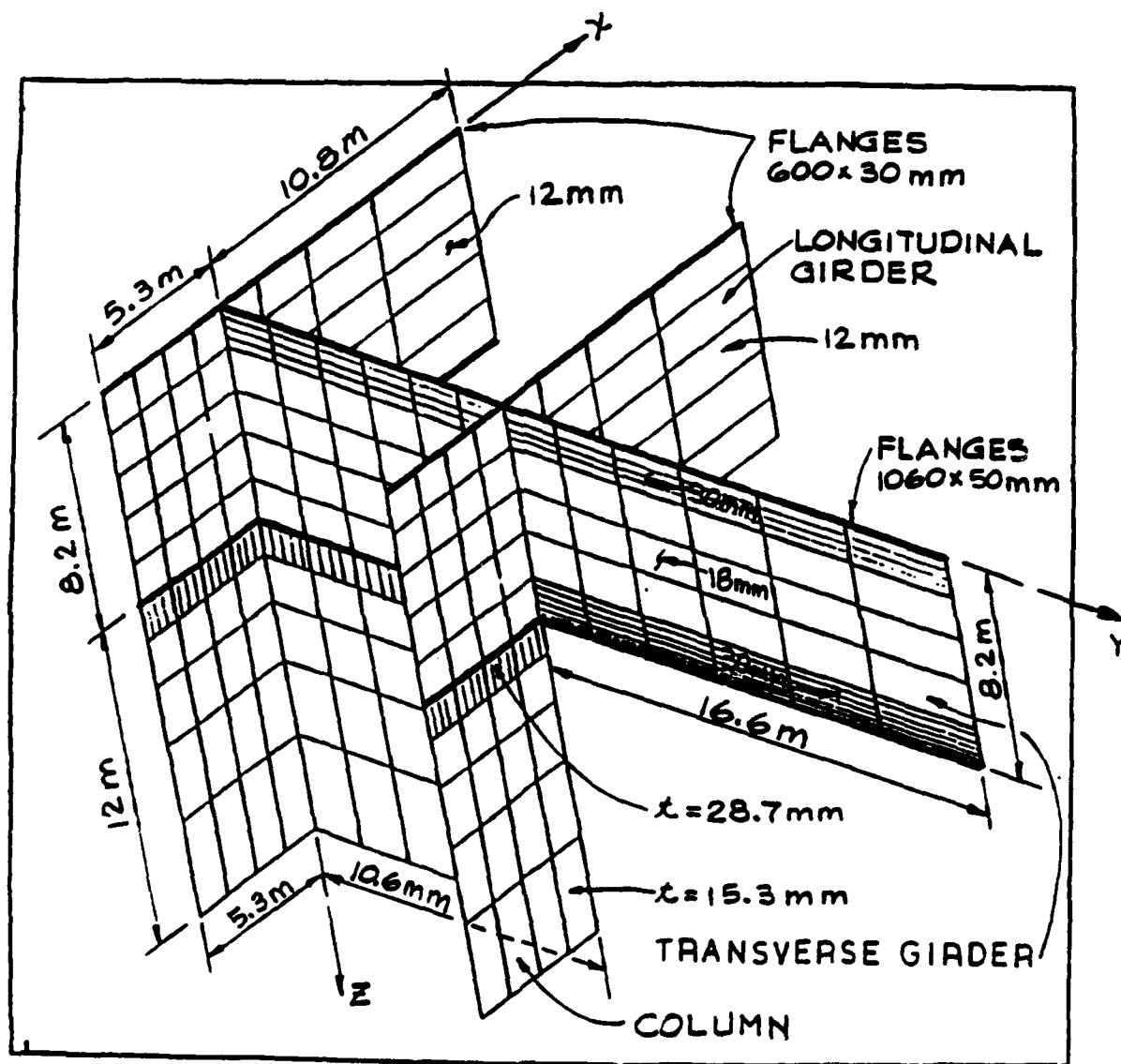


Figure C.4-3 Finite Element Model and Dimensions of Column-to-Girder Connection

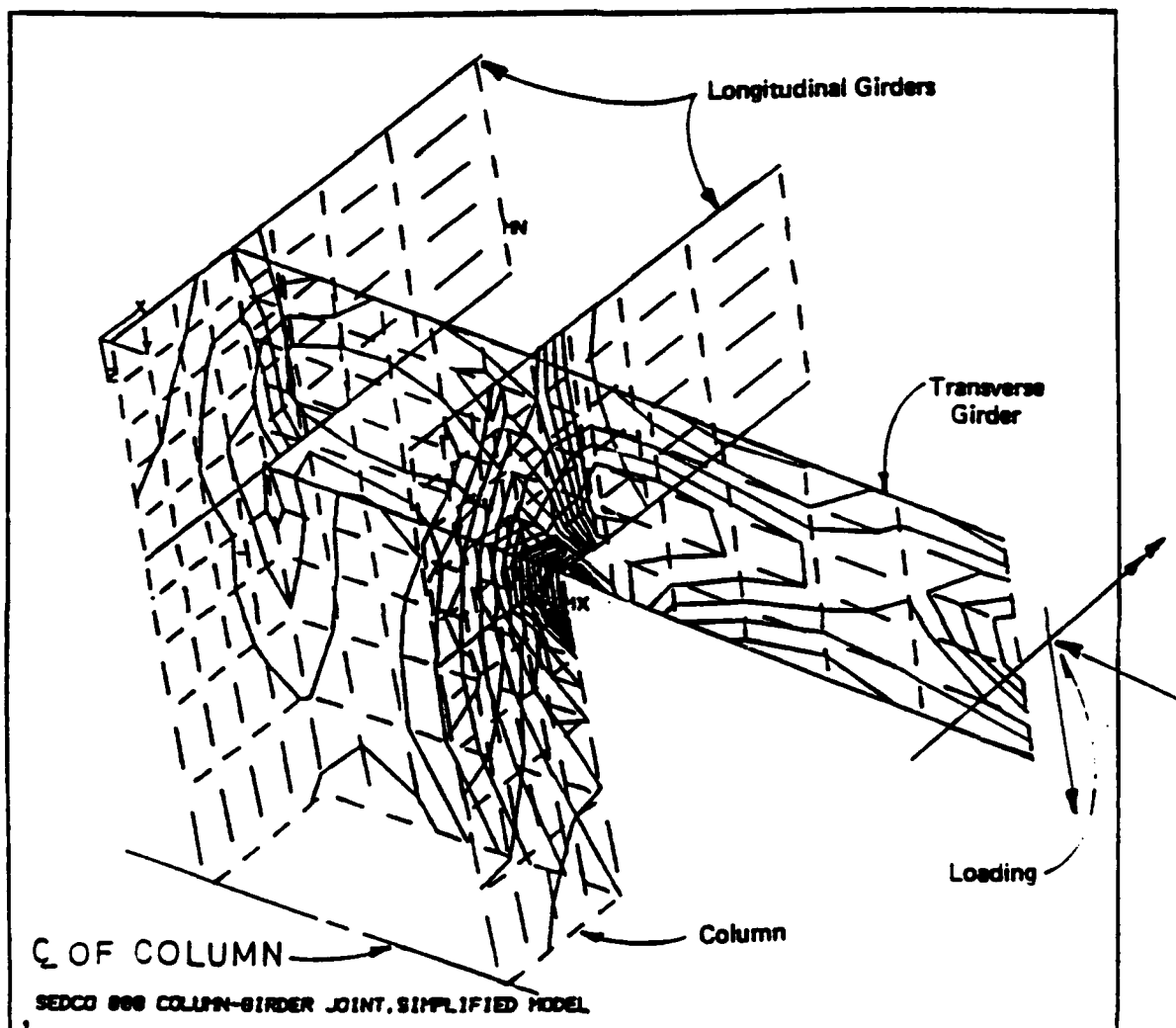


Figure C.4-4 Equivalent Stress Contour Plot for the Column-to-Girder Connection

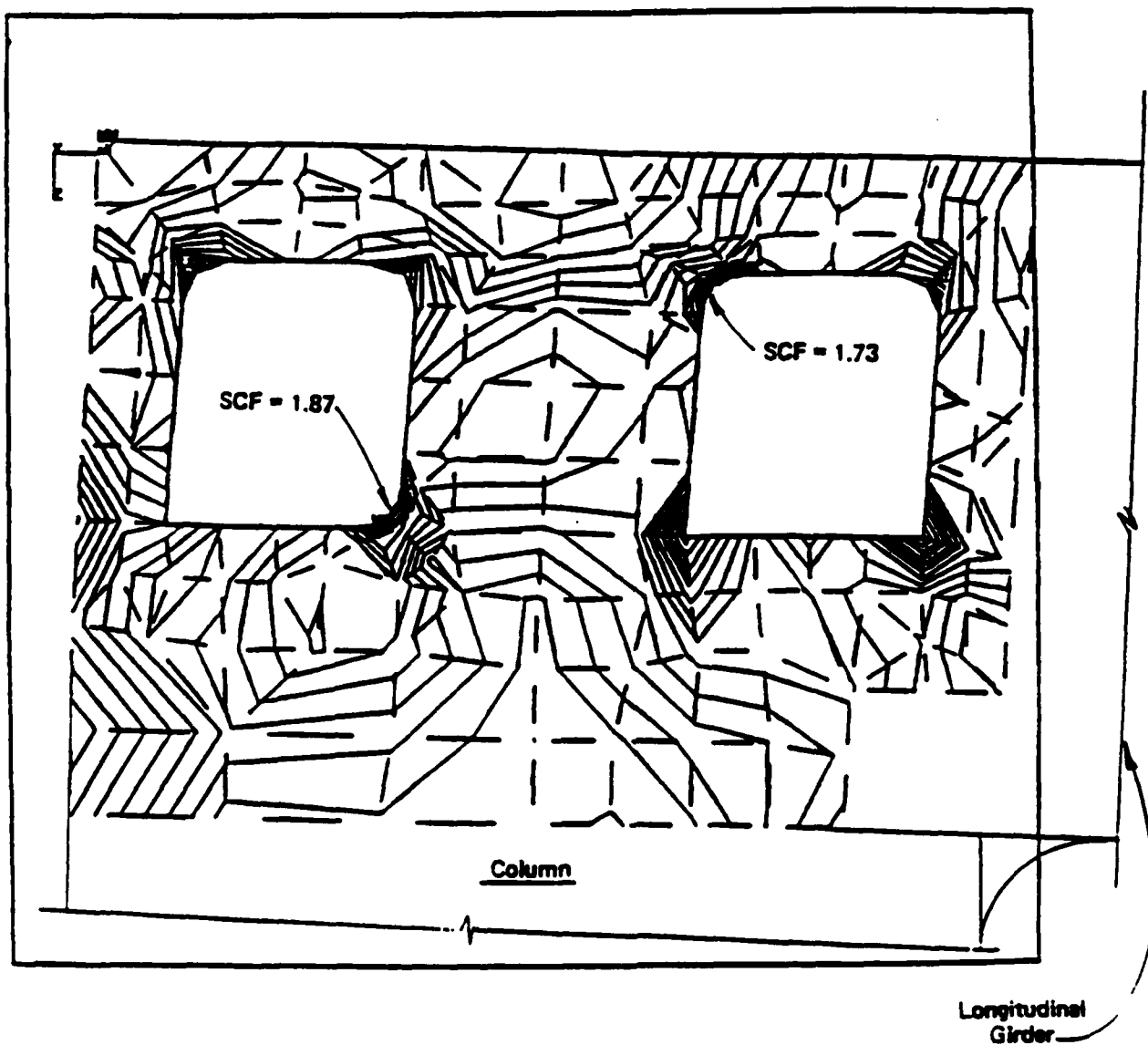


Figure C.4-5 Equivalent Stress Contour Plot of Windlass Holes

C.5

REFERENCES

- C.1 Kuang, J.G. et al., "Stress Concentrations in Tubular Joints," Proceedings of Offshore Technology Conference, OTC Paper No. 2205, Houston, TX. 1975 (Revisions introduced in SPE Journal, pp. 287-299, August 1977).

- C.2 Wordsworth, A.C., "Stress Concentration Factors at K and KT Tubular Joints," Fatigue in Offshore Structural Steels, Institution of Civil Engineers, London, February 1981.

- C.3 Wordsworth, A.C., "Aspects of Stress Concentration Factors at Tubular Joints," TS8, Proceedings of the 3rd International Offshore Conference on Steel in Marine Structures, (SIMS 87), Delft, The Netherlands, June 1987.

- C.4 Gibstein, M.B., "Parametric Stress Analyses of T Joints," Paper No. 26, European Offshore Steels Research Seminar, Cambridge, November 1978.

- C.5 Gibstein, M.B., "Stress Concentration in Tubular K Joints with Diameter Ratio Equal to One," TS10, International Offshore Conference on Steel in Marine Structures (SIMS 87), Delft, The Netherlands, 1985.

- C.6 Efthymiou, M., et al. "Stress Concentrations in T/Y and Gap/Overlap K Joints," The 4th International Conference on Behavior of Offshore Structures (BOSS 1985), Amsterdam, The Netherlands, 1985.

- C.7 Marshall, P.W. and Luyties, W.H., "Allowable Stresses for Fatigue Design," International Conference on Behavior of Offshore Structures (BOSS 1982), Cambridge, Massachusetts, August 1982.

- C.8 Underwater Engineering Group, "Design of Tubular Joints for Offshore Structures," UEG Publication, UR33, 1985.
- C.9 Kellogg, M.W., "Design of Piping Systems", Second Edition, Wiley, 1956.
- C.10 Delft, van D.R.V. et al. "The Results of the European Fatigue Tests on Welded Tubular Joints Compared with SCF Formulas and Design Lives," Paper No. TS 24, Proceedings of the 3rd International Conference on Steel in Marine Structures (SIMS 87), Delft, The Netherlands, June 1987.
- C.11 Ma, S.Y., Tebbett, I.E., "Estimations of Stress Concentration Factors for Fatigue Design of Welded Tubular Connections," Proceedings of the 20th Annual Offshore Technology Conference, OTC Paper No. 5666, Houston, TX., May 1988.
- C.12 Tebbett, I.E., and Lalani, M., "A New Approach to Stress Concentration Factors for Tubular Joint Design," Proceedings of 16th Annual Offshore Technology Conference, ITC Paper No. 4825, Houston, TX, May 1984.
- C.13 Tolloczko, J.A., and Lalani, M., "The Implications of New Data on the Fatigue Life Assessment of Tubular Joints," Proceedings of the 20th Annual Offshore Technology Conference, OTC Paper No. 5662, Houston, TX, May 1988.

(THIS PAGE INTENTIONALLY LEFT BLANK)

APPENDIX D

VORTEX SHEDDING AVOIDANCE AND FATIGUE DAMAGE COMPUTATION

CONTENTS

NOMENCLATURE

D.

VORTEX SHEDDING

D.1 INTRODUCTION

D.2 VORTEX SHEDDING PARAMETERS

D.3 SUSCEPTIBILITY TO VORTEX SHEDDING

D.3.1 In-Line Vortex Shedding

D.3.2 Cross-Flow Vortex Shedding

D.3.3 Critical Flow Velocities

D.4 AMPLITUDES OF VIBRATION

D.4.1 In-Line Vortex Shedding Amplitudes

D.4.2 Cross-Flow Vortex Shedding Amplitudes

D.5 STRESSES DUE TO VORTEX SHEDDING

D.6 FATIGUE LIFE EVALUATION

D.7 EXAMPLE PROBLEMS

D.7.1 Avoidance of Wind-Induced Cross-Flow Vortex Shedding

D.7.2 Analysis for Wind-Induced Cross-Flow Vortex Shedding

D.8 METHODS OF MINIMIZING VORTEX SHEDDING OSCILLATIONS

D.8.1 Control of Structural Design

D.8.2 Mass and Damping

D.8.3 Devices and Spoilers

D.9 REFERENCES

NOMENCLATURE

C_D	=	Coefficient of drag
CL_j	=	Design lift coefficient
CL_0	=	Base lift coefficient
D	=	Fatigue damage
D_{tot}	=	Total fatigue damage
D_1	=	Fatigue damage due to vortex shedding
D_2	=	Fatigue damage due to storm
E	=	Modulus of elasticity
H	=	Submerged length of member
I	=	Member moment of inertia
I	=	Turbulence parameter
I_0	=	Turbulence parameter
K	=	Constant representing member fixity
K_s	=	Stability parameter
L	=	Span between member supports
N	=	Number of cycles to failure at hot spot stress range
Re	=	Reynolds number
S	=	Hot spot stress range
S	=	Member section modulus
SCF	=	Stress concentration factor
St	=	Strouhal number
S_1	=	Corresponding hot spot stress range
T	=	Wave period
T_e	=	Time for which V_{min} is exceeded
V	=	Flow velocity normal to member axis
V_m	=	Maximum orbital velocity due to wave motion
V_{max}	=	Maximum water particle velocity
V_{min}	=	Minimum V_r , required for motion
V_r	=	Reduced velocity
Y	=	Member midspan deflection
Y_m	=	Maximum member midspan deflection
Y_R	=	Refined maximum member midspan deflection

a	=	Maximum modal amplitude
a_n	=	Natural frequency coefficient
b	=	Pit depth
d	=	Member diameter
f_v	=	Member vortex shedding frequency
f_{ar}	=	Turbulence parameter
f_b	=	Member bending stress
f_{bmax}	=	Member maximum bending stress
f_H	=	Member maximum hot spot stress
f_n	=	Member natural frequency
f_s	=	Member vortex shedding frequency
m	=	Mass of member per unit length excluding marine growth
\bar{m}	=	Effective mass per unit length
m_1	=	Mass of member per unit length including marine growth
m_j	=	Generalized mass per unit length for mode j
n	=	Mode of vibration
n_e	=	Member end condition coefficient
n_o	=	Total number of occurrences per year
n_s	=	Actual number of cycles at hot spot stress range
n_w	=	Number of oscillations during one wave cycle
t	=	Nominal caisson thickness
V	=	Applied velocity
v_{cr}	=	Critical wind velocity
V_r	=	Reduced velocity
w	=	Load per unit length
w_o	=	Weight per unit length of member
w_1	=	Weight per unit length of supported items
$y(x)$	=	Fundamental mode shape
$y'(x)$	=	Equivalent fundamental mode shape
δ	=	Logarithmic decrement of damping
ϵ	=	Damping ratio
ν	=	Kinematic viscosity
η_N	=	Ratio of midspan deflection to member diameter (Y/d)
ρ	=	Mass density of fluid

(THIS PAGE INTENTIONALLY LEFT BLANK)

D. VORTEX SHEDDING

D.1. INTRODUCTION

When a fluid flows about a stationary cylinder, the flow separates, vortices are shed, and a periodic wake is formed. Each time a vortex is shed from the cylinder, the local pressure distribution is altered, and the cylinder experiences a time-varying force at the frequency of vortex shedding.

In steady flows, vortices are shed alternately from either side of the cylinder producing an oscillating lift force transverse to the flow direction at a frequency equal to that at which pairs of vortices are shed. In the flow direction, in addition to the steady drag force, there is a small fluctuating drag force associated with the shedding of individual vortices at a frequency twice that of the lift force.

As the flow velocity increases, the vortex shedding frequency increases. Thus, provided the flow velocity is high enough, a condition will be reached where the vortex shedding frequency coincides with the natural frequency of the flexible element.

In general, marine members and appurtenant pipework are of a diameter and length that preclude the occurrence of in-line vibrations induced by vortex shedding. However, all susceptible members must be analyzed to ensure that the stresses due to in-line vibrations and possible synchronized oscillations are small and do not result in a fatigue failure.

Response to vortex shedding cannot be predicted using conventional dynamic analysis techniques since the problem is non-linear. The motion of the structure affects the strength of the shedding which, in turn affects the motion of the structure. This feedback mechanism causes the response to be either significantly large or negligibly small. Once excited, there is also a tendency for the vortex

shedding frequency to synchronize with the natural frequency of the structure. This results in sustained resonant vibration even if the flow velocity moves away from the critical velocity.

Oscillations can be predominantly in-line with the flow direction or transverse to it. In-line motion occurs at lower flow velocities than transverse or cross-flow motion, but the latter is invariably more severe and can lead to catastrophic failure due to a small number of cycles of oscillation.

Response to vortex shedding is further complicated as the excitational force is not necessarily uniform along the length of the members and the actual amplitude of oscillation depends to a large extent on the degree of structural damping.

D.2. VORTEX SHEDDING PARAMETERS

A number of parameters are common to this phenomenon:

Reduced velocity (V_r)

$$V_r = V/f_n d$$

where:

$$\begin{aligned} V &= \text{flow velocity normal to the member axis} \\ f_n &= \text{fundamental frequency of the member (Hz)} \\ d &= \text{diameter of the member} \end{aligned}$$

Reynolds number (R_e)

$$R_e = Vd/\nu$$

where:

$$\nu = \text{kinematic viscosity of the fluid}$$

The Strouhal number (S_t) is a function of the Reynolds number for circular members. The Reynolds number for typical cylindrical members under storm current ranges from 3.5×10^5 to 1.0×10^6 . The Strouhal number is reasonably approximated as 0.21 for this range of Reynolds numbers.

Vortex Shedding Frequency (f_v)

$$f_v = \frac{S_t V}{d} = \text{vortex shedding frequency of the member}$$

If the vortex shedding frequency of the member coincides with the natural frequency of the member, resonance will occur.

Stability parameter (K_s)

$$K_s = 2 \bar{m} \delta / \rho d^2$$

where:

$$\delta = 2 \pi \epsilon = \text{logarithmic decrement}$$

$$\epsilon = \text{damping ratio}$$

$$\rho = \text{mass density of the fluid}$$

$$\bar{m} = \text{effective mass per unit length}$$

$$= \frac{\int_0^L m [y(x)]^2 dx}{\int_0^L [y'(x)]^2 dx}$$

$$L = \text{span between member supports}$$

$$m = \text{mass of member per unit length}$$

$$y(x), \text{ \& } y'(x) = \text{fundamental mode shapes as a function of the ordinate } x \text{ measured from the lower support along the longitudinal axis of the member}$$

As given in References D.1 and D.2, the effective mass is used to equate the real structure with an equivalent structure for which

deflection and stability parameters are known. The deflected form of this equivalent structure is a cantilever, while typical structure members and appurtenances deflect as a simply supported beam. Hence, the equivalent structure has a mode shape given by:

$$y'(x) = a - a \cos\left(\frac{\pi x}{2L}\right)$$

while the real structure has a mode shape given by:

$$y(x) = a \sin\left(\frac{\pi x}{L}\right)$$

Substituting into the effective mass formulation, we obtain:

$$m = \frac{\int_0^L [m] \left[a \sin \frac{\pi x}{L} \right]^2 dx}{\int_0^L \left[a - a \cos \frac{\pi x}{2L} \right]^2 dx}$$

where:

$$a = \text{maximum modal amplitude}$$

Integration of the above equation leads to the relationship:

$$\bar{m} = 2.205 \, m \text{ for simple supported span}$$

$$\bar{m} = 1.654 \, m \text{ for fixed supports}$$

$$\bar{m} = m \text{ for cantilever span}$$

Damping Ratio

Welded marine structures exhibit very low values of structural damping. Vibratory energy is typically dissipated by material and aerodynamic (radiation) damping. Individual members subjected to large vibratory motions dissipate energy through the connections to the main structure largely as dispersive bending and compression

waves. When only isolated members undergo large vibration response, energy dispersion exceeds reflected energy and represents a major source of damping.

Structural members may be grouped into two classes, depending on the fixity of their supports. Tubular braces welded on to regions of high rigidity, such as structure columns or legs, are defined as Class 1 members. Tubular braces welded on to regions of low rigidity, such as other braces, are defined as Class 2 members. The damping ratio applicable for structural members are:

Structural Member - Class 1 Damping ratio $\epsilon = 0.0035$

Structural Member - Class 2 Damping ratio $\epsilon = 0.0015$

Although the recommended damping ratios are for vibrations in air, they may be conservatively used for vibrations in water.

Non-structural continuous members, such as tubulars supported by multiple guides, have both structural and hydrodynamic damping. The hydrodynamic damping occurs due to sympathetic vibration of spans adjacent to the span being evaluated for shedding. Recent work by Vandiver and Chung (Reference D.3) supports the effectiveness of hydrodynamic damping mechanism. The lower bound structural damping ratio for continuous tubulars supported by loose guides is given as 0.009 by Blevins (Reference D.4). The applicable damping ratios are assumed to be:

Non-Structural Members - Continuous Spans

Damping ratio $\epsilon = 0.009$ in air

Damping ratio $\epsilon = 0.02$ in water

Natural Frequency

The fundamental natural frequency (in Hz) for uniform beams may be calculated from:

$$f_n = \frac{a_n}{2\pi} (EI/m_1 L^4)^{1/2}$$

where:

I = the moment of inertia of the beam

a_n = 3.52 for a beam with fix-free ends (cantilever)
 = 9.87 for a beam with pin-pin ends
 = 15.4 for a beam with fix-pin ends
 = 22.4 for a beam with fix-fix ends

L = length

n = mode of vibration

m_1 = mass per unit length

The amount of member fixity assumed in the analysis has a large effect on vortex shedding results, because of its impact on member stiffness, natural period, amplitude of displacement, and member stress. Hence, careful consideration should be given to member end conditions. Members framing into relatively stiff members can usually be assumed to be fixed. Other members, such as caissons and risers, may act as pinned members if supports are detailed to allow member rotation.

For members with non-uniform spans, complex support arrangements or non-uniform mass distribution, the natural frequency should be determined from either a dynamic analysis or from Tables provided in References D.5 and D.6. Reid (Reference D.7) provides a discussion and a model to predict the response of variable geometry cylinders subjected to a varying flow velocities.

The natural frequency of a member is a function of the member's stiffness and mass. For the purposes of vortex shedding analysis and design, the member's stiffness properties are computed from the

member's nominal diameter and thickness. The member mass per unit length m is taken to include the mass of the member steel including sacrificial corrosion allowance, anodes, and contained fluid. For the submerged portion of the member, the added mass of the surrounding water is also included. This added mass is the mass of water that would be displaced by a closed cylinder with a diameter equal to the nominal member outside diameter plus two times the appropriate marine growth thickness.

Because of insufficient knowledge of the effect of marine growth on vortex shedding, the member diameter " d " in vortex-shedding parameters V_r , R_e , K_s , and the member effective mass \bar{m} in parameter K_s do not include any allowance for the presence of marine growth.

D.3. SUSCEPTIBILITY TO VORTEX SHEDDING

The vortex shedding phenomena may occur either in water or in air. The susceptibility discussed and the design guidelines presented are applicable for steady current and wind. Wave induced vortex shedding has not been investigated in depth. Since the water particle velocities in waves continually change both in magnitude and direction (i.e. restricting resonant oscillation build-up), it may be reasonable to investigate current-induced vortex shedding and overlook wave actions.

To determine susceptibility of a member to wind- or current-induced vortex shedding vibrations, the reduced velocity (V_r) is computed first. For submerged members, the stability parameter (K_s) is also calculated. Vortex shedding susceptibility defined here is based upon the method given in Reference D.8, with a modified lower bound for current-induced shedding to reflect present thinking on this subject (Reference D.9).

D.3.1 In-Line Vortex Shedding

In-line vibrations in wind and current environments may occur when:

Current Environment

$$1.2 \leq V_r < 3.5$$
$$\text{and } K_s \leq 1.8$$

Wind Environment

$$1.7 < V_r < 3.2$$

The value of V_r may be more accurately defined for low K_s values from Figure D-1, which gives the reduced velocity necessary for the onset of in-line motion as a function of combined mass and damping parameter (i.e. stability parameter). Corresponding amplitude of motion as a function of K_s is given on Figure D-2. As illustrated on this Figure, in-line motion is completely suppressed for K_s values greater than 1.8.

Typical marine structure members (i.e. braces and caissons on a platform) generally have values of K_s greater than 1.8 in air but less than 1.8 in water. Hence, in-line vibrations with significant amplitudes are often likely in steady current but unlikely in wind.

D.3.2 Cross-Flow Vortex Shedding

The reduced velocity necessary for the onset of cross-flow vibrations in either air or in water is shown on Figure D-3 as a function of Reynold's number, R_e , cross flow vibrations in water and in air may occur when:

Current Environment

$$3.9 \leq V_r \leq 9$$
$$\text{and } K_s \leq 16$$

Wind Environment

$$4.7 < V_r < 8$$

The cross-flow vibrations of members in steady current will invariably be of large amplitude, causing failures after small number

of cycles. Thus, the reduced velocity necessary for the onset of cross-flow vibrations in steady current should be avoided.

D.3.3 Critical Flow Velocities

The criteria for determining the critical flow velocities for the onset of VIV can be expressed in terms of the reduced velocity (Section D.2):

$$V_{cr} = (V_r)_{cr} (f_n \cdot d)$$

where:

$$\begin{aligned} (V_r)_{cr} &= 1.2 \text{ for in-line oscillations in water} \\ &= 1.7 \text{ for in-line oscillations in air} \\ &= 3.9 \text{ for cross-flow oscillations in water} \\ &= 4.7 \text{ for cross-flow oscillations in air} \end{aligned}$$

D.4. AMPLITUDES OF VIBRATION

Amplitudes of vibrations can be determined by several methods. A DnV proposed procedure (Reference D.8) is simple to apply and allows determination of member natural frequencies, critical velocities and maximum amplitudes of vortex-shedding induced oscillations. The procedure yields consistent results, comparable to the results obtained by other methods, except for oscillation amplitudes. The DnV calculation of oscillation amplitudes is based on a dynamic load factor of a resonant, damped, single-degree-of-freedom system. This approach is not valid unless the nonlinear relationship between the response and damping ratio is known and accounted for. Consequently, in-line and cross-flow vortex shedding amplitudes are assessed separately.

D.4.1 In-Line Vortex Shedding Amplitudes

The reduced velocity and the amplitude of vibrations shown on Figures D-1 and D-2, respectively, as functions of stability parameter are based on experimental data. The experimental data obtained are for the cantilever mode of deflection for in-line and cross-flow vibrations.

Sarpkaya (Reference D.10) carried out tests on both oscillatory flow and uniform flow and observed smaller amplitudes of vibration for the oscillatory flow than for the uniform flow. It is also suggested by King (Reference D.1) that the maximum amplitude for an oscillatory flow is likely to occur at a V_r value in excess of 1.5 (as opposed to 1.0 assumed by DnV) and that an oscillation build-up of about 15 cycles is required before "lock-in" maximum-amplitude vibration occurs. In light of this evidence, the amplitude of vibrations shown in Figure D-2 is based on Hallam et al (Reference D.2) rather than the DnV (Reference D.8).

Since typical marine structure members have stability parameters (K_s) in excess of 1.8, in-line vibrations of these members in air are unlikely.

D.4.2 Cross-flow Vortex Shedding Amplitudes

The amplitude of the induced vibrations that accompanies cross-flow vibration are generally large and creates very high stresses. Therefore, it is desirable to preclude cross-flow induced vibrations. Figure D-4 illustrates a curve defining the amplitude of response for cross-flow vibrations due to current flow and based on a cantilever mode of deflection.

Cross-flow oscillations in air may not be always avoidable, requiring the members to have sufficient resistance. The DnV procedure (Reference D.8) to determine the oscillation amplitudes is derived from a simplified approach applicable to vortex shedding due to

steady current, by substituting the mass density of air for the mass density of water. Hence, the oscillation amplitude is not linked with the velocity that causes vortex-induced motion. The resulting predicted amplitudes are substantially higher than amplitudes predicted based on an ESDU (Reference D.11) procedure that accounts for interaction between vortices shed and the forces induced.

The iterative ESDU procedure to determine the amplitudes can be simplified by approximating selected variables. The peak amplitude is represented in Equation 9 of the ESDU report by:

$$\frac{Y}{d} = \eta_N = \frac{0.00633}{\epsilon} \rho \frac{d^2}{m_j} \frac{1}{S_t^2} \quad CL_j = \frac{0.0795 CL_j}{K_s S_t^2}$$

Using this formulation, a corresponding equation can be established for a structure, while making assumptions about the individual parameters. Following step 3 of the procedure, the parameters may be set as:

m_j = generalized mass/unit length for mode j
 = 2.205 m for pinned structure,
 = 1.654 m for fixed structure

K_s = stability parameter = $\frac{2m_j \delta}{\rho d^2}$

ρ = mass density of air = 1.024 kg/m³

δ = decrement of damping = $2\pi\epsilon$

ϵ = damping parameter = 0.002 for wind

S_t = Strouhal Number = 0.2

CL_0 = base lift coefficient = 0.29 high Reynolds number
 = 0.42 low Reynolds number

CL_j = design lift coefficient = $CL_0 \times f_{ar} \times I_0 \times \frac{I}{I_0} \times 1.2$

f_{ar} = turbulence parameter = 1.0

$\frac{I}{I_0}$ = turbulence parameter = 1.0

I_0 = turbulence parameter = 0.45

Evaluating the equation based on the high Reynolds number ($Re > 500,000$) leads to:

$$\eta_N = 0.0795 (0.29)(1.0)(0.45)(1.0)(1.2)/[K_s(0.2)^2]$$

$$\eta_N = \frac{0.3114}{K_s} \quad (\text{high Reynolds number, } Re > 500,000)$$

or

$$\eta_N = \frac{0.4510}{K_s} \quad (\text{low Reynolds number, } Re < 500,000)$$

The amplitude can also be determined iteratively by utilizing the ESDU recommended turbulence parameter and following steps 1 through 5.

Step 1: Determine correlation length factor, I_0 . Depending on the end fixity, I_0 is:

I_0 = 0.66 for fixed and free (cantilever)
 = 0.63 for pin and pin (simple beam)
 = 0.58 for fixed and pin
 = 0.52 for fixed and fixed

Step 2: Assume $I/I_0 = 1.0$ and calculate the amplitude.

Step 3: Obtain a new value of I/I_0 based on initial amplitude.

Step 4: Recompute the amplitude based on the new value of I/I_0 .

Step 5: Repeat Steps 3 and 4 until convergence.

D.5. STRESSES DUE TO VORTEX SHEDDING

Once the amplitude of vibration has been calculated, stresses can be computed according to the support conditions. For a simply supported beam with a uniform load w , the midspan deflection Y , and the midspan bending stress f_b are given as follows:

$$\begin{aligned}\frac{Y}{d} &= \frac{5}{384} \cdot \frac{w L^4}{EI} \cdot \frac{1}{d} \\ w &= \frac{384}{5} \cdot \frac{EIY}{L^4} \\ M_{\max} &= \frac{w L^2}{8} = \frac{384}{40} \frac{EIY}{L^2} \\ f_{b\max} &= \frac{M}{I} \cdot \frac{d}{2} = 4.8 \frac{EDY}{L^2} \quad \text{at midspan}\end{aligned}$$

$$\text{Expressing } f_{b\max} = K \cdot \frac{EDY}{L^2}$$

The K value varies with support conditions and location as shown on Table D-1.

<u>Fixity</u>		<u>Mid-Span</u>	<u>Ends</u>
Fix	Fix	8.0	16.0
Fix	Pin	6.5	11.6
Pin	Pin	4.8	0
Fix	Free	N.A.	2.0

Table D-1 K Values Based on Fixity and Location

The vortex shedding bending stress is combined with the member axial and bending stresses due to global deformation of the marine structure.

D.6. FATIGUE LIFE EVALUATION

The fatigue life evaluation can be carried out in a conservative two-step process. First, the fatigue damage due to the vortex-induced oscillations is calculated as D_1 . Second, a deterministic fatigue analysis is performed by computer analysis. Hot spot stress range vs wave height (or wind velocity) for the loading directions considered is determined from the computer analysis. The critical direction is determined and a plot is made. From the plot of hot spot stress range vs wave height (or wind velocity), the stress ranges for the fatigue waves are determined. The maximum vortex-induced stress ranges for the fatigue environment are added to the deterministic fatigue stress ranges. Then, the standard deterministic fatigue analysis is performed using the increased stress range. The fatigue damage calculated in this second step is D_2 . Therefore the total fatigue damage is equal to the sum of D_1 and D_2 , or $D_{tot} = D_1 + D_2$. The fatigue life in years is therefore calculated as $1/D_{tot}$.

A typical fatigue life evaluation procedure is given below:

Step 1:

- a. Calculate the natural frequency f_n (H_z) of the member.
- b. Calculate the stability parameter of the member.

$$K_s = \frac{2\bar{m}\delta}{\rho d^2}$$

- c. Determine the minimum V_r required for vibrations based on K_s in Figure D-1.
- d. Calculate V_{min} , the minimum velocity at which current- or wind-

vortex shedding will occur, i.e., $V_{min} = V_r(\text{req'd}) \times f_n \times d$.

- e. Check the applied velocity profile to see if V_{max} is greater than V_{min} . If V_{max} is less than V_{min} , then no vortex oscillations can occur.
- f. For V_{max} greater than V_{min} , vortex oscillations can occur. The displacement amplitude is based on stability parameter K_s , and is determined from Figure D-2 for in-line vibration. A conservative approach is used to determine Y/d vs K_s . For $K_s < 0.6$ the first instability region curve is used. For $K_s > 0.6$ the second instability region curve is used. This conservatively represents an envelope of maximum values of Y/d vs K_s from Figure D-2. Displacement amplitude is normalized to Y/d .
- g. Given (Y/d) , calculate the bending stress, f_b .
- h. Multiply bending stress f_b by an SCF of 1.5 to produce hot spot stress f_H . A larger SCF will be used where necessary.
- i. From the maximum hot spot stress, the hot spot stress range is calculated as $2f_H$.
- j. Allowable number of cycles to failure (N) should be calculated using an applicable S-N curve (based on weld type and environment).
- k. Assume conditions conducive to resonant vortex shedding occur for a total time of T (seconds) per annum (based on current or wind data relevant to applicable loading condition).
- l. Hence, in time T , number of cycles $n = f_n T$ and the cumulative damage $D1 = n/N = f_n T/N$ in one year.

Step 2:

- a. Depending on marine structure in service conditions (i.e. structure in water or in air) run an applicable loading analysis. Assuming a marine environment, run a storm wave deterministic fatigue analysis and obtain the results of hot spot stress range vs wave height for the wave directions considered and as many hot spots as are needed.
- b. Determine the critical hot spot and wave direction and draw the hot spot stress range vs wave height graph.
- c. Determine the hot spot stress range for each of the fatigue waves.
- d. For the larger fatigue waves in which vortex-induced oscillations occur, add the increase in stress range due to vortex-induced oscillations to the stress range from the deterministic fatigue analysis.
- e. Calculate the fatigue damage D_2 over a 1 yr period for the full range of wave heights:

$$D_2 = \sum_1^H \left(\frac{n}{N} \right)$$

- f. Calculate the total fatigue damage:

$$D_{tot} = D_1 + D_2$$

- g. Calculate the fatigue life in years as:

$$\text{Life} = \frac{1}{D_{tot}}$$

- h. The fatigue life may be modified to include the effects of corrosion pitting in caissons. Corrosion pitting produces an SCF at the location of the pit. The SCF is calculated as:

$$SCF = \frac{1}{(1 - \frac{b}{t})} + \frac{3 (\frac{b}{t})}{(1 - \frac{b}{t})^2}$$

where:

b = pit depth
t = nominal caisson thickness

The new life including corrosion damage is calculated as:

$$\text{New Life} = \frac{\text{Old Life}}{(SCF)^3}$$

This estimate of fatigue damage can, if necessary, be refined by consideration of the number of wave occurrences for different directions and evaluation of the damage at a number of points around the circumference of the member.

D.7. EXAMPLE PROBLEMS

D.7.1 Avoidance of Wind-Induced Cross-Flow Vortex Shedding

It can be shown that for a steel beam of circular cross section, the following relationship holds:

where:

$$V_{cr} = \frac{c \cdot V_{r n_e}^2}{(L/d)^2} \left[\frac{w_0}{w_0 + w_1} \right]^{1/2}$$

V_{cr} = critical wind velocity of the tubular necessary for the onset of cross-flow wind-induced vortex shedding

c	=	constant (See <u>NOTE</u> , next page)
V_r	=	reduced velocity
n_e	=	member end efficiency
	=	1.5 fixed ends
	=	1.0 pinned ends
w_0	=	weight per unit length of tubular
w_1	=	weight per unit length of supported item (e.g., anodes)
L	=	beam length
d	=	tubular mean diameter

For $V_r = 4.7$, $n_e = 1.5$ (fixed condition), and $w_1 = 0$, this reduces to:

$$\begin{aligned} V_{cr} &= 97240/(L/d)^2 \text{ ft/sec} \\ &= 29610/(L/d)^2 \text{ m/sec} \end{aligned}$$

Hence, if maximum expected wind speed is 65.6 ft/s (20 m/s), then setting all brace L/d ratios at 38 or less precludes wind-induced cross-flow vortex shedding, and no further analyses or precautions are required.

However, maximum wind speeds may be so high that the above approach may be uneconomical. In this case, either precautionary measures must be taken or additional analyses considering strength and fatigue must be undertaken.

NOTE:

The relationship given is based on:

$$V_{cr} = V_r f_n d = V_r \left(\frac{a_n}{2\pi} \left[EI/M_1 L^4 \right]^{\frac{1}{2}} \right) d$$

substituting

$$a_n = (n_e \pi)^2$$

$$m_1 = (w_0 + w_1)/g$$

$$I = \pi d^3 t / 8$$

$$E = 4176 \times 10^6 \text{ lbs/ft}^2 \quad (200,000 \text{ MN/m}^2)$$

$$g = 32.2 \text{ ft/sec}^2 \quad (9.806 \text{ m/sec}^2)$$

$$w_0 = \gamma_s \pi d t$$

$$\gamma_s = \text{weight density of steel, } 490 \text{ lbs/ft}^3 \quad (0.077 \text{ MN/m}^3)$$

$$V_{cr} = V_r \left(\frac{n_e^2 \pi^2}{2\pi} \right) \left[\frac{E (\pi d^3 t / 8) g}{(w_0 + w_1) L^4} \right]^{\frac{1}{2}} \cdot d$$

$$V_{cr} = V_r \left(\frac{n_e^2 \pi}{2} \right) \left[\frac{E (w_0 / \gamma_s) d^2 g}{8 (w_0 + w_1) L^4} \right]^{\frac{1}{2}} \cdot d$$

Substituting for E, γ_s , and g

$$V_{cr} = V_r \cdot \frac{C n_e^2}{(L/d)^2} \left[\frac{w_0}{w_0 + w_1} \right]^{\frac{1}{2}}$$

where

$$\begin{aligned} \text{constant } C &= 9195 && \text{for } V_{cr} \text{ as ft/sec} \\ &= 2800 && \text{for } V_{cr} \text{ as m/sec} \end{aligned}$$

D.7.2 Analysis for Wind-Induced Cross-flow Vortex Shedding

Using procedures discussed in Section D.4 a flare structure bracing members are analyzed for crossflow oscillations produced by vortex shedding. The analysis is performed using a Lotus spreadsheet. The general procedure is as follows:

- (a) Member and environmental parameters are input.
- (b) Critical velocity, peak amplitudes of oscillation and corresponding stress amplitudes are computed.
- (c) The time (in hours) of crossflow oscillation required to cause fatigue failure is computed.

Analysis Description

The following is a detailed description of the spread sheet input and calculation.

(a) Spread Sheet Terminology

Columns are labeled alphabetically while rows are labeled numerically. A "cell" is identified by referring to a specific row and column.

(b) General Parameters

The following are parameters common to all members analyzed as given at the top of the spread sheet.

CELL C5: DAMPING RATIO = ϵ

CELL C6: AIR MASS DENSITY = ρ

CELL C7: KINEMATIC VISCOSITY = ν

CELL C8: STRESS CONCENTRATION FACTOR = SCF

CELL C9: MODULUS OF ELASTICITY = E

CELL K5: RATIO OF GENERALIZED MASS TO EFFECTIVE MASS = $(\frac{m_j}{m_e})$

CELL K6: FIXITY PARAMETER IN FORMULA FOR CRITICAL VELOCITY = n_e

CELL K7: FIXITY PARAMETER IN FORMULA FOR STRESS AMPLITUDE = C

CELL K8: FIXITY PARAMETER IN FORMULA FOR MEMBER FREQUENCY = a_n

(c) Specific Member Analysis

The following describes the content of each column in analyzing a specific member. Entries and formulas for vortex shedding analysis of member group H1 on line 16 are also provided. Formula coding is described in the LOTUS 1-2-3 Users Manual.

COLUMN A: ENTER THE MEMBER GROUP IDENTIFIER

COLUMN B: ENTER THE EFFECTIVE SPAN OF THE MEMBER = L (m)

COLUMN C: ENTER THE OUTSIDE DIAMETER OF THE TUBULAR = d (mm)

COLUMN D: ENTER THE TOTAL OUTSIDE DIAMETER = D (mm) INCLUDING AS APPLICABLE, MARINE GROWTH, FIRE PROTECTION, ETC.

COLUMN E: ENTER THE TUBULAR WALL THICKNESS = t (mm)

COLUMN F: ENTER ADDED MASS (kg/m), IF APPLICABLE

COLUMN G: THE MOMENT OF INERTIA OF THE TUBULAR = I (cm⁴) IS COMPUTED.

$$I = \frac{\pi}{4} \left[\left(\frac{d}{2} \right)^4 - \left(\frac{d}{2} - t \right)^4 \right] \quad (\text{cm}^4)$$

COLUMN H: THE TOTAL EFFECTIVE MASS IS COMPUTED

$$m_e = \pi \left[\left(\frac{d}{2} \right)^2 - \left(\frac{d}{2} - t \right)^2 \right] (0.785) + m_a \quad (\text{kg/m})$$

COLUMN I: THE CRITICAL VELOCITY FOR CROSSFLOW OSCILLATION IS COMPUTED.

$$V_{cr} = \frac{13160 \, n_e^2}{(L/D)^2} \quad (\text{m/s})$$

COLUMN J: ENTER THE THRESHOLD WIND VELOCITY = V_{thr}

COLUMN K: THE STABILITY PARAMETER IS COMPUTED

$$K_s = \frac{2m_e (2\pi E)}{PD^2}$$

COLUMN L: THE REYNOLDS NUMBER IS COMPUTED

$$R_e = \frac{V_{cr}}{D_v}$$

Before performing calculation in the following columns, the critical velocity is compared with the threshold velocity. If the critical velocity is larger, crossflow oscillations will not occur and the computations are suppressed. An "N.A." is then inserted in each column.

If the critical velocity is less than the threshold value, the following computations are performed.

COLUMN M: THE AMPLITUDE OF VIBRATION IS COMPUTED

$$Y = \frac{\alpha D}{\left(\frac{m_j}{m_e} \right) K_s}$$

Where $\alpha = 0.04925$ for $Re > 500,000$
and $\alpha = 0.07178$ for $Re < 500,000$

COLUMN N: THE STRESS AMPLITUDE IS COMPUTED

$$f_b = \frac{CEdY}{L^2} \quad (\text{MPa})$$

where C depends on beam end fixity (see Section D.4)

COLUMN O: THE HOT SPOT STRESS RANGE IS COMPUTED

$$S = 2 (\text{SCF}) f_b \quad (\text{MPa})$$

COLUMN P: THE NUMBER OF CYCLES TO FAILURE UNDER THE HOT SPOT STRESS RANGE IS COMPUTED.

$$N = 10^{(14.57 - 4.1 \log_{10} S)} \quad (\text{cycles})$$

COLUMN Q: THE MEMBER NATURAL FREQUENCY IS COMPUTED

$$f_n = \frac{a_n}{2\pi} \left(\frac{EI}{m_e L^4} \right)^{\frac{1}{2}} \quad (\text{Hz})$$

where a_n depends on beam end fixity (see Section D.2)

COLUMN R: THE TIME IN HOURS TO FATIGUE FAILURE UNDER N CYCLES OF STRESS RANGE S IS COMPUTED

$$T = \frac{N}{f_n}$$

D.8. METHODS OF MINIMIZING VORTEX SHEDDING OSCILLATIONS

D.8.1 Control of Structural Design

The properties of the structure can be chosen to ensure that critical velocity values in steady flow do not produce detrimental oscillations.

Experiments have shown that for a constant mass parameter ($m/\rho d^2 = 2.0$), the critical velocity depends mainly on the submerged length/diameter (L/d) ratio of the member.

Thus, either high natural frequency or large diameter is required to avoid VIV's in quickly flowing fluid. A higher frequency will be obtained by using larger diameter tubes, so a double benefit occurs. An alternative method of increasing the frequency is to brace the structure with guy wires.

D.8.2 Mass and Damping

Increasing the mass parameter, $m/\rho d^2$, and/or the damping parameter reduces the amplitude of oscillations; if the increase is large enough, the motion is suppressed completely. While high mass and damping are the factors that prevent most existing structures from vibrating, no suitable design criteria are presently available for these factors, and their effects have not been studied in detail.

Increasing the mass of a structure to reduce oscillatory effects may not be entirely beneficial. The increase may produce a reduction in the natural frequency (and hence the flow speeds at which oscillation will tend to occur). It is thus possible that the addition of mass may reduce the critical speed to within the actual speed range. However, if increased mass is chosen as a method of limiting the amplitude of oscillation, this mass should be under stress during the motion. If so, the mass will also contribute to the structural damping. An unstressed mass will not be so effective.

If the structure is almost at the critical value of the combined mass/damping parameter for the suppression of motion, then a small additional amount of damping may be sufficient.

D.8.3 Devices and Spoilers

Devices that modify flow and reduce excitation can be fitted to tubular structures. These devices (see Figure D-5) work well for isolated members but are less effective for an array of piles or cylinders. Unfortunately, there is no relevant information describing how the governing stability criteria are modified. The most widely used devices are described below.

Guy Wires

Appropriately placed guy wires may be used to increase member stiffness and preclude wind-induced oscillations. Guy wires should be of sufficient number and direction to adequately brace the tubular member; otherwise, oscillations may not be eliminated completely and additional oscillations of the guys themselves may occur.

Strakes or Spoilers

Strakes and spoilers consist of a number (usually three) of fins wound as a helix around the tubular. These have proven effective in preventing wind-induced cross-flow oscillations of structures, and there is no reason to doubt their ability to suppress in-line motion, provided that the optimum strake design is used. This comprises a three-star helix, having a pitch equal to five times the member diameter. Typically each helix protrudes one-tenth of the member diameter from the cylinder surface. To prevent in-line motion, strakes need only be applied over approximately in the middle one-third of the length of the tubular with the greatest amplitude. Elimination of the much more violent cross-flow motion requires a longer strake, perhaps covering the complete length of tube. The main disadvantage of strakes, apart from construction difficulties and problems associated with erosion or marine growth, is that they increase the time-averaged drag force produced by the flow. The drag coefficient of the straked part of the tube is independent of the Reynold's number and has a value of $C_D = 1.3$ based on the tubular diameter.

Shrouds

Shrouds consist of an outer shell, separated from the tubular by a gap of about 0.10 diameter, with many small rectangular holes. The limited data available indicates that shrouds may not always be effective. The advantage of shrouds over strakes is that their drag penalty is not as great; for all Reynold's numbers, $C_D = 0.9$ based on the inner tubular diameter. Like strakes, shrouds can eliminate the in-line motion of the two low-speed peaks without covering the complete length of the tubular. However, any design that requires shrouds (or strakes) to prevent cross-flow motion should be considered with great caution. Their effectiveness can be minimized by marine growth.

Offset Dorsal Fins

This is the simplest device for the prevention of oscillations. It is probably the only device that can be relied upon to continue to work in the marine environment over a long period of time without being affected adversely by marine growth. It has some drag penalty, but this is not likely to be significant for most designs.

The offset dorsal fin is limited to tubular structures that are subject to in-line motion due to flow from one direction only (or one direction and its reversal, as in tidal flow).

This patented device comprises a small fin running down the length of the tubular. Along with the small drag increase there is a steady side force. This may be eliminated in the case of the total force on multi-tubular design by placing the fin alternately on opposite sides of the tubulars.

- D.1 King, R., "A Review of Vortex Shedding Research and Its Application," Ocean Engineering, Vol. 4, pp. 141-171, 1977.
- D.2 Hallam, M.G., Heaf, N.J., Wootton, L.R., Dynamics of Marine Structures, CIRIA, 1977.
- D.3 Vandiver, J.K., and Chung, T.Y., "Hydrodynamic Damping in Flexible Cylinders in Sheared Flow," Proceedings of Offshore Technology Conference, OTC Paper 5524, Houston, 1988.
- D.4 Blevins, R.D., Flow Induced Vibrations, Van Nostrand Reinhold, 1977.
- D.5 Blevins, R.D., Formulas for Natural Frequency and Mode Shape, Van Nostrand Reinhold, 1979.
- D.6 Gorman, D.I., Free Vibration Analyses of Beams and Shafts, Wiley-Interscience, 1975.
- D.7 Reid, D.L., "A Model for the Prediction of Inline Vortex Induced Vibrations of Cylindrical Elements in a Non-Uniform Steady Flow," Journal of Ocean Engineering, August 1989.
- D.8 Det Norske Veritas, "Rules for Submarine Pipeline Systems," Oslo, Norway, 1981.
- D.9 Griffin, O.M. and Ramberg, S.E., "Some Recent studies of Vortex Shedding with Application to Marine Tubulars, and Risers," Proceedings of the First Offshore Mechanics and Arctic Engineering/Deep Sea Systems Symposium, March 7 - 10, 1982, pp. 33 - 63.
- D.10 Sarpkaya, T., Hydroelastic Response of Cylinders in

Harmonic Flow, Royal Institute of Naval Architects, 1979.

- D.11 Engineering Sciences Data Unit, Across Flow Response Due to
Vortex Shedding, Publication No. 78006, London, England,
October, 1978.

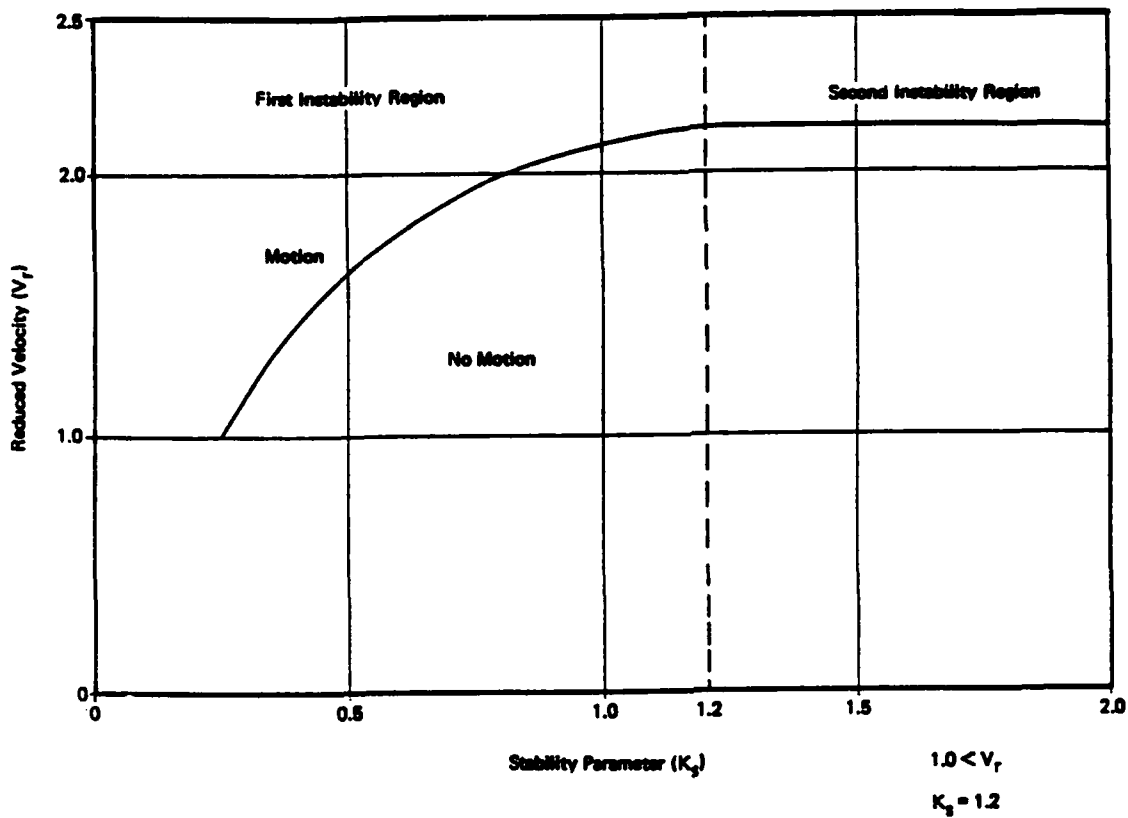


Figure D-1 Oscillatory Instability Relationship

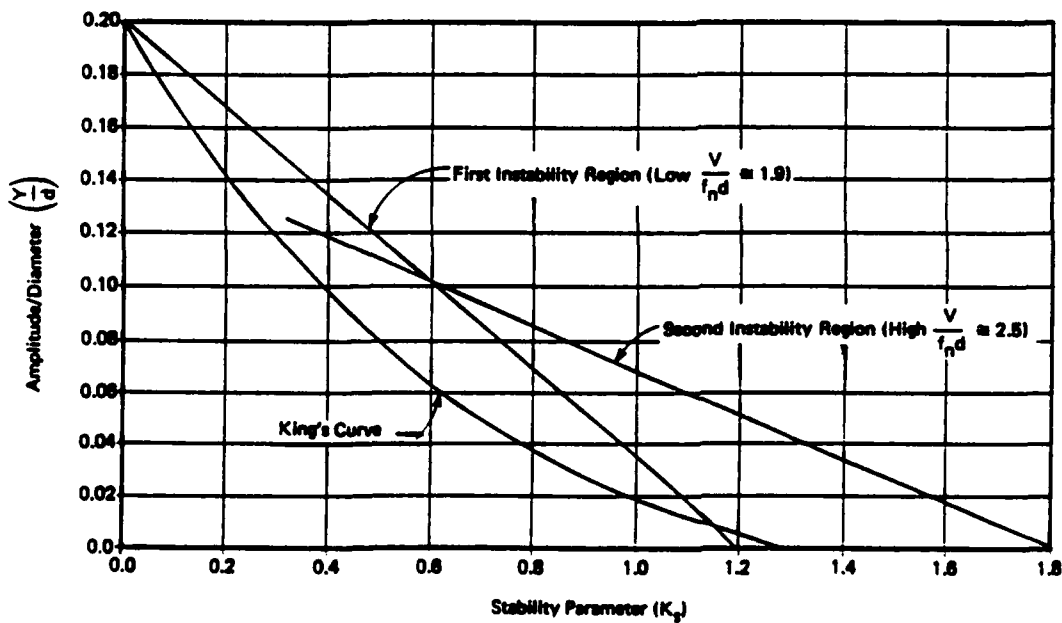


Figure D-2 Amplitude of Response for In-Line Vibrations

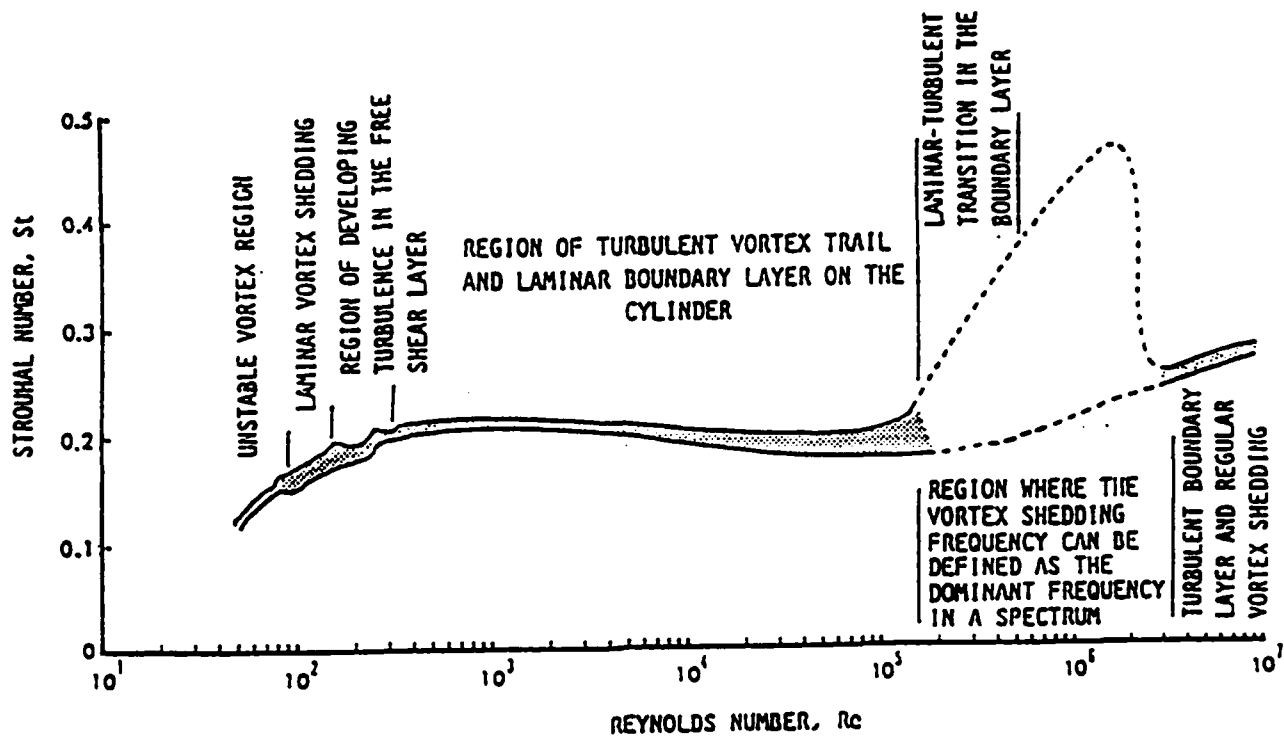


Figure D-3 The Strouhal versus Reynold's Numbers for Cylinders

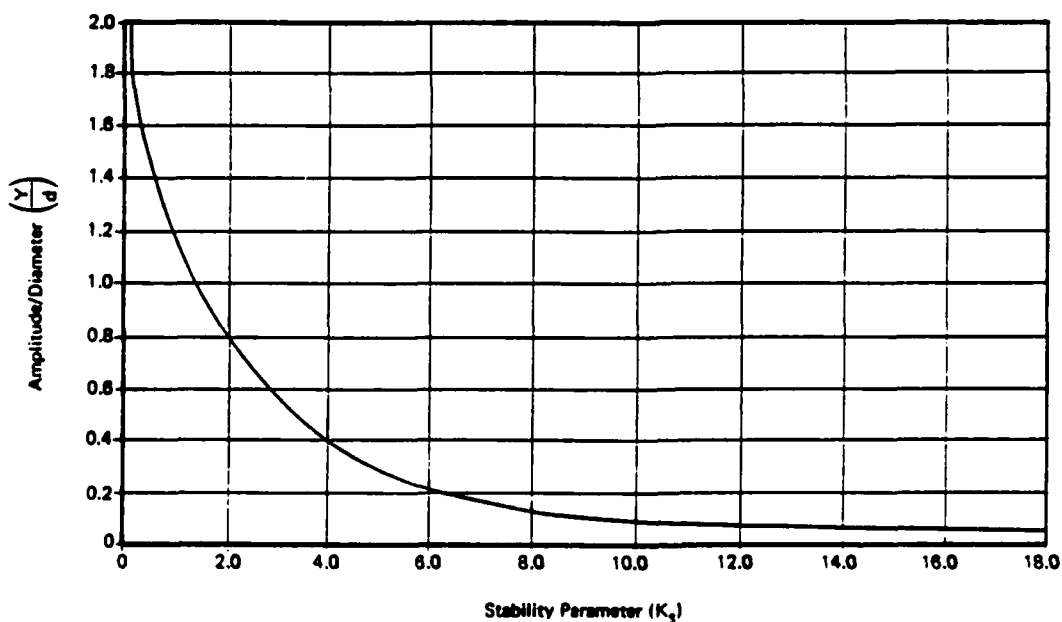
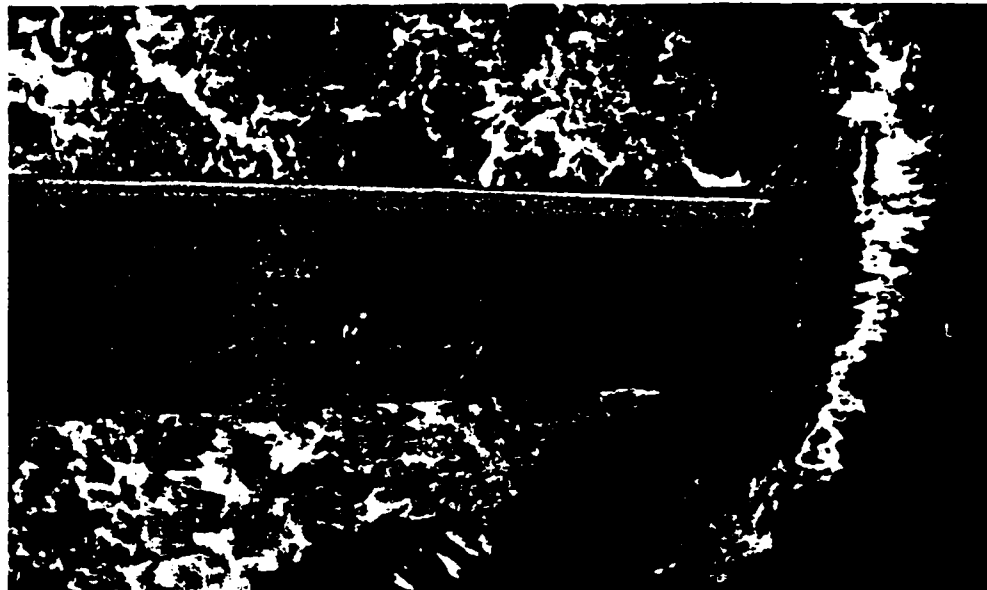
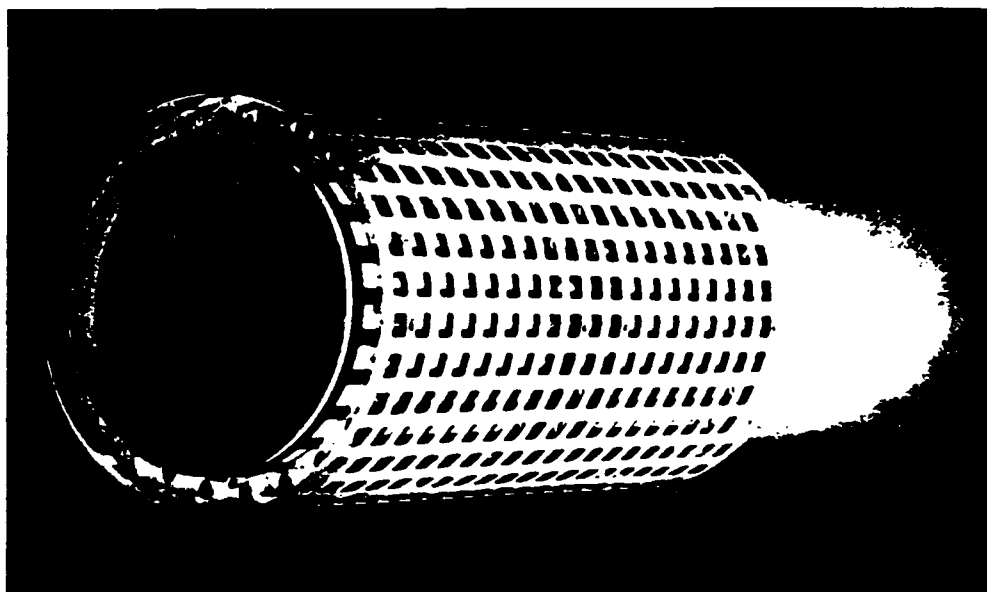


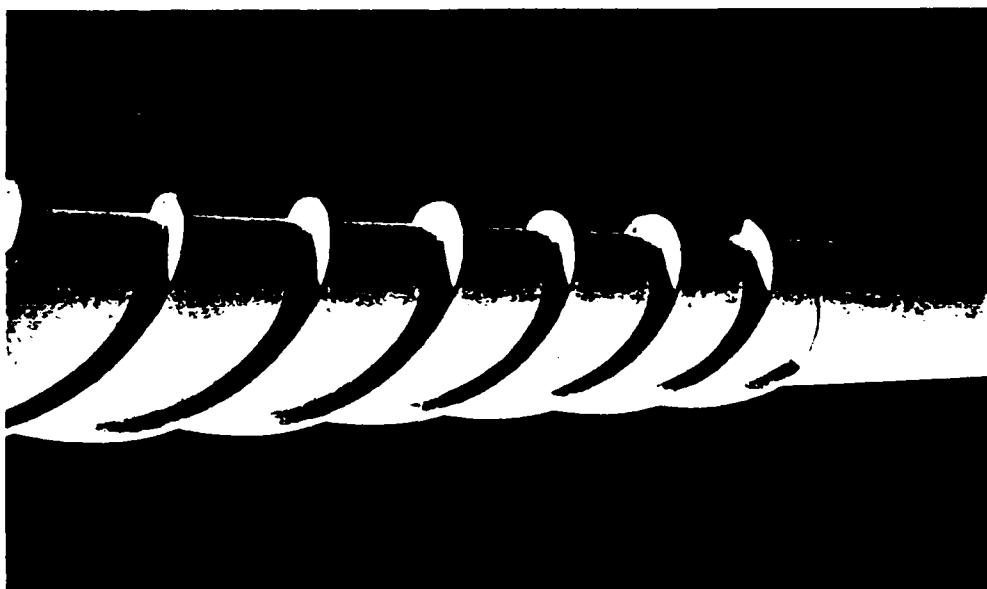
Figure D-4 Amplitude of Response for Cross-Flow Vibrations



Offset Dorsal Fin



Shrouds



Strakes

Figure D-5 Typical Devices and Spoilers

(THIS PAGE INTENTIONALLY LEFT BLANK)

COMMITTEE ON MARINE STRUCTURES

Commission on Engineering and Technical Systems

National Academy of Sciences – National Research Council

The COMMITTEE ON MARINE STRUCTURES has technical cognizance over the interagency Structure Committee's research program.

Peter M. Palermo Chairman, Alexandria, VA

Mark Y. Berman, Amoco Production Company, Tulsa, OK

Subrata K. Chakrabarti, Chicago Bridge and Iron, Plainfield, IL

Rolf D. Glasfeld, General Dynamics Corporation, Groton, CT

William H. Hartt, Florida Atlantic University, Boca Raton, FL

Alexander B. Stavovy, National Research Council, Washington, DC

Stephen E. Sharpe, Ship Structure Committee, Washington, DC

LOADS WORK GROUP

Subrata K. Chakrabarti Chairman, Chicago Bridge and Iron Company, Plainfield, IL

Howard M. Bunch, University of Michigan, Ann Arbor, MI

Peter A. Gale, John J. McMullen Associates, Arlington, VA

Hsien Yun Jan, Martech Incorporated, Neshanic Station, NJ

Naresh Maniar, M. Rosenblatt & Son, Incorporated, New York, NY

Solomon C. S. Yim, Oregon State University, Corvallis, OR

MATERIALS WORK GROUP

William H. Hartt Chairman, Florida Atlantic University, Boca Raton, FL

Santiago Ibarra, Jr., Amoco Corporation, Naperville, IL

John Landes, University of Tennessee, Knoxville, TN

Barbara A. Shaw, Pennsylvania State University, University Park, PA

James M. Sawhill, Jr., Newport News Shipbuilding, Newport News, VA

Bruce R. Somers, Lehigh University, Bethlehem, PA

Jerry G. Williams, Conoco, Inc., Ponca City, OK

SHIP STRUCTURE COMMITTEE PUBLICATIONS

- SSC-351 An Introduction to Structural Reliability Theory by Alaa E. Mansour 1990
- SSC-352 Marine Structural Steel Toughness Data Bank by J. G. Kaufman and M. Prager 1990
- SSC-353 Analysis of Wave Characteristics in Extreme Seas by William H. Buckley 1989
- SSC-354 Structural Redundancy for Discrete and Continuous Systems by P. K. Das and J. F. Garside 1990
- SSC-355 Relation of Inspection Findings to Fatigue Reliability by M. Shinozuka 1989
- SSC-356 Fatigue Performance Under Multiaxial Load by Karl A. Stambaugh, Paul R. Van Mater, Jr., and William H. Munse 1990
- SSC-357 Carbon Equivalence and Weldability of Microalloyed Steels by C. D. Lundin, T. P. S. Gill, C. Y. P. Qiao, Y. Wang, and K. K. Kang 1990
- SSC-358 Structural Behavior After Fatigue by Brian N. Leis 1987
- SSC-359 Hydrodynamic Hull Damping (Phase I) by V. Ankudinov 1987
- SSC-360 Use of Fiber Reinforced Plastic in Marine Structures by Eric Greene 1990
- SSC-361 Hull Strapping of Ships by Nedret S. Basar and Roderick B. Hulla 1990
- SSC-362 Shipboard Wave Height Sensor by R. Atwater 1990
- SSC-363 Uncertainties in Stress Analysis on Marine Structures by E. Nikolaidis and P. Kaplan 1991
- SSC-364 Inelastic Deformation of Plate Panels by Eric Jennings, Kim Grubbs, Charles Zanis, and Louis Raymond 1991
- SSC-365 Marine Structural Integrity Programs (MSIP) by Robert G. Bea 1992
- SSC-366 Threshold Corrosion Fatigue of Welded Shipbuilding Steels by G. H. Reynolds and J. A. Todd 1992
- None Ship Structure Committee Publications – A Special Bibliography